**Evaluation of emerging screening technologies for the on-site detection and identification of methamphetamine and its precursors in simulated clandestine lab operations**

Alexis Wilcox, B.S.

Thesis submitted
to the **Eberly College of Arts and Sciences**
at **West Virginia University**

in partial fulfillment of the requirements for the degree of

**Master of Science** in
**Forensic and Investigative Science**

**Dr. Luis E. Arroyo, Ph.D., chair**
**Dr. Tatiana Trejos, Ph.D.**
**Dr. Casper Venter, Ph.D.**
**Dr. Edward Sisco, Ph.D.**

**Department of Forensic and Investigative Science**

**Morgantown, West Virginia**
**2023**

**Keywords:**
Raman Spectroscopy, Direct Analysis in Real-Time Mass Spectrometry, Machine Learning, Forensic Science, Clandestine Methamphetamine Laboratories

# ABSTRACT

Evaluation of emerging screening technologies for the on-site detection and identification of methamphetamine and its precursors in simulated clandestine lab operations

**Alexis Wilcox**

Stimulant drugs comprise one of the top drug categories abused in the United States. Due to its accessibility, low price, and manufacturing simplicity, methamphetamine is frequently placed within the top 10 seized drugs in the country. As of March 2023, methamphetamine is the most seized controlled substance in the United States, with 34,291 kg. In 2022, the United States seized over 79,000 kg of methamphetamine. One reason for the proliferation of methamphetamine is related to the production itself, which does not require large warehouses but can be manufactured in houses using relatively accessible materials and small containers. When a clandestine laboratory is investigated, law enforcement and CSIs must be able to identify what drug is being produced and what hazards are associated with the production method being utilized by the clandestine laboratory.

Due to shifting manufacturing routes by underground chemists, it has become difficult for forensic scientists to identify illicit substances and their respective precursors reliably. Indeed, rapid analytical tools that facilitate the identification of legal and scheduled drugs are highly desirable for first responders, health personnel, and forensic chemists. This thesis addresses this deficit by investigating Raman Spectroscopy and Direct Analysis in Real-Time Mass Spectrometry (DART-MS) to determine ways to improve mixture identification. This research focuses on methamphetamine and its precursors, ephedrine, and pseudoephedrine. However, the scope was expanded to include several other drugs and cutting agents of concern in the United States.

This research compared three Portable Raman instrumentations for detecting methamphetamine and its precursors in binary mixtures. From a practical perspective, the TacticID GP from B&W Tek (Newark, DE) and the Mira XTR DS from Metrohm USA (Riverview, FL) were determined to be suitable for on-site detection due to their simple operation and color-coded results that provide immediate safety information for the results, in case the user is not familiar with the compound. The mixture analysis function allowed for better identification of the controlled substance due to the controlled substance being the minor component in most cases. The iRaman Prime from B&W Tek (Newark, DE) had limitations for the mixtures. Software used to compare the collected spectrum to the library does not include the mixture analysis function to

help identify complex samples. There are other software present; however, the software requires an additional understanding of statistical analysis that first responders may not be equipped with.

This research also sought to improve Raman's detection of mixtures using machine learning, specifically convolutional neural networks or CNN. The iRaman Prime from B&W Tek (Newark, DE) was used for this purpose, which had the most difficulty identifying mixtures due to the built-in software available. Using CNN, the ability to identify both components in the mixtures improved to 94.0 % compared to 71.5 % using cosine similarity. However, the algorithm had difficulty identifying the drugs and adulterants in the authentic samples. The difficulty is because the authentic samples consisted of more complex samples, with more than two compounds present. Further research can be done to train the algorithm with more complex samples or include the class of compounds to give an overall result for compounds not in the training set.

Lastly, the utility of DART-MS was investigated for methamphetamines. The Data Interpretation Tool (DIT) *v. 2* from NIJ/NIST was used to see how well DART-MS could identify multiple components in mixtures. Authentic samples from the Maryland State Police Forensic Sciences Division were used as more complex samples to compare these instruments with more realistic ones. The DIT and DART-MS identified 82.5 % of the binary mixtures. The DIT also successfully identified at least one controlled substance in the samples containing controlled substances. This thesis demonstrates that the combination of Raman Spectroscopy with CNN and DART-MS with DIT improves their respective instrument's ability to detect mixtures, making them better equipped for use in clandestine operations and regular forensic casework.

# ACKNOWLEDGMENT

# Table of Contents

# LIST OF FIGURES

# LIST OF Tables

# LIST OF ABBREVIATIONS

**Part II: Comparison of Portable Raman Instruments**

| | |
|---|---|
| ADHD | Attention deficit hyperactivity disorder |
| APLD-MS | Ambient pressure laser desorption-mass spectrometry |
| CCD | Charged coupled device |
| CMEA | Combat methamphetamine epidemic act |
| CSI | Crime scene investigators |
| HQI | Hit quality index |
| IMS | Ion mobility spectrometry |
| IR | Infrared |
| NIJ | National Institute of Justice |
| ORS | Orbital raster scan |
| P2P | Phenyl-2-propanone |
| PLS | Partial Least Squares Regression |
| PCA | Principal component analysis |
| SVM | Support Vector Machine |
| SWGDRUG | Scientific working group for the Analysis of Seized Drugs |
| TOS | TacticID operating system |

**Part III: Improving Raman Spectroscopy Using Machine Learning**

| | |
|---|---|
| 4-MEC | 4-Methylethcathinone |
| 4-MMC | 4-Methylmethcathinone |
| 6-MAM | 6-monoacetylmorphine |
| Δ9-THC | Delta-9-tetrahydrocannabinol |
| ANN | Artificial neural networks |
| CNN | Convolutional neural networks |
| DL | Deep learning |
| ML | Machine learning |
| MSP FSD | Maryland State Police Forensic Science Division |
| ReLU | Rectified linear activation function |

**Part IV: Direct Analysis in Real-Time Mass Spectrometry**

AccuTOF          Accurate time-of-flight

API              Atmospheric pressure interface

DART-MS          Direct analysis in real-time mass spectrometry

DIT              Data interpretation tool

ESI              electron spray ionization

FPIE             Fraction of peak intensity explained

is-CID           In-source collision-induced dissociation

LFPM IRD         Low fragmentation protonated molecule isotope ratio difference

OA               Orthogonal acceleration

PEG              polyethylene glycol

RevMF            Reverse match factor

TD               Thermal Desorption

# Part I: Introduction
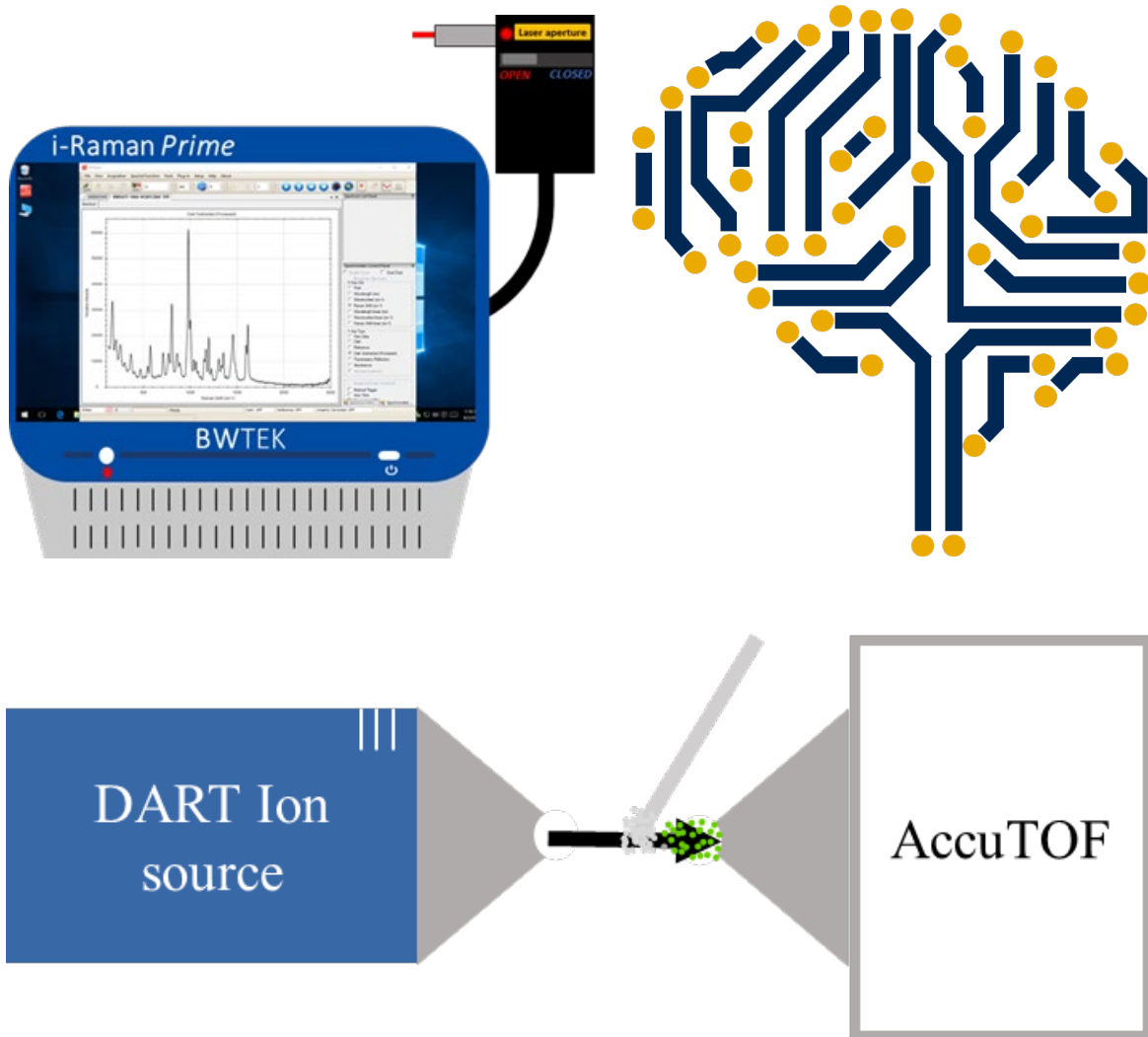


Chapter 1: Purpose of Research and Objectives

*1.1 Problem Statement*

      Stimulant drugs comprise one of the main drug categories abused in the United States. Due to its accessibility, price, and manufacturing simplicity, methamphetamine is frequently one of the country's top 10 seized drugs. The growth and spread of the illicit manufacture and trade of methamphetamine continued to upsurge despite efforts by the government to control and punish users, distributors, and manufacturers. The Comprehensive Methamphetamine Control Act of 1996 enhanced penalties regarding the manufacture and trafficking of methamphetamine, and the Combat Methamphetamine Epidemic Act of 2005 set stronger regulations for precursor chemicals.[1] This act limited the domestic clandestine laboratories, as seen by the decrease in incidents in **Figure 1**.
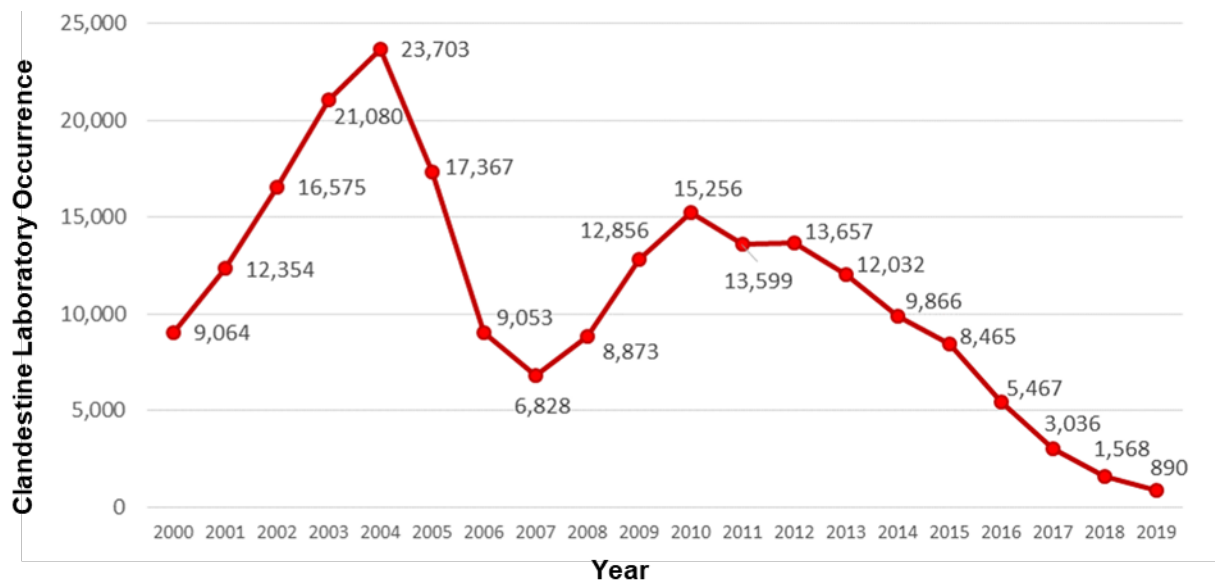


**Figure 1:** Number of domestic incidents for clandestine methamphetamine production. [2]

      Despite the many laws and government entities overseeing and enforcing methamphetamine regulations (e.g., Schedule II drugs), the ingenuity of the illegal drug market has continued to allow the trade and use of methamphetamine within the United States to grow. Indeed, today the manufacture and trafficking of methamphetamine have become a global problem and a profitable worldwide market.[3] As of March 2023, methamphetamine was reported to be the most seized controlled substance in the United States, with 34,291 kg. As a reference, during the 2022 fiscal year, the United States seized over 79,000 kg of methamphetamine. [11] The

COVID-19 pandemic has had little to no effect on the production, distribution, and use of methamphetamine, and its abuse proliferated. [12]

**Figure 2** shows the main trafficking routes described by the United Nations on Drugs and Crime (UNODC). [4] North America is identified as a significant departure and destination country for methamphetamine trafficking, as seen in **Figure A - 1**and **Figure A - 2** in the **Appendix**. According to the 2020 National Threat Assessment from the Drug Enforcement Administration (DEA) [2], most methamphetamine entry points on the United States' southern border are produced in Mexico by large cartel operations. Most precursors come to the United States via maritime shipments from China and India. Most manufactured methamphetamine comes from Mexico through the southern border using various techniques. Privately owned vehicles can transport kilograms of methamphetamine concealed in the tires or other natural voids in the vehicle. Fuel tanks can conceal both packages and solutions of methamphetamine. Traffickers often will conceal methamphetamine using odors and liquids.
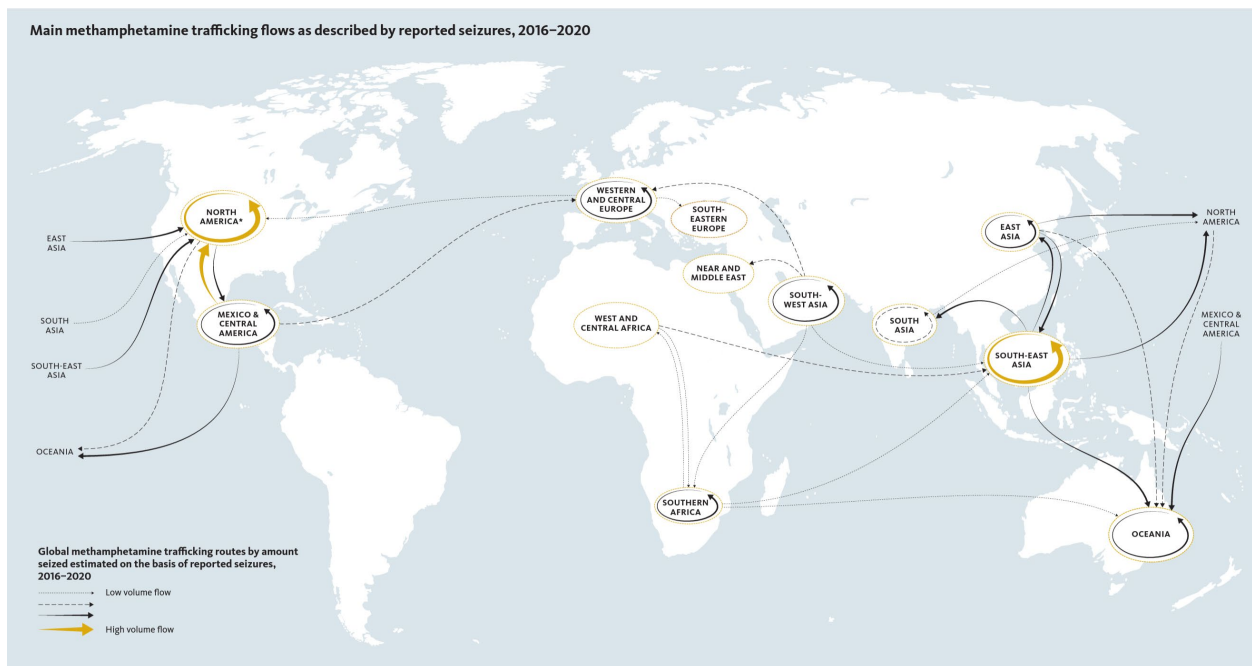


**Figure 2:** Main methamphetamine trafficking routes as described by the UNODC. North America is listed as a main destination and departure for methamphetamine. [5]

Methamphetamine and amphetamine-type substances (ATS) are central nervous system stimulants, producing alertness, euphoria, increased heart rate and body temperature, memory loss, hypertension, hallucinations, paranoia, and violent behavior. ATS are derived from the

phenethylamine structure and are commonly snorted, smoked, ingested, or injected. [6] ATS represents a group of synthetic drugs. Many drugs of abuse result from plant-based compounds or semi-synthetic routes based on plant compounds. ATS are fully synthetic compounds and not the result of plant-based extractions. Since the 1930s, methamphetamine has been utilized for medical purposes. Its use and over-prescription during World War II and to the general public have contributed to its illicit use today, including the clandestine synthesis since the 1960s.[7]

Unfortunately, the synthesis of methamphetamine is well-understood, published, and relatively simple. As a result, the purity and potency of methamphetamine within the United States remain very high and can be obtained at meager prices.[8] Because of this, the number of seizures and methamphetamine-related crimes continues to grow. Over 53,000 kilograms of methamphetamine were seized in the United States in 2019, resulting in over 400,000 reports to the National Forensic Laboratory Information System (NFLIS), where the average purity of methamphetamine was astonishing 97 %.[8] Interestingly, it has appeared that the COVID-19 epidemic has had little impact on the production, distribution, and use of methamphetamine.

One reason for the proliferation of methamphetamine is related to the production itself, which does not require large warehouses but can be manufactured in houses using relatively accessible materials and small containers. As the government tries to control and limit the production of methamphetamine, clandestine laboratories alter how methamphetamine is produced to avoid drug laws. [9]

Due to the numerous regulations and control over methamphetamine synthesis, several methods have been developed, each using its reactants, precursors, and synthetic routes. These different synthesis methods can be traced to specific precursors and impurities originating from low-quality reactants, incomplete reactions, and/or inadequate purification steps. [10] Determining the synthetic route is vital to provide investigative information regarding the types of precursors used and available and track where the seizure originated. [11][12] For example, in the first half of 2019, 99 % of the methamphetamine seized was determined to have been produced using the P2P method.[8] Mexico has seen a shift to 1-phenyl-2-propanone (P2P) synthesis methods based on the availability of chemicals and regulations imposed. Also, changing towards phenylacetic acid (PAA), its derivatives (representing a classic P2P synthesis), benzaldehyde, and nitroethane.[13] Designer precursors have also been seen, which can be classified as masked precursors or chemical intermediates. Like other synthesis routes, their use is based on chemical

availability and legislative control.[13] Interestingly, the methamphetamine trade in Mexico and the United States is that many precursors are typically purchased from overseas countries like China or India and shipped using maritime methods. Still, the majority of methamphetamine trafficking occurs over land.[8]

A general understanding of the operation of clandestine laboratories is critical to this project since it would offer a clear perspective for law enforcement personnel and crime scene investigators (CSI) to recognize solvents, precursors, and equipment used in the illicit manufacture of drugs. This theme will be addressed in Part II of this thesis. When a clandestine laboratory is investigated, law enforcement and CSIs must be able to identify what drug is being produced and what hazards are associated with the production method being utilized by the clandestine laboratory. This information is also crucial for firefighters who are usually called to attend fires that could involve a clan lab or dump site.
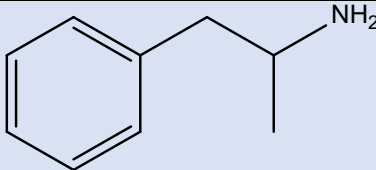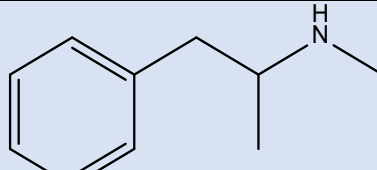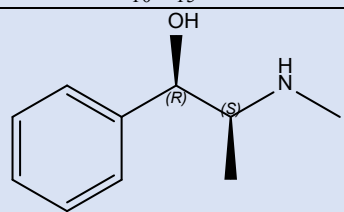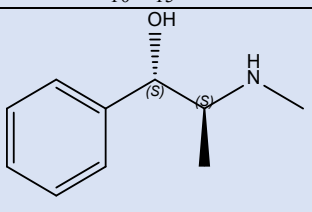
Despite the number of local clan labs and dump sites declining in the past decade (Figure 1), their presence still represents a significant risk to the general population. Indeed, rapid analytical screening tools that facilitate the identification of legal and scheduled drugs are highly desirable for first responders, health personnel, and forensic chemists. Two methods that provide structural information about the molecule being analyzed include Raman Spectroscopy and Direct Analysis in Real Time Mass Spectrometry (DART-MS). However, both instruments have limitations when it comes to impure samples. This is a problem with seized drugs because most controlled substances are cut with additional ingredients to limit the toxic effects and increase the product yield. Therefore, this research investigated ways to improve the detection of complex samples for Raman and DART-MS as a fast analytical technique that can identify multiple sample components. This thesis will demonstrate the use of machine learning and the Data Interpretation Tool (DIT) to improve the detection of mixtures for Raman and DART-MS, respectively.
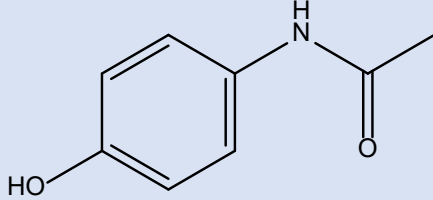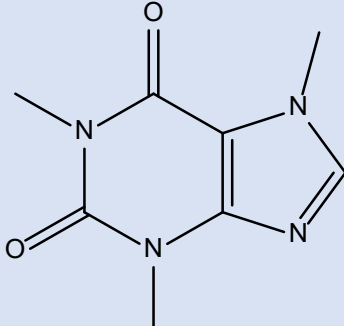
*1.2 – Goals and Objectives*

This study investigated the use of Raman Spectroscopy and DART-MS for mixtures related to methamphetamine clandestine laboratories. Six of the main standards used throughout the study are shown in **Table 1**. Several different data analysis tools were used to improve the detection of mixtures. The samples analyzed were expanded from the six standards proposed to 38 standards to include other compounds that may not be related to clandestine methamphetamine production. This expansion was to make the CNN algorithm more beneficial for seized drug analysis. The goal

for each analytical technique was to get over 80 % identification. Additional aspects of each technique were compared such as portability, cost of the instrument, and consumables required to identify the advantages and disadvantages of each instrument and improve the understanding of the utility of Raman spectroscopy and DART-MS for this field.

**Table 1:**List of the six main drugs of interest and important information about each.

| Drug | Amphetamine | Methamphetamine |
|---|---|---|
| Formula (PubChem) | $C_9H_{13}N$ | $C_{10}H_{15}N$ |
| Structure (PubChem) |  |  |
| Molecular weight (PubChem) | 135.206 g/mol | 149.2370 g/mol |
| CAS #(PubChem) | 300-62-9 | 537-46-2 |
| ChemSpider # (ChemSpider) | 13852819 | 1169 |
| Category (PubChem) | Schedule II | Schedule II |
| Pka (PubChem) | 9.9 | 9.9 |
| Raman bands of interest [14] | 500 cm$^{-1}$ ← ν chain<br>942 cm$^{-1}$ ← ν chain<br>1251 cm$^{-1}$ ← ν CC | 522 cm$^{-1}$ ← ν chain<br>1300 cm$^{-1}$ (couplet) ← ν chain<br>1450 cm$^{-1}$ (shoulder)← 2$^{nd}$ amine |
| Common isotopes (ChemDraw) | 135.1048 (100.0 %)<br>136.1082 (9.7 %) | 149.1204 (100.0 %)<br>150.1238 (10.8 %) |
| Characteristic Ions (DART-AccuTOF) (DIT) | *m/z* 136.133← PM<br>*m/z* 137.116 ← +1 Isotope (PM)<br>*m/z* 91.055 ← BP | *m/z* 150.129 ← PM<br>*m/z* 151.131 ← +1 Isotope (PM)<br>*m/z* 91.055 ← BP |
| **Drug** | **Ephedrine** | **Pseudoephedrine** |
| Formula (PubChem) | $C_{10}H_{15}NO$ | $C_{10}H_{15}NO$ |
| Structure (PubChem) |  |  |
| Molecular weight (PubChem) | 165.2360 | 165.2360 |
| CAS #(PubChem) | 98299-42-3 | 90-82-4 |
| ChemSpider # (ChemSpider) | 8935 | 6761 |
| Category (PubChem) | Schedule 2 | Schedule 2 |
| Pka (PubChem) | 9.68 | 9.52 |

| | | |
|---|---|---|
| Raman bands of interest | 238 cm$^{-1}$, 402 cm$^{-1}$, 750 cm$^{-1}$ stereoscopic differences between CN and CO bonds for ephedrine/pseudoephedrine | 260 cm$^{-1}$, 427 cm$^{-1}$, 550 cm$^{-1}$ stereoscopic differences between CN and CO bonds for ephedrine/pseudoephedrine |
| Common isotopes (ChemDraw) | 165.1154 (100.0 %) 166.1187 (10.8 %) | 165.1154 (100.0 %) 166.1187 (10.8 %) |
| Characteristic Ions (DART-AccuTOF) (DIT Library) | $m/z$ 166.123 ← PM $m/z$ 167.126 ← +1 Isotope (PM) $m/z$ 148.113 ← BP | $m/z$ 166.123 ← PM $m/z$ 167.125 ← +1 Isotope (PM) $m/z$ 148.113 ← BP |
| **Drug** | **Acetaminophen** | **Caffeine** |
| Formula (PubChem) | $C_8H_9NO_2$ | $C_8H_{10}N_4O_2$ |
| Structure (PubChem) | | |
| Molecular weight (PubChem) | 151.16 | 194.19 |
| CAS #(PubChem) | 103-90-2 | 58-08-2 |
| ChemSpider # (ChemSpider) | 1906 | 2424 |
| Category (PubChem) | N/A | N/A |
| Pka (PubChem) | 9.38 | 14 |
| Raman bands of interest [15] | 650 cm$^{-1}$ ← ν CO 1240 cm$^{-1}$ ← ν CO 1650 cm$^{-1}$ ← ν CO | 740 cm$^{-1}$ ← δ rings 554 cm$^{-1}$ ← δ pyrimidine ring 1330 cm$^{-1}$ ← ν imidazole ring |
| Common isotopes (ChemDraw) | 151.06 (100.0 %) 152.07 (8.8 %) | 194.08 (100.0 %) 195.08 (10.2 %) |
| Characteristic Ions (DART-AccuTOF) (DIT) | $m/z$ 152.073 ← PM $m/z$ 153.076 ← +1 Isotope (PM) $m/z$ 110.063 ← MF | $m/z$ 195.088 ← PM $m/z$ 196.090 ← +1 Isotope (PM) |

N/A = not scheduled drug, PM = protonated molecule, BP = Base peak ion, MF, Major fragment ion

**Part I** of this thesis explains the problem this thesis addresses. It also explains the goals and objectives used to address the problem. The main objective of this thesis was to understand how existing technology (both portable and benchtop) could benefit first responders and forensic laboratories in identifying unknown materials by comparing their performance metrics for the detection of complex mixtures. This goal was achieved through the completion of the following sub-objectives:

1. Compare portable Raman instruments for the detection of complex samples relating to methamphetamine clandestine laboratories.
2. Improve portable Raman instruments using machine learning.
3. Investigate the use of DIT for the analysis of complex DART-MS spectra.

**Part II** of this thesis compared three portable Raman instruments for their ability to detect two targeted compounds in 42 in-house binary mixtures related to clandestine methamphetamine production. These binary mixtures are combinations of methamphetamine, amphetamine, common cutting agents (acetaminophen and caffeine), and precursors (ephedrine and pseudoephedrine). Two pharmaceutical pills were also analyzed, including pseudoephedrine, which is used to make methamphetamine, and phenylephrine, which has been used to replace pseudoephedrine. Cosine similarity was used as a more direct comparison of the collected spectra.

**Part III** of this thesis proposed using machine learning to improve the portable Raman's ability to identify complex samples. Machine learning algorithms can be trained to learn the complexity of datasets and use this information to make predictions on new data. The machine learning algorithm used was convolutional neural networks (CNN). CNN was compared to cosine similarity, a more traditional similarity technique. The samples analyzed in this part were expanded to include other controlled substances and cutting agents to make the algorithm more realistic for casework. A total of 38 drug standards were used as the dataset/library, and 100 binary mixtures were analyzed as a test set. Twelve authentic samples from the Maryland State Police Forensic Sciences Division (MSP FSD) were analyzed as more complex entities.

**Part IV** of the thesis used the Data Interpretation Tool (DIT) to detect mixtures analyzed with DART. DIT is an improved software developed by NIJ and NIST that identifies patterns in the complex spectra that could be related to the pure spectra in the library. Sixty binary mixtures from Part III and the same twelve authentic samples were also analyzed by DART-AccuTOF and identified using the DIT.

**Part V** compared the ability of both Raman Spectroscopy and DART-MS to detect complex samples. It also looked at the analysis cost and consumables required for each analytical technique to summarize the advantages and limitations of using Raman spectroscopy and DART-MS to detect mixtures, specifically methamphetamine and its precursors.

# Part II: Comparison of Portable Raman Instruments



ADMIN

✔ Match

Scan Index:

Search Result:

1. Methamphetamine

Mixture 📷 Notes

TacticID

MIRA XTR

Scan: #

Mixture   Identification

Methamphetamine HQI: #

Metrohm

Laser aperture

OPEN   CLOSED

i-Raman *Prime*

BWID

Acquired Data

Methamphetamine

ID

View   Print

Add

MATCH

Methamphetamine

BWTEK
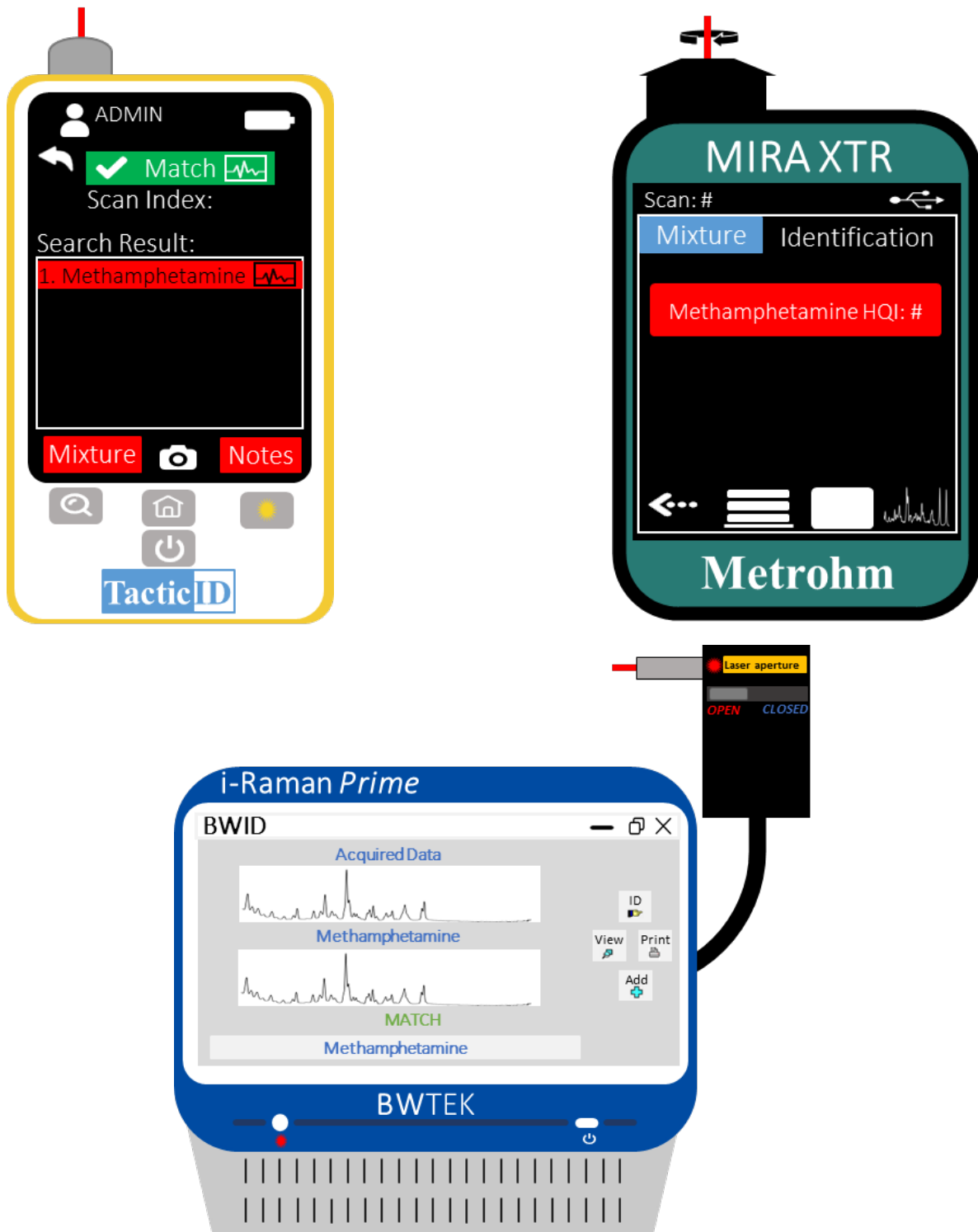
## Chapter 1: Relevant Literature Review

*1.1 – Methamphetamine*

Methamphetamine is a central nervous system (CNS) stimulant that increases the brain's norepinephrine and dopamine activity. [16] According to the DEA, methamphetamine is considered a Schedule II drug. [17] Schedule II substances are defined as "drugs with a high potential for abuse, with use potentially leading to severe psychological or physical dependence"; however, Schedule II drugs also have accepted medical use. [18] Methamphetamine is FDA approved medication called Desoxyn® and is used to treat attention deficit hyperactivity disorder (ADHD). [19] The typical dosage for ADHD is 20-25 mg per day. [20] Some common side effects of short-term methamphetamine/Desoxyn include fast heartbeat, tremors, trouble sleeping, decreased appetite, headache, dizziness, stomach upset, dry mouth, and weight loss. [16] Professionals do not recommend Desoxyn for an extended period due to methamphetamine's addictive nature. [19] Chronic methamphetamine side effects include weight loss, psychosis, hallucinations, sagging skin, body sores, inflamed heart lining, formication, meth mouth (tooth decay and cracked teeth), and heightened risk of brain damage, coma, stroke, or death. [21]

*1.2 – Clandestine Laboratories*

Clandestine laboratories (or clan labs) are those locations where illicit substances are illegally produced. Most clandestine laboratories are large industrial labs that are highly organized and produce tons of illicit substances trafficked worldwide. [22] **Figure 3** shows some examples of industrial clandestine methamphetamine laboratories from Mexico. These pictures were taken from various news outlets. However, not all clandestine laboratories are this large. The second most common type of clandestine lab is small user-based clandestine laboratories, where a drug user will self-produce the drug, they are addicted to and maybe some extra to support their close associates. [22] These labs can be found in kitchens and cars; since synthetic approaches can be performed in a simple plastic bottle with easily obtained materials. **Figure 4** shows some examples of small user-based clandestine methamphetamine laboratories from Mexico. These pictures were taken from various news outlets.

**Figure 3:** Examples of large industrial clandestine methamphetamine laboratories in Mexico taken from news articles. The respective news outlets these pictures are adapted from are present in the bottom left corner for each picture.
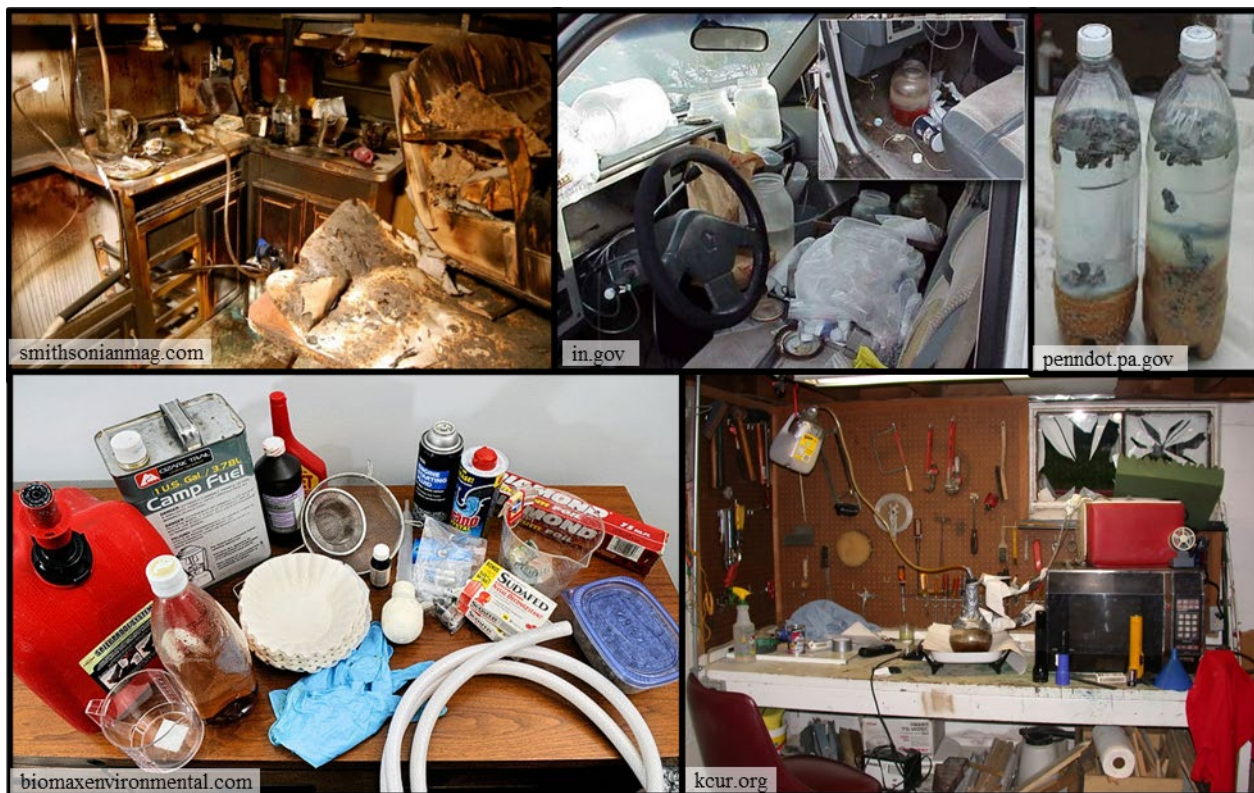
**Figure 4:** Examples of small user-based clandestine methamphetamine laboratories from the United States. The respective news outlets these pictures are adapted from are present in the bottom left corner for each picture.

Clandestine laboratories are defined by the processes they perform and the materials they use. Four main steps are involved in clandestine laboratory operations: Extraction, synthesis, purification, and cutting/diluting/tableting. [23] **Extraction labs** will extract the compound(s) of interest from bulk starting material. Examples include extracting ephedrine/pseudoephedrine from cough syrup for methamphetamine production or extracting opium from the poppy plant for heroin production. These labs will also extract illicit drugs from concealment after trafficking. **Synthesis labs** use precursors, reagents, and solvents to produce the illicit drug. **Purification labs** will remove unwanted colors, odors, and contaminants from the pure drug. **Cutting/diluting/tableting labs** will add additional materials (diluents) to increase the bulk or limit the toxic effects of pure drugs like fentanyl. The methods used by clandestine laboratories provide valuable information about how illicit substances are being made, which will help labs and police correctly identify potential clandestine laboratories.

*1.3 – Methamphetamine Production*

The illicit substances of interest in this research are amphetamine and methamphetamine. There are several precursors used to produce these two drugs, including ephedrine, pseudoephedrine, and phenyl 2-propanone (P2P). [23] Due to their legitimate medical use, ephedrine and pseudoephedrine are excellent raw materials available for the illicit manufacturing of methamphetamine. According to the 2022 Annual Precursors Report, approximately 1.17 million pseudoephedrine and 66,200 kg of ephedrine were traded globally. The United States ranked first in the largest imports of pseudoephedrine and fifth in the ephedrine imports. [9] **Figure 5** and **Figure 6** are from the 2022 Annual Precursor Report. These two figures show that even though seizures of pure ephedrine and pseudoephedrine are declining (**Figure 5**), the seizures of pseudoephedrine in medical preparation form are increasing (**Figure 6**).
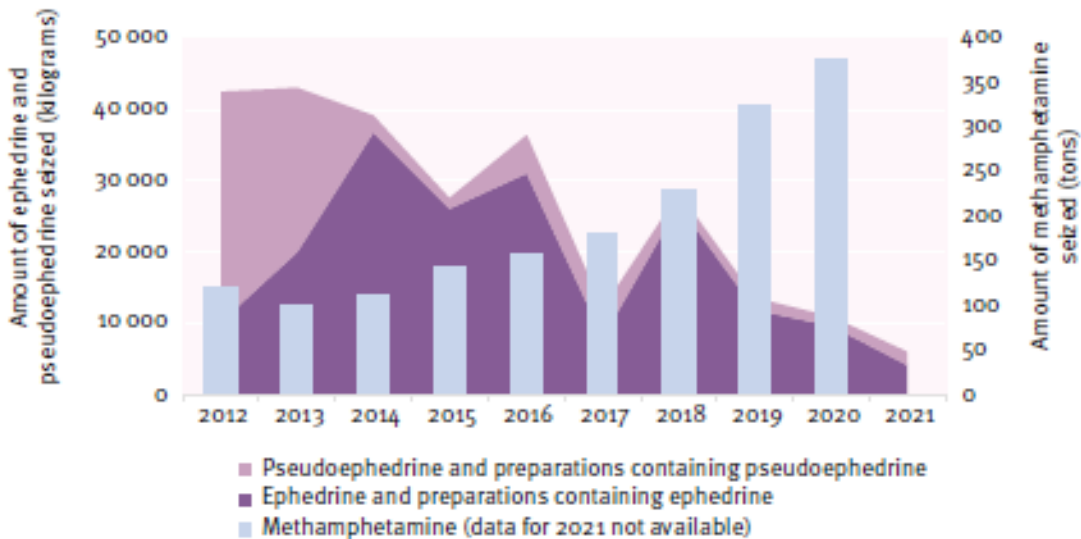


**Figure 5:** Seizures of ephedrine and pseudoephedrine compared to seizures of methamphetamine. [9]
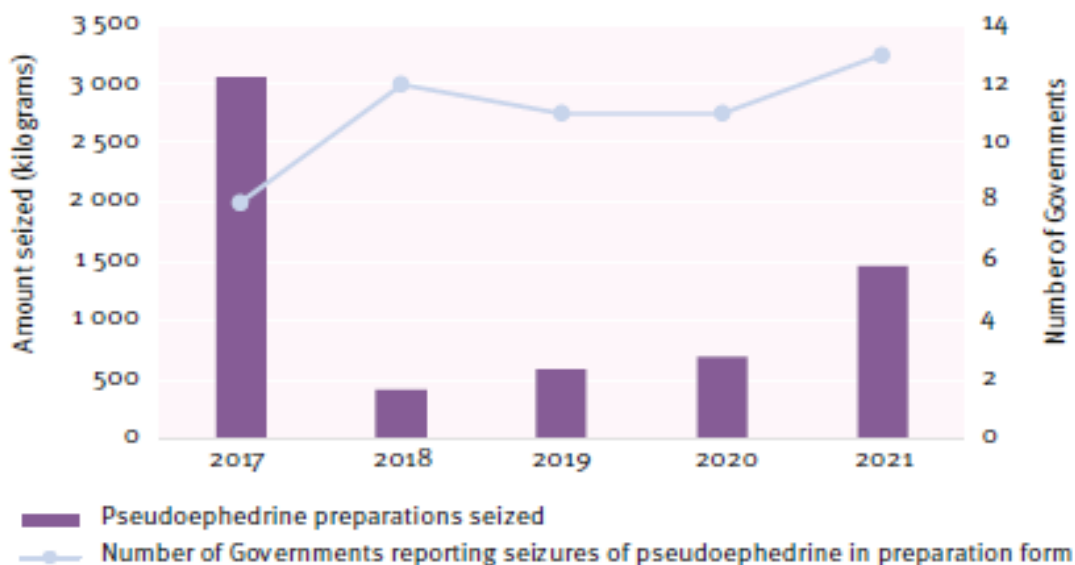
**Figure 6:** Seizures of pseudoephedrine preparations and the number of governments reporting the pseudoephedrine seizures. [9]

Another common precursor is phenyl-2-propanone (P2P), commonly used in larger clandestine laboratories like the Mexico drug cartels. This is because P2P provides a higher yield. However, the materials and equipment needed for this production are more expensive and harder to get.

1.3.1 – Phenyl-2-propanone Methods

There are three methods to produce methamphetamine or amphetamine using phenyl-2-propanone or P2P. **Reductive amination** uses either an amine (for amphetamine) or methylamine (for methamphetamine), which reacts with the carbonyl group on P2P to form an imine intermediate which is then reduced to the desired drug. An example of reductive amination to produce methamphetamine can be seen below:
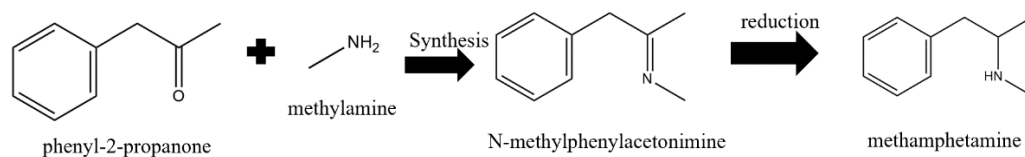


**Figure 7:** Synthetic Route for the Synthesis of Methamphetamine using P2P and Methylamine via Reductive Amination.

Another method using P2P is the **Leuckart method**. Depending on the choice of drug, either formamide (amphetamine) or methyl-formamide (methamphetamine) reacts with P2P to form an N-formyl intermediate, which then gets hydrolyzed to produce the desired drug. [23] An example of using the Leuckart method to produce amphetamine can be seen below:
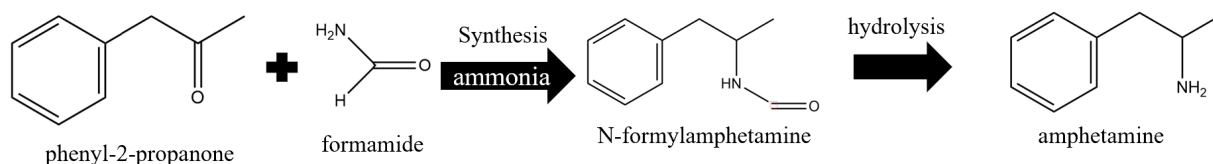


**Figure 8:** Synthetic Route for the synthesis of Amphetamine using P2P and a formamide via the Leuckart method.

The final method to make either methamphetamine or amphetamine with P2P is the **Nitrostyrene method**. This method uses benzaldehyde and nitroethane to form a phenyl-2-nitropropene which can either be directly reduced to form amphetamine or reduced and hydrolyzed to form P2P, which can then be used with the other two methods to form methamphetamine. [23] Both of these variations of the nitrostyrene method can be seen below:
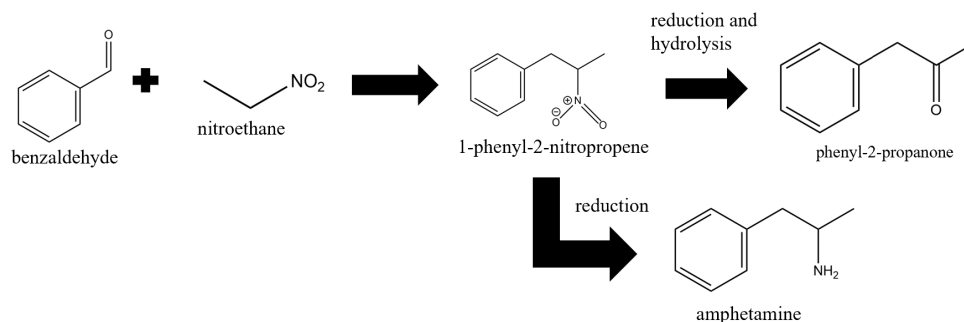


**Figure 9:** Synthetic Route for the synthesis of P2P or amphetamine using a benzaldehyde and a nitroethane via the Nitrostyrene method.

1.3.2 – Ephedrine/pseudoephedrine Routes

Five common methods are used to produce methamphetamine directly from these starting drugs. These precursors are not typically used to make amphetamine because the N-CH$_3$ bond would have to be broken. Three different methods can be grouped as the **iodine/red phosphorus methods**. [24] These methods use the same direct synthesis but with different reagents, as seen in **Figure 10**. **The Nagal method** uses HCl and red phosphorus. The **Moscow method** uses iodine, red phosphorus, and water. The **Hypo method** uses hypophosphorous (H$_3$PO$_2$) acid as a reducing

agent and iodine. There are benefits and limitations to each method. Red phosphorus can be recovered and reused. However, this creates an extra extraction step and creates phosphine, a poisonous red-P byproduct. The Hypo method has a higher percent yield, but all reagents must be replaced after each batch. These methods require the mixtures to be refluxed for a length of time. Household items can be repurposed for user labs, but large-scale labs need scientific equipment.
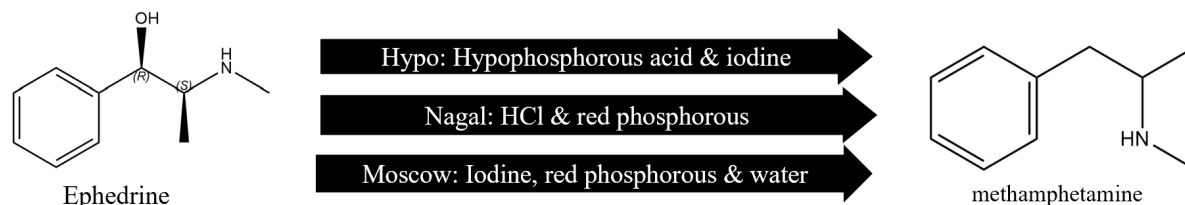


**Figure 10:** Three different synthetic routes and methods for the synthesis of methamphetamine using ephedrine or pseudoephedrine via direct synthesis.

The **Birch Reduction method** reacts ammonia and lithium metal with ephedrine to produce methamphetamine (**Figure 11**). [24] Fertilizers and single-use batteries are commonly used for this method. A common variation of the Birch Reduction is called the "one pot" method. [25] This variation puts all the reagents and precursors into one pot, like a soda bottle. The ammonia is produced in-situ with sodium hydroxide and ammonium salt, which then reacts with the lithium metal and ephedrine to produce methamphetamine.
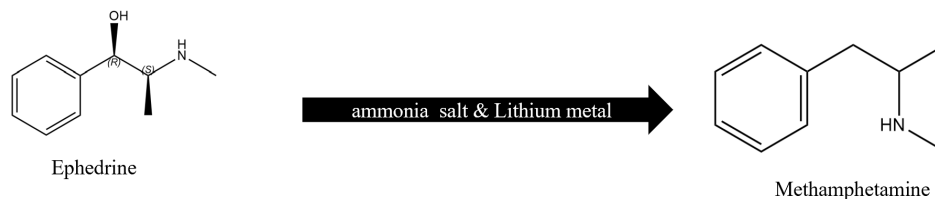


**Figure 11:** Synthesis of methamphetamine using either ephedrine or pseudoephedrine via the Birch Reduction

The final method is the **Emde method** (**Figure 12**). This method reacts with ephedrine and thionyl chloride to make a chloroephedrine intermediate, which then gets hydrogenated with high pressure to form methamphetamine. [23] This method is typically used in large-scale laboratories due to the high pressure required. Caution is needed because thionyl chloride reacts violently with water and is highly corrosive.
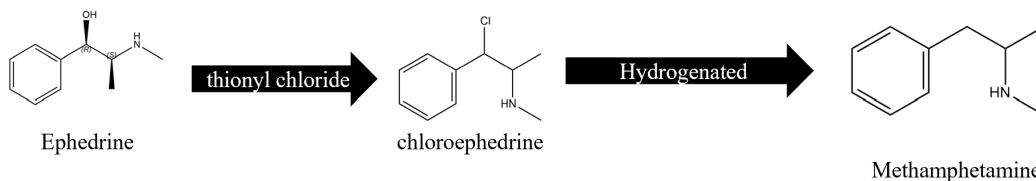
**Figure 12:** Synthesis of methamphetamine using either ephedrine or pseudoephedrine via the Emde method.

1.3.3 – Methamphetamine impurities and previous research

Government agencies aim to understand the dynamics of the manufacturing methods of classic and emerging substances for intelligence purposes. To this end, researchers at the DEA have developed screening and confirmatory methods to detect impurities in methamphetamine to trace manufacturing routes. These impurities establish links between the clandestine laboratory, suppliers, and users. [26] Most of these impurities come from the intermediates during the manufacturing process. For example, the Emde route, which uses thionyl chloride and ephedrine/pseudoephedrine, has an intermediate of (+)-chloropseudoephedrine and (-)-chloroephedrine. [27] The Leuckart method that uses P2P and methyl-formamide has two route-specific impurities, α,α'dimethyldiphenethylamine and N, α,α'dimethyldiphenethylamine. [28]

Several groups have reported activities investigating methamphetamine in clandestine laboratories, including surface contamination [25], social organizations [29], building contamination [30–32], environmental contamination [33], property values [34], precursor chemicals [35], impurities in methamphetamine tablets[26,36–39], and conversion efficiency [40]. An article from Reiss et al. [41] compared three different analytical techniques for on-site detection in clandestine methamphetamine laboratories, including immunoassays, ion mobility spectrometry (IMS), and ambient pressure laser desorption-mass spectrometry (APLD-MS). The authors selected these instruments because they offer the potential for on-site detection of trace materials. Immunoassays are straightforward, but IMS requires training and prior experience, and APLD-MS requires expert/highly trained personnel. The author's study used clandestine laboratory glassware contaminated with 3,4-methylenedioxy-N-methamphetamine (MDMA) and amphetamine. All three analytical techniques were able to detect MDMA and amphetamine. IMS and APLD-MS detected the amphetamine intermediate (N-formylamphetamine), and only APLD-MS could detect the precursors (alpha-phenylacetoacetonitril and benzyl methyl ketone). Raman

spectroscopy was not used in this study by Reiss et al. because Raman suffers when performing trace analysis.

While the reagents, solvents, and impurities are out of the scope of this research, it is highly valuable to identify rapid interrogation tools which will help identify legal and scheduled drugs. First responders, health personnel, and forensic scientists comprised the core of interested parties that may benefit when attending their specific activities. [24] The traditional screening methods used to detect illicit substances and their precursors have limitations. Traditional screening methods, including chemical color tests, are prone to false positives and false negatives due to the subjective nature of the results. Whereas traditional confirmatory tests are not prone to such problems and include gas chromatography-mass spectrometry (GC-MS), these confirmatory methods can create bottlenecks due to the time required for analysis and sample preparation, like extractions and separation steps.

*1.4 – Raman Spectroscopy*

Dr. CV Raman won a Nobel Prize in Physics in 1930 for discovering the Raman effect used in Raman Spectroscopy. The Raman effect is the change in the wavelength of light that results when a light beam interacts with the electron density of the chemical bond in a molecule. This method was improved further with the invention of the laser in the 1960s, where it became more applicable with the addition of a laser light source due to the high intensity, single wavelength source. [42] Two different variations of scattered light occur when the incident photons or laser interacts with the molecules in the sample. The majority of the scattered light is called Rayleigh scattering. Rayleigh scattering has the same wavelength at the incident light source. This shift provides no information about the chemical structure of the molecules hit by the light because the scattered light is unchanged. The other type of scattered light is called Raman scattering. Raman scattering occurs when the scattered light has a different wavelength or frequency than the incident light source. There are two different types of Raman scattering. Stokes shifts occur when the frequency of the scattered light is lower than the light source. Anti-stokes occur when the frequency of the scattered light is higher than the light source. [43] These shifts can be explained using the energy equations below:

**Equation 1:**  $E_{ex} = hv_{ex}$ ← Rayleigh scattering
**Equation 2:**  $E = h\,(v_{ex} - v_v) - v_{ex}$ ← stoke lines

**Equation 3:** $E = h(v_{ex} + v_v) - v_{ex}$ ← anti-stokes lines

Where $E_{ex}$ is the energy from the light source, h is Plank's constant ($6.626 \times 10^{-34}$ Js), $v_{ex}$ is the exciting frequency, and $v_v$ is the vibrational frequency.

Stokes is the most common scattered light used in Raman spectroscopy because it is more intense than anti-Stokes. The simplest explanation is that Stokes scattering occurs from the ground state, while anti-Stokes occur from an excited state. At room temperature and standard conditions for experiments, the ground state will be more populated, resulting in more scattering occurring from that state. The scattered light occurs from the laser interacting with an oscillating dipole moment of a vibrating molecule which alters the frequency of the light source. Therefore, samples must have a change in polarizability to be Raman active. This altered frequency gets dispersed with a gradient and is detected with a charged coupled device (CCD). The CCD converts the photons to a charge which is turned into a readable spectrum using bands. The spectra created are unique to the analyzed molecule, making Raman a confirmatory technique according to SWGDRUG, providing structural information.

There are many advantages to Raman spectroscopy. Raman spectroscopy is selective and non-destructive. SWGDRUG considers Raman a category A technique, providing structural information about a molecule. [44] Raman can analyze substances through clear containers with little to no sample prep. Clear containers, like plastic baggies, are commonly seen in forensic laboratories to hold drugs. One advantage of Raman versus other vibrational spectroscopic methods like infrared (IR) is that water is inactive and can be used as a solvent. Raman can also be portable and taken into the field for on-site analysis.

No analytical technique is perfect, and there are also limitations to Raman spectroscopy. Raman scattered light accounts for roughly 1 in $10^6$ scattered lights, making Raman scattering weak compared to other spectroscopic techniques.[45] Fluorescence is also an issue. Fluorescence occurs when photons get excited to a higher energy state. Light is emitted as fluorescence when the excited molecule returns to its lower energy state. This light will create broader bands across the spectrum, hiding the Raman scattering. Colored samples can be challenging to analyze. Darker samples can get burned, and brighter colors can increase the fluorescence. One of the main issues with Raman is mixtures. Bands from multiple components convolute the Raman spectrum, which makes data interpretation difficult. Mixtures will be addressed further in **Part III: Improving Raman Spectroscopy Using Machine Learning.**

*1.5 – Portable Raman Instrumentation*

Portable Raman systems have different features that affect their ability to identify components. One feature is the laser wavelength. The laser's wavelength will affect the laser's energy, as shown in **Equation 4**. Shorter wavelengths, like 532 or 785 nm, have more energy than longer wavelengths, like 1064 nm. More energy will increase the intensity of the Raman signal. However, more energy will also increase the risk of fluorescence, which blocks the Raman signal. [46] Increasing the area size improves the intensity of the signal without losing resolution.

**Equation 4:** $$E = \frac{hc}{\lambda}$$

Where E is photons energy, h is Planck's constant (6.626 x $10^{-34}$ J*s), c is the speed of light (3 x $10^8$ m/s), and $\lambda$ is the photon wavelength.

Instruments can also have different optical devices that can influence the collected spectra. The laser aperture size can influence the spectrum. [47] Smaller apertures allow for high resolution, but the signal is weak and may miss the target compound. A larger aperture can increase the sample area; However, this will decrease the resolution of the spectrum. The Mira has an orbital raster scan (ORS) that addresses this aperture size problem, shown in **Figure 13**. [48] The ORS uses a moveable mirror instead of a fixed mirror in other models, like the TacticID. The movable mirror increases the sample area of a tightly focused laser beam.
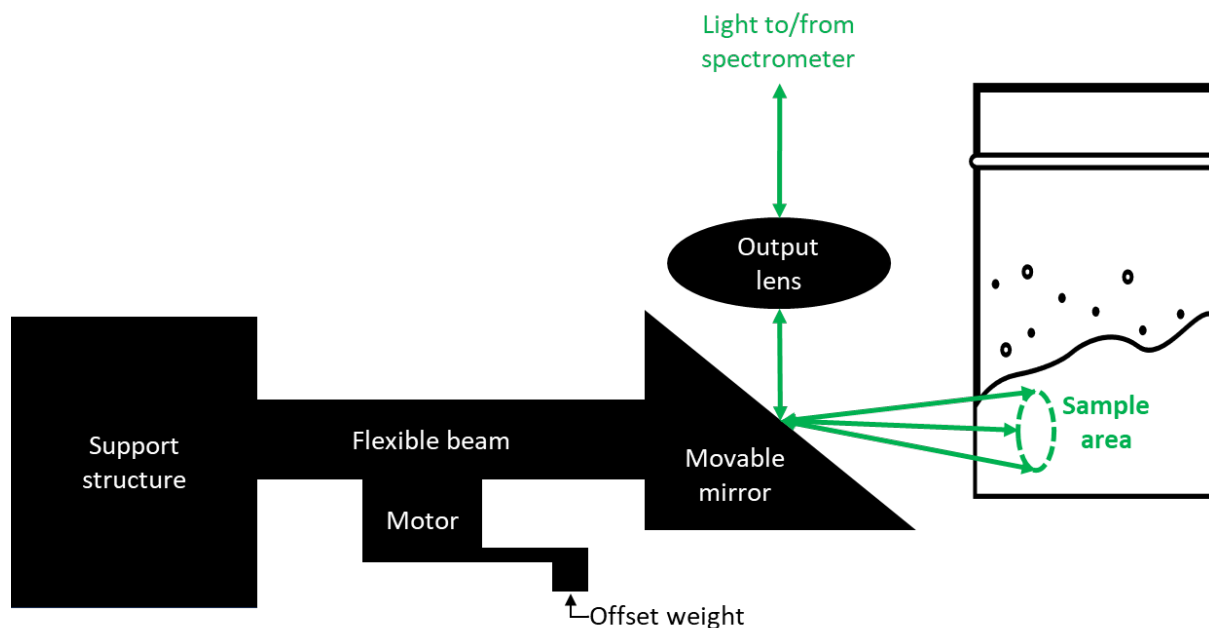


**Figure 13:** Diagram of the ORS optical element. Adapted from [47]

Another feature that affects their ability is the software used for data analysis. Some software can consider the possibility of mixtures, which will improve the identification of complex samples. One example includes the software on TacticID. The software on TacticID is called the TacticID operating system (TOS). This software uses a spectral similarity score called Hit Quality Index (HQI). HQI is considered a correlation algorithm and uses dot products to calculate the similarity between the known library spectrum and an unknown test spectrum, as shown in **Equation 5**. [49] HQI divides the squared dot product from the two spectra divided by the dot product of the library spectrum and the dot product of the test spectrum. Scores closer to 100 % demonstrate a high spectral correlation, and scores closer to 0 % indicate a low correlation. In instances where mixtures are analyzed, the HQI could be below the instrument's threshold set by the user due to the presence of multiple bands for each compound being present in a single spectrum. In such cases, the mixture analysis software provides a spectral weight is used. The spectral weight provides a percent contribution of each compound to the overall observed spectrum.

**Equation 5:** $$HQI = \frac{(Library * Test)^2}{(Library * Library)(Test * Test)}$$

However, other software, like the BWID (*v 2.04*) on the iRaman Prime, can only compare the collected samples to the pure library spectra using HQI and does not consider mixtures. [50] The iRaman prime has other software that is beneficial for a forensic laboratory. One software is the BWIQ, which is a multivariate analysis software package. The BWIQ (*v 4.1.4*) allows for regression classification modeling. [51] Regression is typically used for quantitative analysis, while classification is used for identification. However, their classification models only allow up to six different classes. [52] Some of the multivariate options include Partial Least Squares Regression (PLS), Principal Component Analysis (PCA), and Discriminant Analysis with Support Vector Machine (SVM). Another software for iRaman Prime is the BWSpec (*v. 4.15_3*), which is used for data acquisition and basic data manipulation. [53] This software allows for easy parameter manipulation, like the integration time and laser power, which allows the analyst to get spectra with better intensity and resolution. BWSpec also allows for simple data processing, like smoothing and baseline correction.

*1.6 – Cosine Similarity*

The software in this section used HQI to compare the questioned spectrum to the library spectrum. HQI has been used in other Raman analysis publications. [54–57] However, several

other spectral similarity scores can be used to compare two spectra, including PCA [58–60], PLS [61,62], SMV [63,64], and cosine similarity [64–68]. This thesis also used cosine similarity as a comparison technique. Like HQI, Cosine similarity is a correlation metric that compares two vectors. In Raman spectroscopy, these vectors comprise the spectral intensity values for the known library and the questioned spectrum. **Equation 6** shows the formula for cosine similarity where x and y are the vectors of spectra.

**Equation 6:** $$\cos\theta = \frac{\sum_{i=1}^{n} x_i * y_i}{\sqrt{\sum_{i=1}^{n} x_i^2}\sqrt{\sum_{i=1}^{n} y_i^2}}$$

A paper by Carey et al. l. explains cosine similarity scores. [68] High scores are given to two spectra with matching wavelengths with high intensities. However, if one of the bands has a low intensity at a particular wavelength, the wavelength will barely contribute to the overall similarity score. This correlation can be seen in **Figure 14**. Cosine similarity is intensity invariant. The paper did not provide the overall similarity score for this comparison.
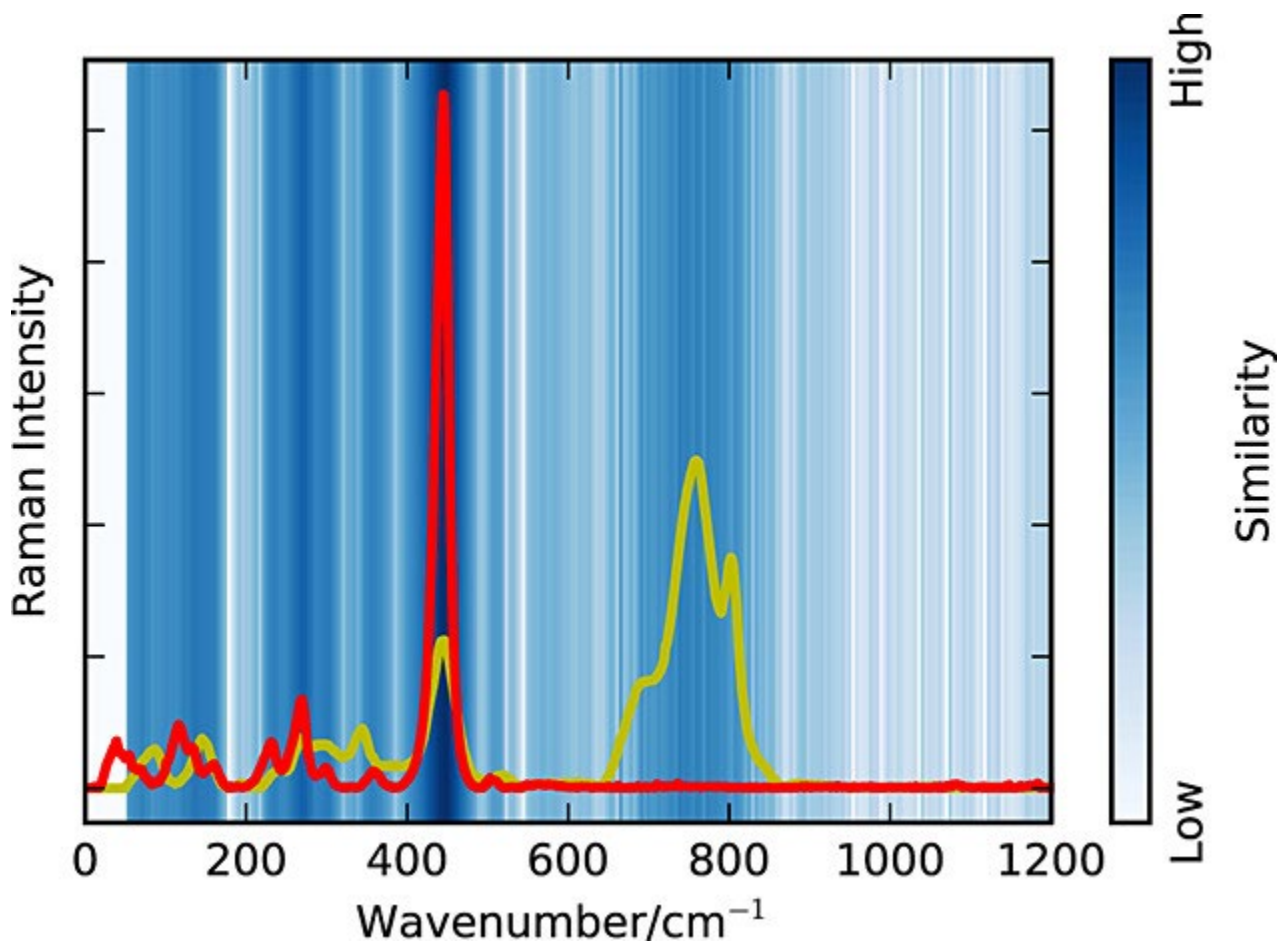
**Figure 14:** Illustration of cosine similarity from Cary et al. [68] Two overlaid spectra of chiolite (red) and cabalzarite (yellow). The dark blue area around 450 cm$^{-1}$ accounted for roughly 85 % of the overall similarity score.

Cosine similarity is also easy to explain, with a resulting score identifying the similarity between two compounds. Scores closer to 100 % demonstrate a high spectral correlation, and scores closer to 0 % indicate a low correlation. HQI and cosine similarity uses the dot product of the two spectra to determine the similarity. However, cosine similarity also considers the length of the spectra, calculating the similarity regardless of the size by dividing the dot product by the Euclidian norms or the magnitude of each vector. One limitation to cosine similarity is that the magnitude of the vectors is not considered, just the directionality. Another limitation between cosine similarity and HQI is that it does not consider mixtures. Therefore, in a complex spectrum where bands from multiple compounds are present, these similarity metrics do not consider bands from multiple compounds, which can, in turn, lower the similarity even if the compound is present.

*1.7 – Purpose*

This section compared three portable Raman instruments to assess their accuracy in identifying simulated street samples created using binary mixtures. These 42 binary mixtures are related to mixtures found in clandestine methamphetamine laboratories. The three instruments include: TacticID, Mira XTR DS (from now on referred to as Mira), and iRaman Prime (from now on referred to as iRaman). These instruments were chosen based on their different properties, as shown in **Table 2**. If available, the software will be compared by their ability to detect both compounds in the binary mixtures using HQI and the default mixture analysis. The TacticID and Mira used the default HQI threshold of 0.85. The iRaman's HQI threshold was lowered to 0.70 because it does not have a mixture analysis function. Their ability will be determined by the number of compounds identified, divided by the total number of expected compounds, using **Equation 6** on page 29.

**Table 2:** Instrument specification for the TacticID, Mira, and the iRaman.

| Instrument | TacticID GP | Mira XTR DS | iRaman Prime |
|---|---|---|---|
| Laser | 785 nm | 785 nm | 1064 nm |
| Manufacturer | B&W Tek | Metrohm | B&W Tek |
| Software | TacticID operating system (TOS) | MIRA Cal | BWID BWIQ BWSpec |
| Type | handheld | handheld | portable |
| Standard | Polystyrene | Polystyrene | Polystyrene |
| HQI threshold | 85 % | 85 % | 75 % |
| **Specifications** | | | |
| ORS | | ✓ | |
| Manufacture library | ✓ | ✓ | ✓ (BWID) |
| In-house library | ✓ | * | ✓(BWID) |
| Mixture analysis function | ✓ | ✓ | |
| Multivariate analysis | | | ✓ (BWIQ) |
| Data processing | | | ✓ (BWIQ) |
| Fluorescence rejection | | ✓ | |
| SERS attachment | ✓ | ✓ | |
| near detection | ✓ | ✓ | ✓ |
| far detection | | ✓ | |

The binary mixtures will also be identified using an in-house cosine similarity algorithm to produce a numerical value for the comparison of the spectra. Cosine similarity will allow the spectra from each instrument to be compared without the influence of the software. The scores from each instrument will provide better insight into the collected spectra' quality. The data from all three instruments will be processed using the same cosine similarity written in Python, with the same parameters. By using the same parameters, the identification of the compounds will only be determined by the quality of the spectra focusing on the laser wavelength and the ORS for the Mira. The top three reported compounds from the cosine similarity algorithm were selected for data analysis. No threshold was used for the cosine similarity, but the lowest score for each instrument in the top three results was 79 % for the iRaman, 75 % for the TacticID, and 74 % for the Mira.
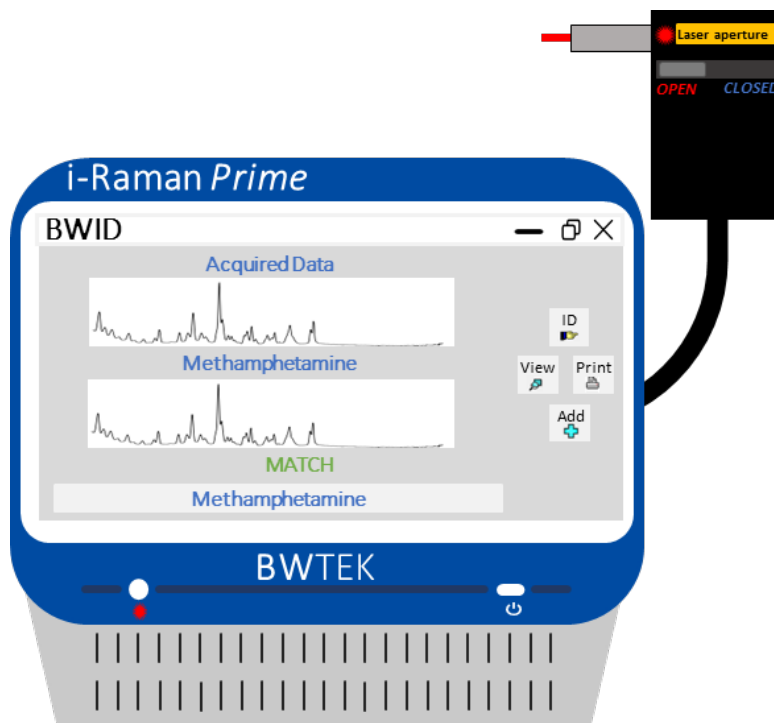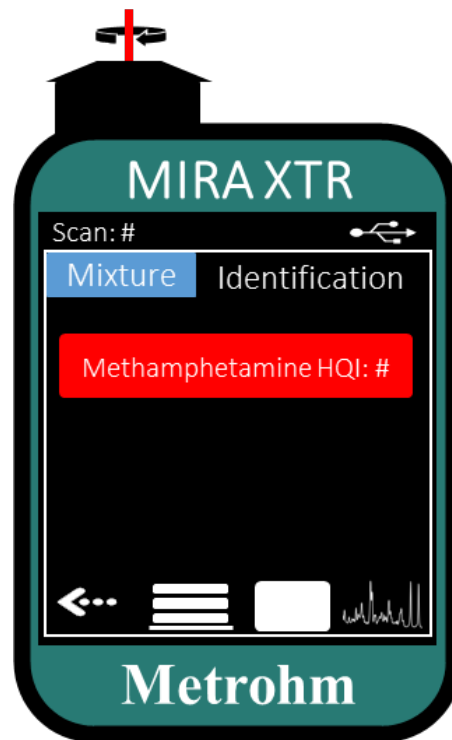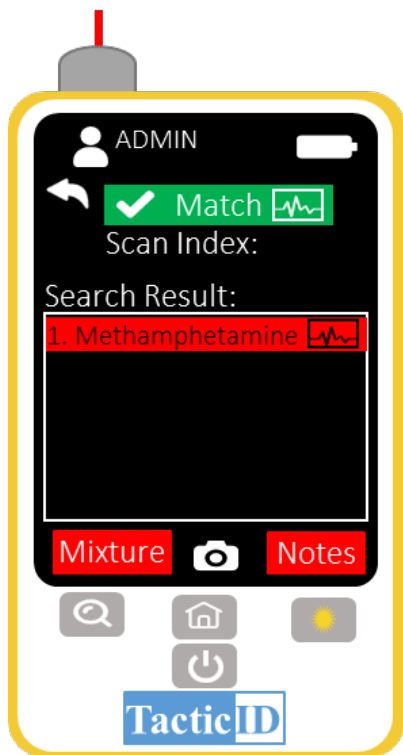
# Chapter 2: Materials, Methods, and Experimental Design

*2.1 – Materials*

Methamphetamine HCl, amphetamine sulfate, ephedrine HCl, and pseudoephedrine were purchased from Millipore-Sigma (St. Louis, MO). Caffeine was purchased from JT Baker (Phillipsburg, NJ), and acetaminophen was purchased from Millipore-Sigma (St. Louis, MO).
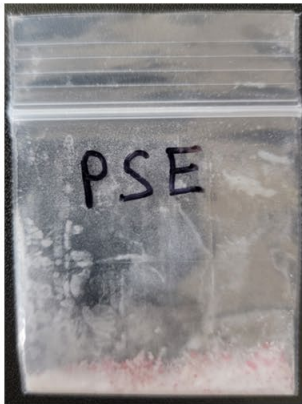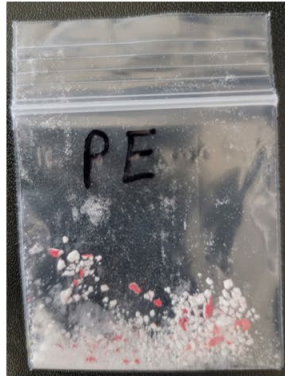
The six standards were used to make 42 mixtures in various ratios, as shown in **Table 3.** All standards and mixtures were analyzed through a plastic bag and in triplicate to account for variability in the sample.

**Table 3:** List of binary mixtures created.

| Mixture | Mixture Ratio | | | |
|---|---|---|---|---|
| | 1:4 | 1:7 | 1:10 | 1:20 |
| Methamphetamine : Pseudoephedrine | ✓ | ✓ | ✓ | ✓ |
| Methamphetamine : Ephedrine | ✓ | ✓ | ✓ | ✓ |
| Methamphetamine : Amphetamine | ✓ | ✓ | | |
| Methamphetamine : Acetaminophen | ✓ | ✓ | ✓ | ✓ |
| Methamphetamine : Caffeine | ✓ | ✓ | ✓ | ✓ |
| Pseudoephedrine : Acetaminophen | ✓ | ✓ | ✓ | ✓ |
| Pseudoephedrine : Caffeine | ✓ | ✓ | ✓ | ✓ |
| Ephedrine : Acetaminophen | ✓ | ✓ | ✓ | ✓ |
| Ephedrine : Caffeine | ✓ | ✓ | ✓ | ✓ |
| Amphetamine : Acetaminophen | ✓ | ✓ | ✓ | ✓ |
| Amphetamine : Caffeine | ✓ | ✓ | ✓ | ✓ |

A pseudoephedrine pharmaceutical behind-the-counter was obtained from a local retailer (Kroger, Inc),  and an over-the-counter phenylephrine HCl from SUDAFED[PE] was also purchased from a retailer pharmacy and analyzed with two portable systems, TacticID and iRaman. The Mira instrument was loaned by Metrohm USA for a very short time, and due to time constraints, these specimens were not measured. One pill from the two pharmaceutical medicines was analyzed in triplicate using three methods. The first method consisted in analyzing the outer coating. The second method was splitting the pill and analyzing the white inner content. The last method consisted in crushing the pill into a powder for analysis through a plastic baggie, like the other binary mixtures created in-house. The different methods for the two pills can be seen in **Table 4**. Due to the red color, Raman spectra were collected at three different laser percentages (energies) to get the best analyte response. The results were compared for both instruments to see how the collection method and the laser wavelength affected the detection of the drugs.

**Table 4:** Pictures demonstrating the different methods of detection for the Pills. Method one is analyzing the outer portion. Method two is analyzing the white inner portion. Method three is crushing the pill into a powder.



*2.2 – Instrumentation*

Three Raman instruments were used. TacticID GP portable 785 nm laser and an iRaman Prime portable 1064 nm laser Raman instruments were from B&W Tek (Newark, DE). A Mira XTR DS 785 nm was from Metrohm USA (Riverview, FL). The three instruments will be called TacticID, Mira, and iRaman. All instruments used hit-quality-index (HQI) to determine the spectral similarities. The Mira and TacticID also used a mixture analysis function on the instrument. All instruments used a compatible polystyrene reference material to ensure each instrument worked properly before any measurements.

2.2.1 – TacticID

The TacticID 785 nm laser unit was operated on N-mode with a laser power of 90 % and a scan delay of 0 sec. The spectral range was from 176 cm$^{-1}$ – 2500 cm$^{-1}$ with a spectral resolution of 9 cm$^{-1}$. The spectra were compared to the instruments store library and an in-house library created with the same instrument. The TacticID's HQI threshold was set to the manufacturer's

recommended 85 %. The point-and-shoot adapter was used for collection. The mixtures were also analyzed via the mixture analysis option, which provides the spectral weight of the compounds identified. The laser power was lowered to 60 % for the pharmaceutical pills because at this energy power, the tested specimen showed limited fluorescence and greater signal for the target molecule.

2.2.2 – Mira

The Mira 785 nm laser unit was operated using the instrument's default procedure as recommended by the product manual. [69] The spectral range was from $400 \text{ cm}^{-1} - 2300 \text{ cm}^{-1}$ with a spectral resolution of $8 - 10 \text{ cm}^{-1}$. The spectra were compared to the instrument's stored library. Mira's default HQI threshold was 85 %. The intelligent Universal Attachment (iUA) set to the second dot was used for data collection. The mixtures were also analyzed via the mixture analysis option, which provides the spectral weight of the compounds identified.

2.2.3 – iRaman

The iRaman 1064 nm laser unit was operated using the BWID software (*v 2.04*) to get the identification of the samples using library search and HQI. Spectra were compared to the instruments store library and an in-house library created with the same instrument. The laser power was set to 90 %, and a scan delay of 0 sec. The spectral range was $200 \text{ cm}^{-1} - 2500 \text{ cm}^{-1}$ with a spectral resolution of $2 \text{ cm}^{-1}$. The same HQI threshold for Mira was used for the iRaman, 75 %. The distance regulator was used for collection. The BWID software on the iRaman instrument did not have an additional option for mixture analysis. Therefore, only the HQI values were used. The laser at 90 % power provided the best signal for pharmaceutical pills.

*2.3 – Data Analysis*

2.3.1 – Instrument Library

The results of each replicate were combined into one set of overall results to account for sample variation. A percent identification was calculated using **Equation 7** based on precision. Only the true positives were included in this calculation. However, the false positives were addressed in the results as well. Percent identification is a simple way to identify the percentage of compounds correctly identified. A higher percent identification means that more compounds were correctly identified. A lower percent identification shows that the instrument could not identify as many present compounds. The results were based on the respective instrument parameters. The TacticID and the Mira threshold were 85 %. The iRaman had a threshold of 75 %. The mixture analysis function for the Mira and TacticID enables the instrument to identify

multiple compounds when the threshold is lower than the HQI. The number of hits, or high spectrally correlated compounds, was set to 5, and the ratio threshold was set to 15 %. These mixture parameters are the default parameters of the instruments.

$$\textbf{Equation 7:} \qquad \text{Percent Identification} = \frac{\text{\# of compounds identified}}{\text{\# of expected compounds}} * 100$$

The mixtures were created at different ratios to simulate authentic samples. The effect of the ratios was identified by separating the mixtures into their respective groups and counting the number of mixtures where either 0, 1, or 2 components were identified.

2.3.2 – Cosine Similarity

Despite the instruments belonging to the same core company (BWTek), the software capabilities in handling and processing the data (e.g., HQI threshold, mixture analysis functions) were different. Therefore, more attention was given to the spectral quality using similar data processing algorithms. Cosine similarity was performed using each instrument collected spectra. Scores closer to 100 % demonstrate a high spectral correlation, and scores closer to 0 % indicate a low correlation. Cosine similarity was chosen over HQI because cosine similarity considers the magnitude of the vectors, while HQI does not. One of the limitations of these similarity scores is that neither considers complex samples where the bands from multiple components convolute the Raman spectrum. This limitation will be addressed in the next section using machine learning.

**Figure 15** shows the data methodology for cosine similarity. The cosine similarity equation (**Equation 6**) divides the dot product of spectra A and spectra B by the Euclidian norm of the two vectors. The collected spectra were truncated to 1,800 cm$^{-1}$. The truncation was utilized to remove the noise regions that did not contribute to any critical bands. Due to the limited number of spectra acquired (n= xyz), data augmentation was performed, resulting in 9,000 spectra for each instrument. This was done by generating 500 random numbers between 0 and 1 using *numpy v* 1.23.3 in Python. Each spectrum was multiplied by every random number, creating new spectra with intensity variations for each compound. Increasing the sample size and adding intensity variations to the spectra can improve similarity scores when low-intensity Raman bands are observed due to interferences from components in mixtures. The cosine similarity algorithm was coded in Python using the cosine similarity function in *sklearn v* 1.1.2. The algorithm compares all compounds in the augmented dataset pairwise and produces the top 3 results based on the highest cosine score. The replicates were combined to account for variation in the mixtures, and the percent identification was calculated for the cosine results.
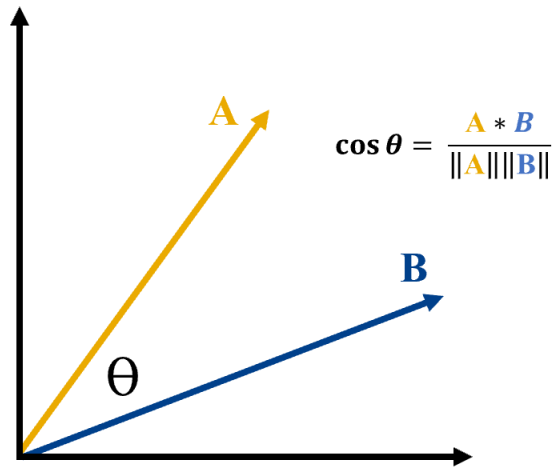
**Figure 15:** Data analysis methodology for cosine similarity. Cosine similarity is the similarity between two vectors.
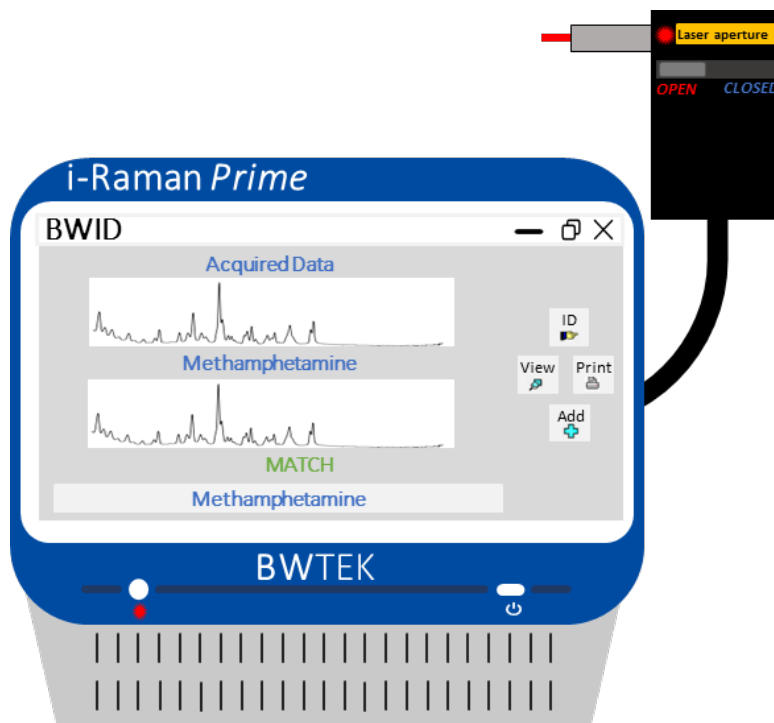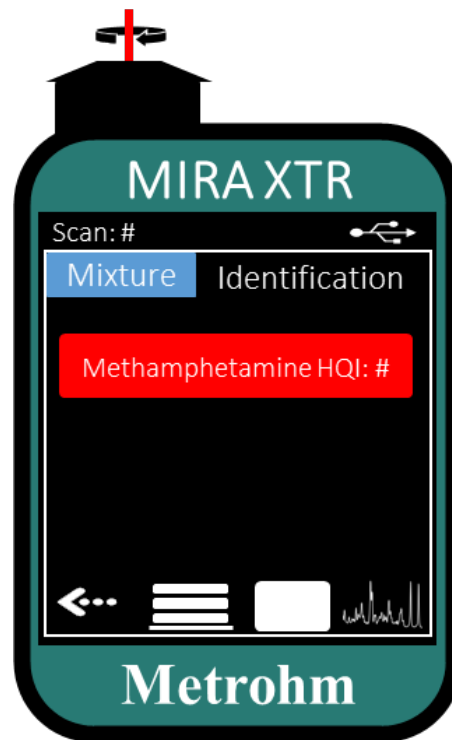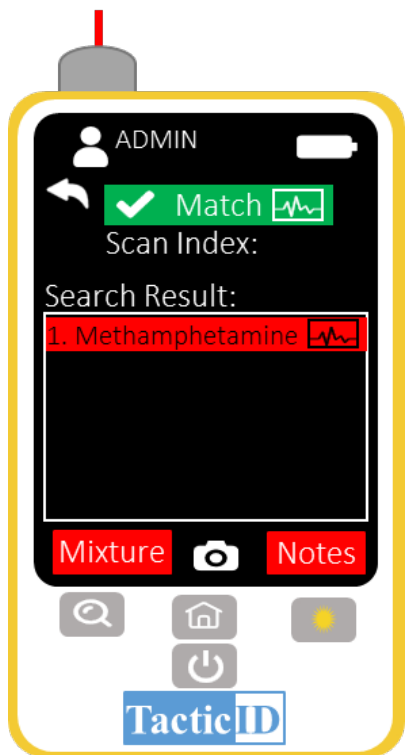
# Chapter 3: Results and Discussion

*3.1 – Raman Band Characterization*

**Figure 16** - **Figure 21** shows each standard spectrum of the three instruments. Each figure has a table that has the most intense bands. [15,70–74]. The ranges are different for each instrument, but the bands present are consistent between the different instruments. Many of the more intense bands are consistent for amphetamine, methamphetamine, ephedrine, and pseudoephedrine, due to their similar structure. However, all standards are differentiable, and the bands can differentiate the standards are discussed later.
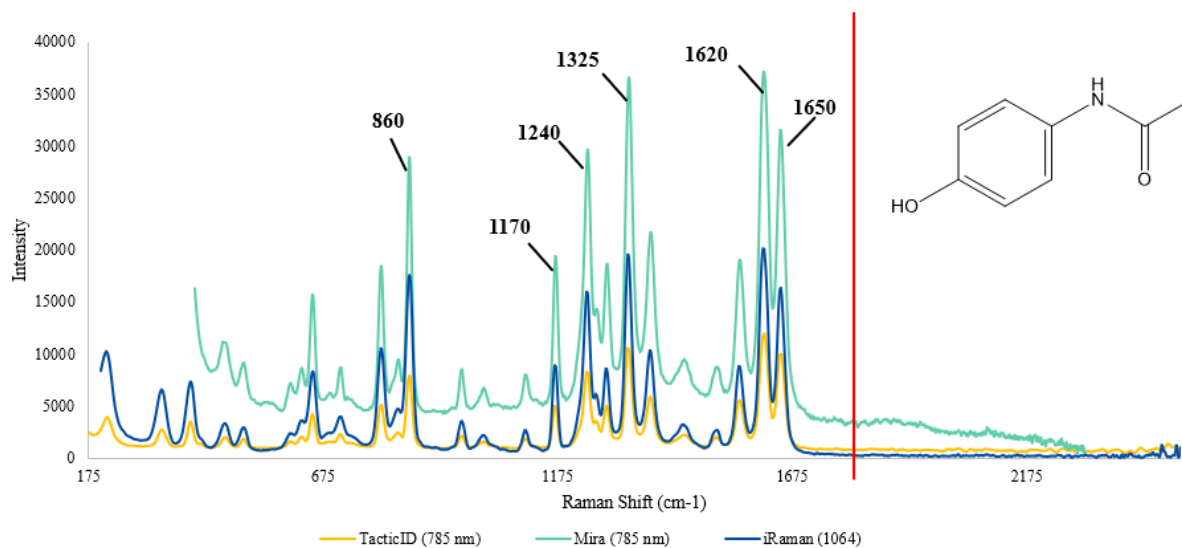


| Raman Shift | Functional group | Raman Shift | Functional group |
|---|---|---|---|
| 860 cm$^{-1}$ | ν C-C | 1325 cm$^{-1}$ | δ C-OH |
| 1170 cm$^{-1}$ | ν C-O | 1620 cm$^{-1}$ | δ Aromatic ring chain |
| 1240 cm$^{-1}$ | ν C-N | 1650cm$^{-1}$ | ν C=O |

**Figure 16:** Comparison of the Raman spectra of each of the three Raman instruments for acetaminophen. The red line shows the cutoff used for the cosine similarity. Some of the most intense Raman bands have been characterized in the table below the spectra. ν = stretching, δ = bending. [72]

**Figure 17:** Comparison of the Raman spectra of each of the three Raman instruments for amphetamine sulfate. The red line shows the cutoff used for the cosine similarity. Some of the most intense Raman bands have been characterized in the table below the spectra. $v$ = vibration, $\delta$ = bending, p = rocking, s = symmetric, IPL = in plane. [74]
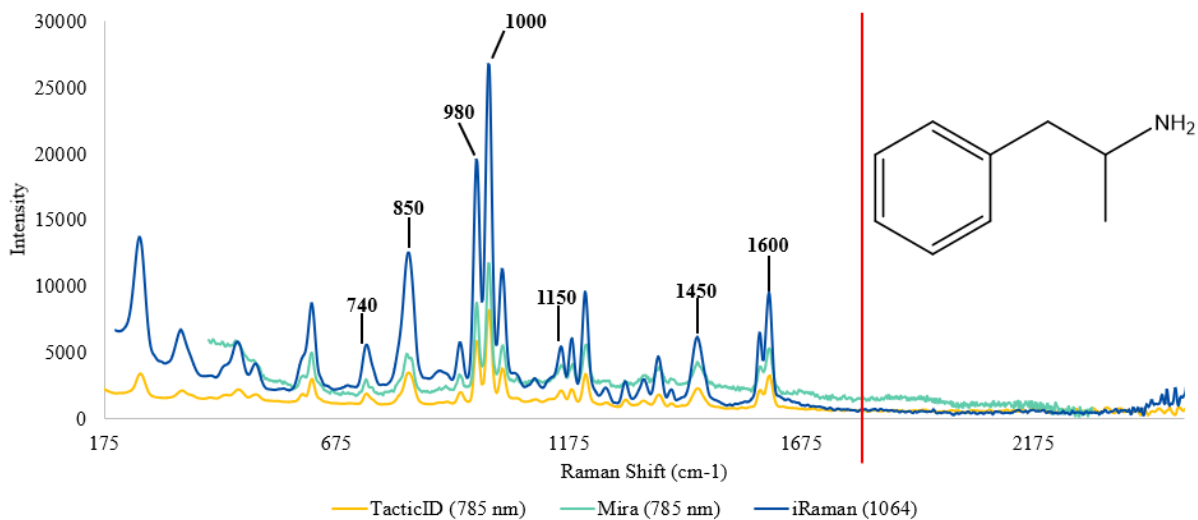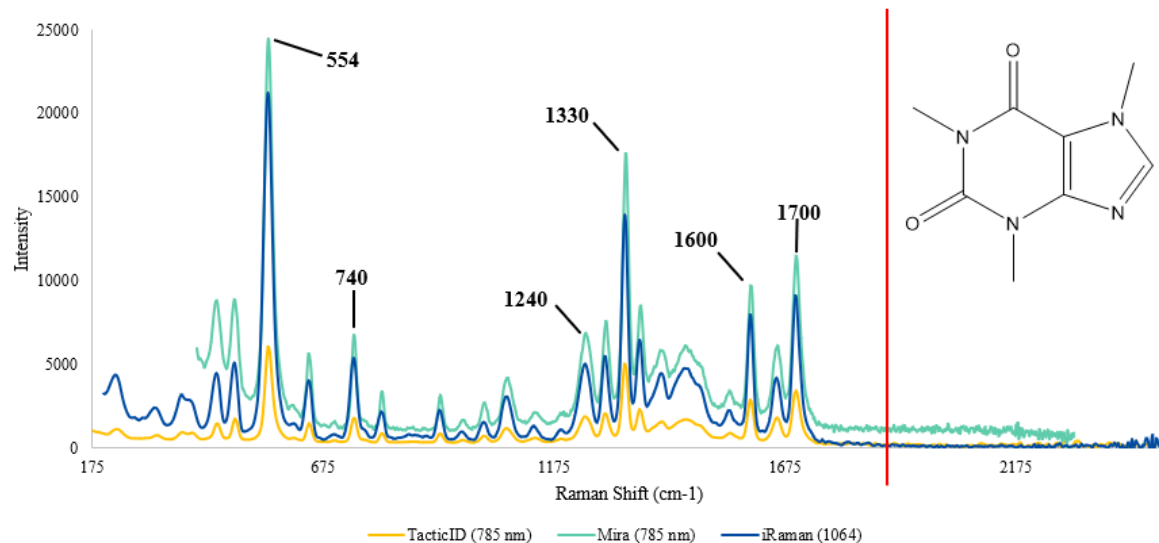
| Raman Shift | Functional group | Raman Shift | Functional group |
|---|---|---|---|
| 850 cm$^{-1}$ | $v$ CC , $\delta_{IPL}$ CH | 1150 cm$^{-1}$ | $v$ C-N (aliphatic amines) |
| 980 cm$^{-1}$ | $v_s$ -SO$_4$ | 1450 cm$^{-1}$ | $\delta_{IPL}$ Aromatic C-H |
| 1000 cm$^{-1}$ | $v_{IPL}$ Aromatic CC | 1600 cm$^{-1}$ | $v$ and $\delta_{IPL}$ Aromatic CC |

| Raman shift | Functional group | Raman shift | Functional group |
|---|---|---|---|
| 740 cm$^{-1}$ | δ(pyrimidine, imidazole ring) + δ(CH3) + ρ(CH3) | 1330 cm$^{-1}$ | ν(imidazole ring) |
| 1240 cm$^{-1}$ | δ(CH−N) + ρ(CH₃) | 1600 cm$^{-1}$ | ν(C=C) + ν(CN) + δ(CH3) |
| 554 cm$^{-1}$ | δ(pyrimidine ring) + δ(CNC) + ρ(CH3) | 1700 cm$^{-1}$ | ν(C=O) in phase |

**Figure 18:** Comparison of the Raman spectra of each of the three Raman instruments for caffeine. The red line shows the cutoff used for the cosine similarity. Some of the most intense Raman bands have been characterized in the table below the spectra. ν = vibration, δ = bending, p = rocking [75]
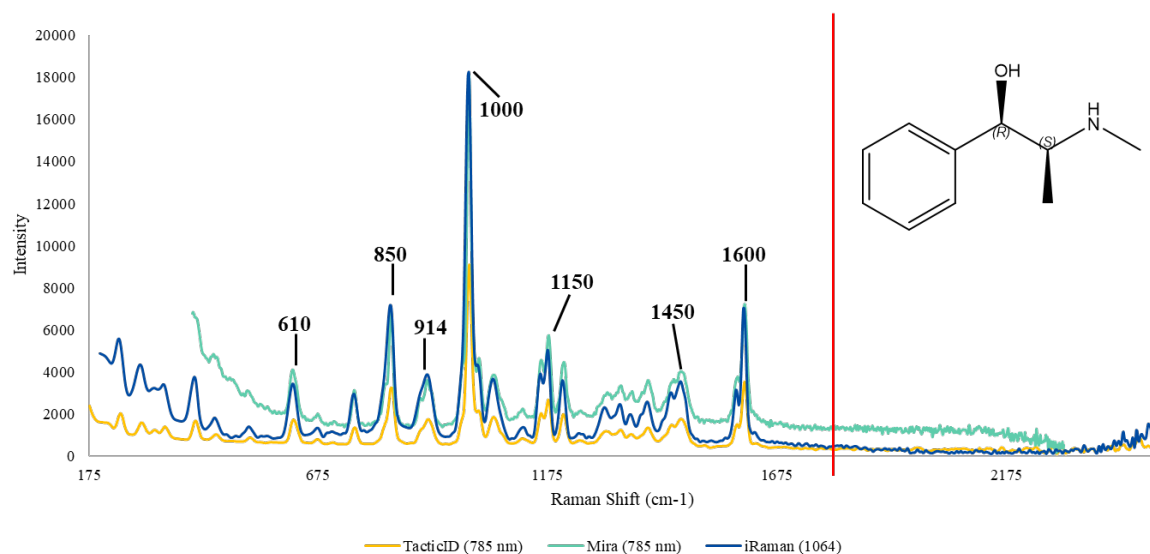
| Raman Shift | Functional group | Raman Shift | Functional group |
|---|---|---|---|
| 610 cm$^{-1}$ | δ aromatic ring | 1150 cm$^{-1}$ | ν C-N (aliphatic amines) |
| 850 cm$^{-1}$ | ν CC , δ$_{IPL}$ CH | 1450 cm$^{-1}$ | δ$_{IPL}$ Aromatic C-H |
| 1000 cm$^{-1}$ | ν$_{IPL}$ Aromatic CC | 1600 cm$^{-1}$ | ν and δ$_{IPL}$ Aromatic CC |

**Figure 19:** Comparison of the Raman spectra of each of the three Raman instruments for ephedrine HCl. The red line shows the cutoff used for the cosine similarity. Some of the most intense Raman bands have been characterized in the table below the spectra. ν = vibration, δ = bending, p = rocking [72,74]

**Figure 20:** Comparison of the Raman spectra of each of the three Raman instruments for methamphetamine HCl. The red line shows the cutoff used for the cosine similarity. Some of the most intense Raman bands have been characterized in the table below the spectra. ν = vibration, δ = bending, IPL = in plane, p = rocking. [72,74,76]
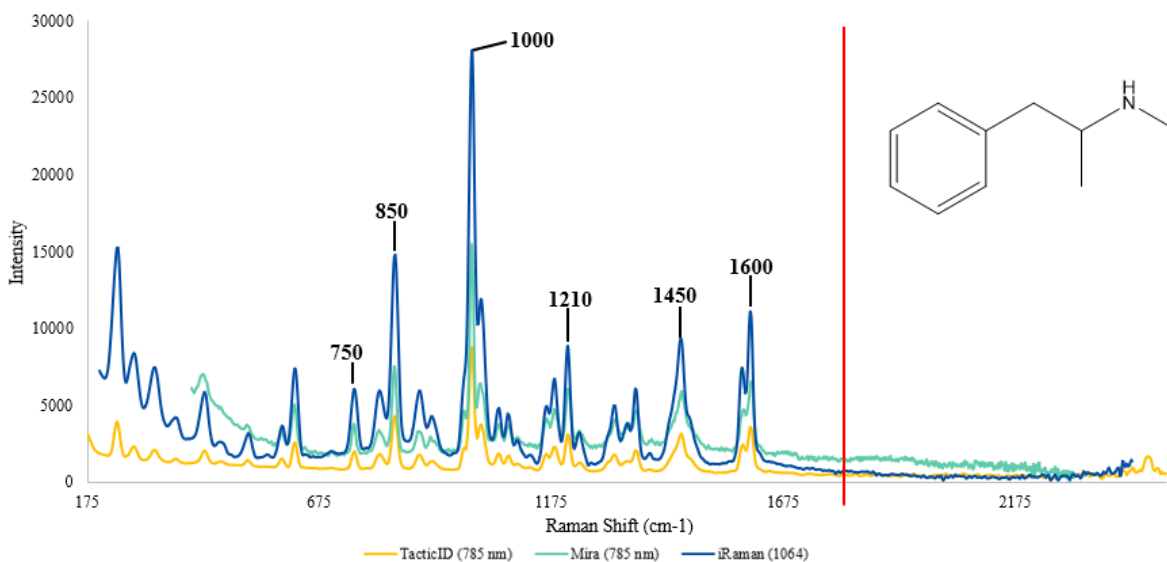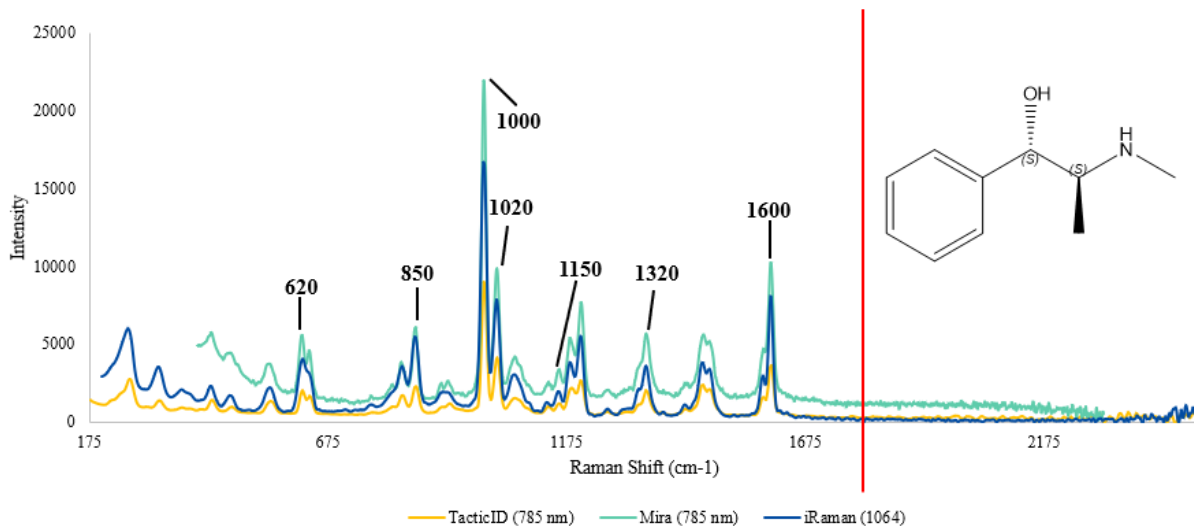
| Raman Shift | Functional group | Raman Shift | Functional group |
|---|---|---|---|
| 750 cm$^{-1}$ | δ NH | 1210 cm$^{-1}$ | ν C-N (aliphatic amines) |
| 850 cm$^{-1}$ | ν CC , δ$_{IPL}$ CH | 1450 cm$^{-1}$ | p CH$_2$, CH$_3$, NH |
| 1000 cm$^{-1}$ | ν$_{IPL}$ Aromatic CC | 1600 cm$^{-1}$ | ν and δ$_{IPL}$ Aromatic CC |

| Raman Shift | Functional group | Raman Shift | Functional group |
|---|---|---|---|
| 620 cm$^{-1}$ | δ aromatic ring | 1150 cm$^{-1}$ | ν C-N (aliphatic amines) |
| 850 cm$^{-1}$ | ν CC , δ$_{IPL}$ CH | 1320 cm$^{-1}$ | δ C-OH |
| 1000 cm$^{-1}$ | ν$_{IPL}$ Aromatic CC | 1600 cm$^{-1}$ | ν and δ$_{IPL}$ Aromatic CC |

**Figure 21:** Comparison of the Raman spectra of each of the three Raman instruments for pseudoephedrine. The red line shows the cutoff used for the cosine similarity. Some of the most intense Raman bands have been characterized in the table below the spectra. ν = stretch, δ = bending, IPL = in plane. [72,74]

Figure 16 shows the collected spectra for acetaminophen. Some crucial bands that identify acetaminophen involve the amide functional group, which is not present in the other standards, specifically the 650 cm$^{-1}$, attributed to the carbonyl stretch and 1240 cm$^{-1}$ relating to the carbon-nitrogen bond.

Figure 18 shows the Raman spectra of caffeine. The essential bands for caffeine are primarily attributed to pyrimidine and imidazole rings, including 740 cm$^{-1}$ relating to the bending of the rings, 554 cm$^{-1}$ relating to the bending of the pyrimidine ring, and 1330 cm$^{-1}$ relating to the imidazole ring stretching.

Amphetamine, methamphetamine, ephedrine, and pseudoephedrine share the highest intensity band at 1004 cm$^{-1}$, attributed to the aromatic ring. The two cutting agents, acetaminophen and caffeine, do not share this intense band. Caffeine does not contain an aromatic ring. Acetaminophen has a band around 1007 cm$^{-1}$; however, it does not have the high intensity as the

other spectra. The amphetamine sulfate has another band in this range, around 980 cm$^{-1}$. This band is from sulfate and not the amphetamine molecule.

Amphetamine and methamphetamine are structurally different on the nitrogen atom. Amphetamine is a primary amine, and methamphetamine is a secondary amine. **Figure 22** shows a comparison of amphetamine and methamphetamine. The main differences in vibrational spectroscopy of primary and secondary amines can be found in the Raman range of 3000 cm$^{-1}$ to 3500 cm$^{-1}$, the range for NH bonds. [72] Secondary amines with one NH bond have a weak band between 3500-3300 cm$^{-1}$. Primary amines with NH$_2$ result in a weak doublet between 3550-3250 cm$^{-1}$. This range is not seen in the collected Raman spectra. The 998 cm$^{-1}$ band in the amphetamine spectrum is from the sulfate. The main differences between amphetamine and methamphetamine are the less intense Raman bands. The 500 cm$^{-1}$, 942 cm$^{-1}$, and 1251 cm$^{-1}$ from the amphetamine spectrum and 522 cm$^{-1}$, 821 cm$^{-1}$, and 1300 cm$^{-1}$ (couplet) from the methamphetamine spectrum relate to the aliphatic chain stretching. The 1251 cm$^{-1}$ band is from the CC linear chain stretching of amphetamine. A shoulder on the 1450 cm$^{-1}$ band from the methamphetamine spectrum is from bending the -CH$_3$ on methamphetamine's secondary amine. [14]
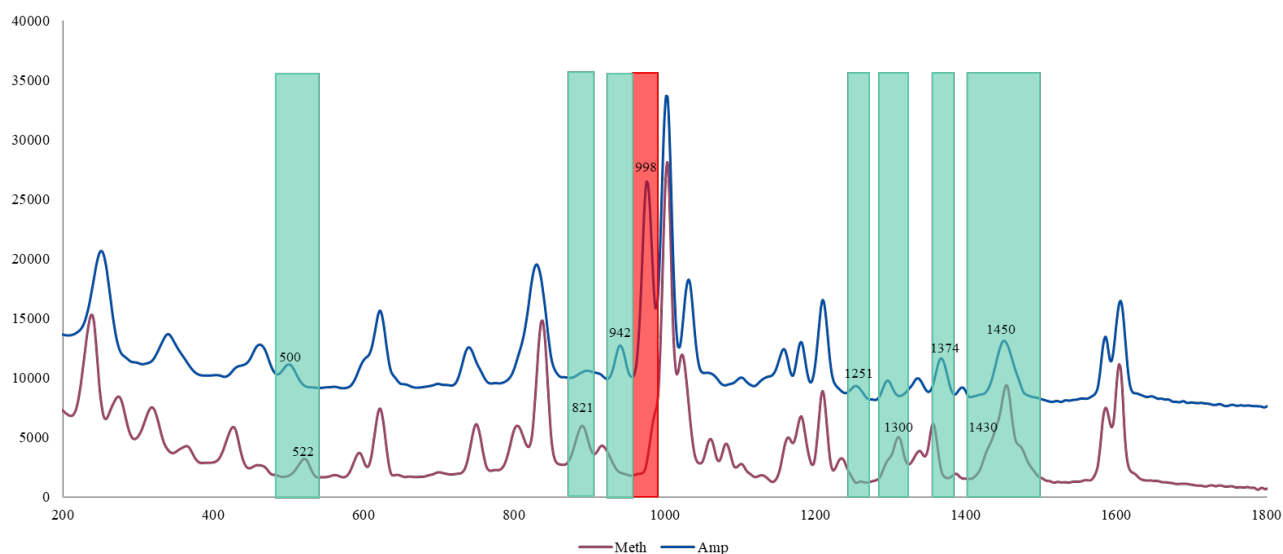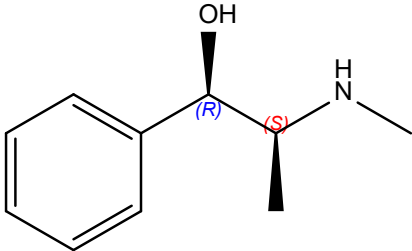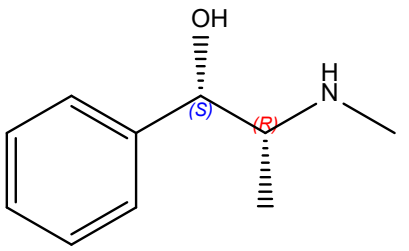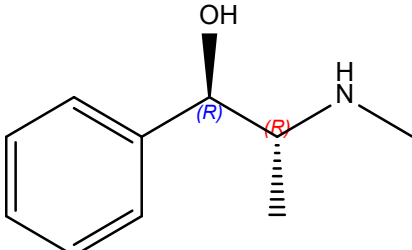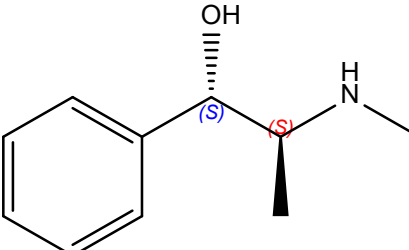


**Figure 22:** Raman Spectra Comparison of Amphetamine and methamphetamine. Some bands are highlighted to show the differences in their respective spectrum. The band highlighted in red is from the sulfate and not an amphetamine. The bands highlighted in green are differences between the two molecules.

Ephedrine and pseudoephedrine are diastereomers with two chiral centers. Therefore, they have four different spatial configurations. The diastereomers and their respective enantiomer can

be seen in **Table 5**. Ephedrine and pseudoephedrine are differentiable based on their Raman spectra, as seen in **Figure 23**. Some more apparent differences include a 750 cm$^{-1}$ band for ephedrine and 550 cm$^{-1}$ for pseudoephedrine. There are also differences in the 200-600 cm$^{-1}$ region. These differences have been seen in previous publications. [73,77] Previous publications demonstrate that the stereoscopic differences in some enantiomers allow for discrimination using Raman spectroscopy. For ephedrine and pseudoephedrine, their stereoscopic differences change the Raman shift for the CN and CO bonds, which occurs in the 200 – 700 cm$^{-1}$ region. This region can differentiate the six standards, as it is considered a fingerprint region for alkaloids [73], as demonstrated in **Figure 24**. Even though some bands, like the 630 cm$^{-1}$, are shared for some of the compounds, the combination of these bands makes each of the compounds able to be differentiated.

**Table 5:** The structure of the enantiomers of ephedrine and pseudoephedrine.

| Common name | Spatial configuration |
|---|---|
| Ephedrine |  |
| Pseudoephedrine |  |
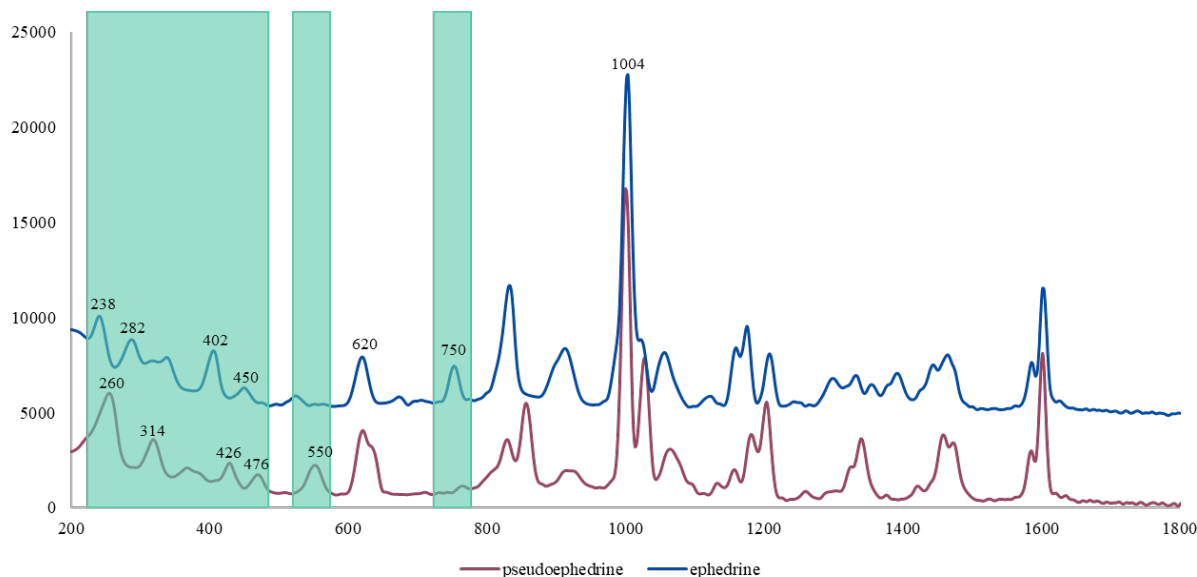
**Figure 23:** Raman spectrum comparison of ephedrine and pseudoephedrine, using the iRaman. The bands in green are consistent with previous publications. [73,77]
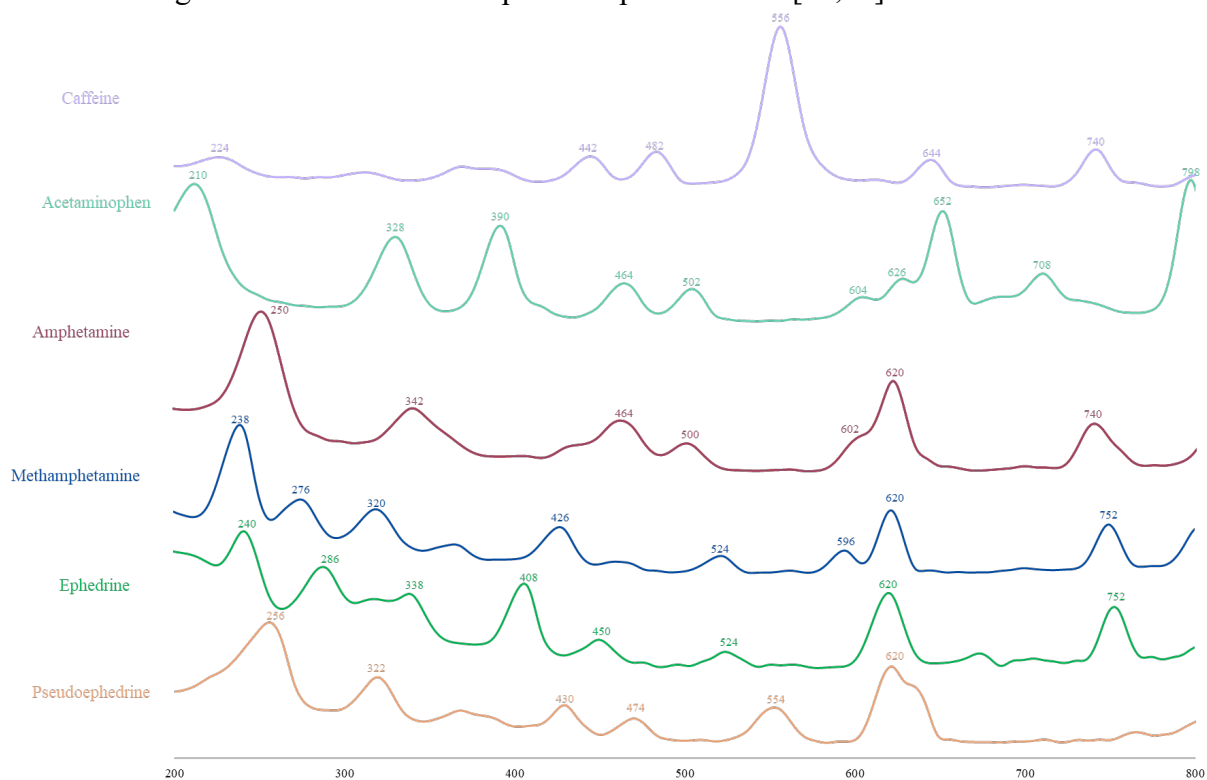


**Figure 24:** The six standards zoomed in to the $200 - 800$ cm$^{-1}$ range. While some bands are shared throughout the six spectra, none of the spectra have the same bands in the same spot.

*3.2 – TacticID*

The TacticID successfully identified the six standards used in this study without any false positives. It could also identify at least one component 100 % of the time. Fourteen of the 42

samples identified both components in the mixture; The other mixtures identified one of the components. The TacticID had an overall percent identification of 66.6 %. In all the binary mixtures, there were no false positives, and all compounds identified were present in the mixtures. Our research group has previously tested the performance of this instrument in a recent publication [54]. The more diluted the samples inhibited the TacticID's ability to identify both components in the mixture, as seen in **Figure 25**.
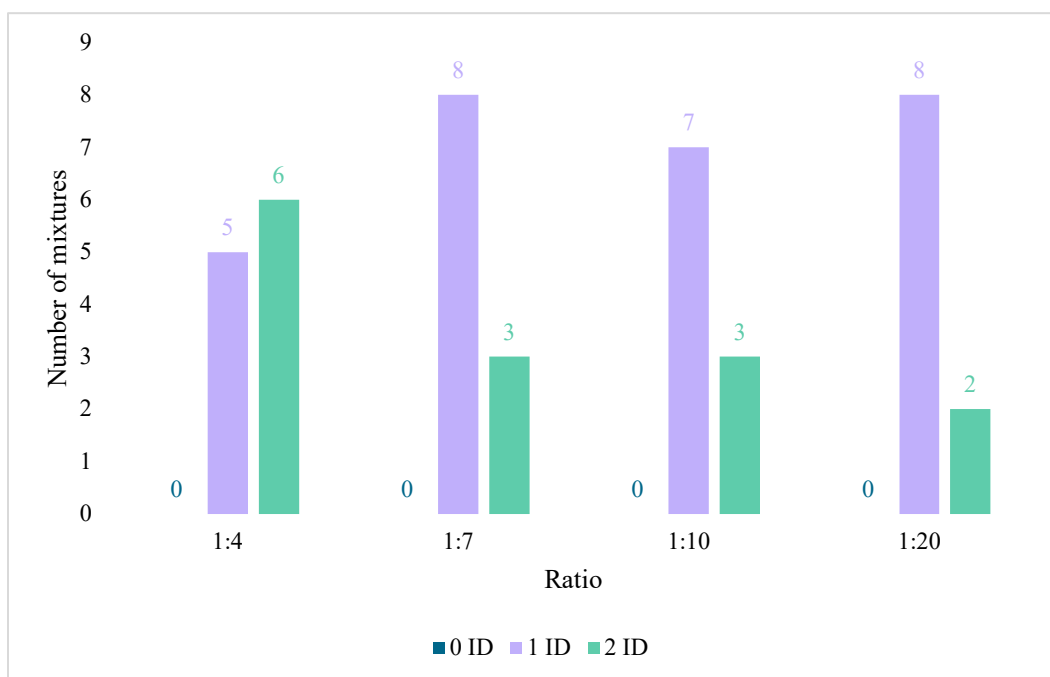


**Figure 25:** A graph showing the trend between the TacticID's ability to identify 0 (blue), 1 (green), and 2 (yellow) components in the mixture. The mixtures are separated into different groups based on the ratio. As the drug gets more diluted, the TacticID's ability to identify both compounds decreases, as seen by the decrease in the green bars from left to right.

*3.3 – Mira*

The Mira was also able to identify all six pure standards. However, the results included false positives for amphetamine sulfate, ephedrine HCl and pseudoephedrine. Like the TacticID, the Mira could identify at least one component for each mixture. Fourteen of the 42 samples identified both components in the mixture; the other mixtures identified one of the components. When only one compound was identified it was always the major component, in most cases the cutting agent. The Mira had an overall percent identification of 66.6 %. There were some issues of false positives. A total of 27 (~20%) replicates included false positive results in the mixture analysis function. Eighteen of the false positives were from the mixtures containing ephedrine HCl, where the

mixture analysis function identified the other standards instead of ephedrine. Three of the other false positives identified 1-N-methylephedrine HCl. This occurred when there was a mixture of ephedrine and methamphetamine. This can be explained with a combination of bands from the ephedrine HCl and the methamphetamine. The compound was only identified using the mixture analysis function. The rest of the false positives had less than 15% spectral weight score. None of the false positives were present for all three standards; Some were present for two replicates. The false positives are most likely due to the libraries used. There are eight libraries in the Mira XTR, including: Controlled and prescription substances; polymers, monomers and processing; organic chemicals; organic chemicals 2; illicit; inorganics and organometallics; nutraceuticals; and flavors and fragrances. Many of the false positives are from compounds not in the drug libraries. These results might be improved if an in-house library was created with the standards used at our lab and by optimizing and validating the method, like our group did for the TacticID. [54] The same trend was seen with Mira's results in **Figure 26**.
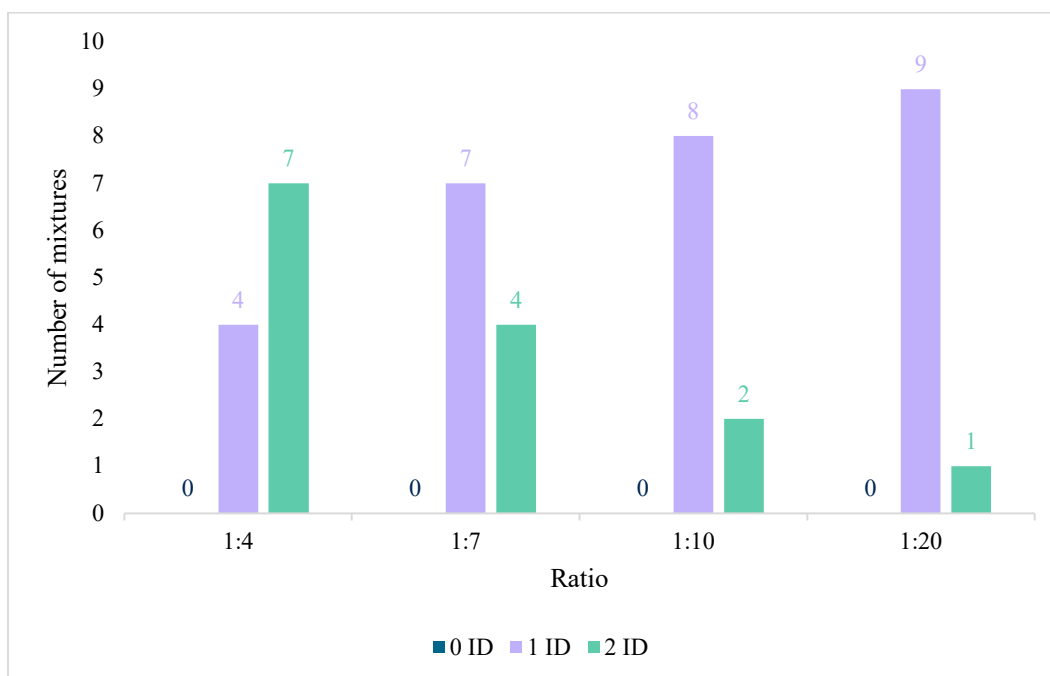


**Figure 26:** A graph showing the trend between the Mira's ability to identify 0 (blue), 1 (green), and 2 (yellow) components in the mixture. The mixtures are separated into different groups based on the ratio. As the drug gets more diluted, Mira's ability to identify both compounds decreases, as seen by the decrease in the green bars from left to right.

*3.4 – iRaman*

The BWID is the only software that can identify compounds using a library for the iRaman instrument. The BWID does not have a function to analyze complex samples. All the six pure standards were correctly identified with no false positives. Only three of the 42 samples identified both components in the mixture. These instances were due to the positioning of the laser rather than the BWID software. An example can be seen in **Figure 27**. The first and third spectra obtained when measuring a 1:4 ratio of methamphetamine and acetaminophen were identified as acetaminophen, with HQI of 99.4 and 99.6. However, the second replicate was identified as methamphetamine with an HQI of 98.2. When the individual results were combined, both components were identified using the threshold of 75. The iRaman had an overall percent identification of 53.6 %. There were no false positives identified for the binary mixtures. All of the compounds identified were present in the mixtures. **Figure 28** shows the effect of the ratio on the instrument's ability to detect both components. The more diluted samples, like the 1:10 and 1:20, could not identify both compounds.
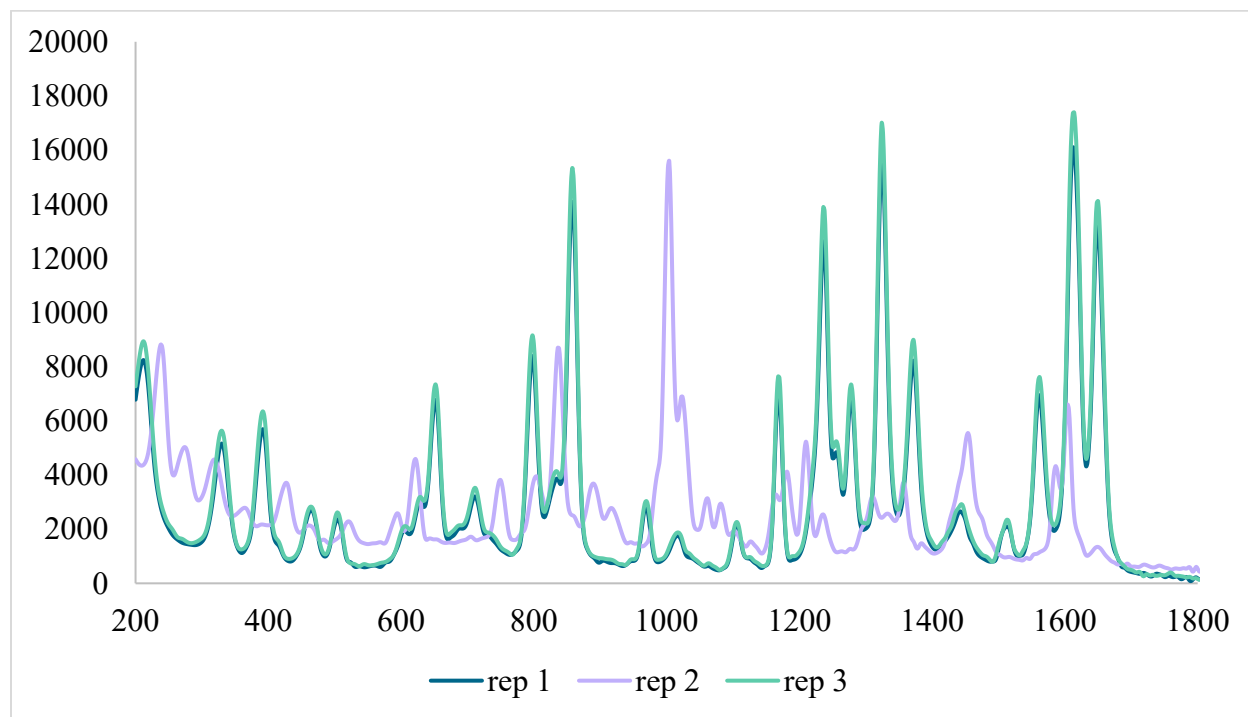


**Figure 27:** Spectra comparison for the three replicates for the 1:4 ratio of methamphetamine and acetaminophen. Rep 1 and 3 were identified as acetaminophen. However, rep 2 was identified as methamphetamine. The bands of rep 1 and 3 do not align with those of rep 2.
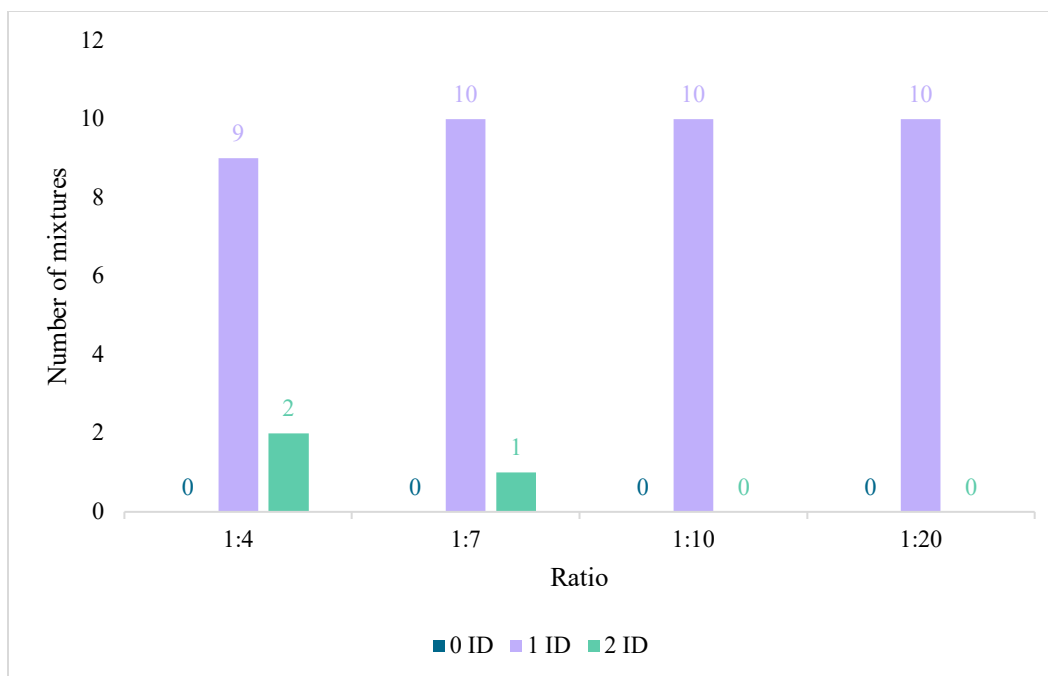
**Figure 28:** A graph showing the trend between the iRaman's ability to identify 0 (blue), 1 (green), and 2 (yellow) components in the mixture. Only three mixtures were able to identify both components in the mixture. The mixtures are separated into different groups based on the ratio. The 1:10 and 1:20 ratios were unable to identify both compounds.

Between the three replicates, all mixtures identified at least one compound. However, some individual replicates gave no result above the HQI threshold. The no result is most likely due to the interference between the two mixtures. The similarity metric used in the BWID software is the HQI, which compares the collected spectrum to the library spectrum. The HQI does not consider bands from multiple components. **Figure 29** shows an example of a replicate with no scores above the 75 % threshold. However, after manual inspection of the spectrum, bands are present that are consistent with methamphetamine and caffeine. Some bands are highlighted as examples; however, all bands are consistent with either caffeine or methamphetamine. This combination of bands prevents the HQI from identifying either compound.
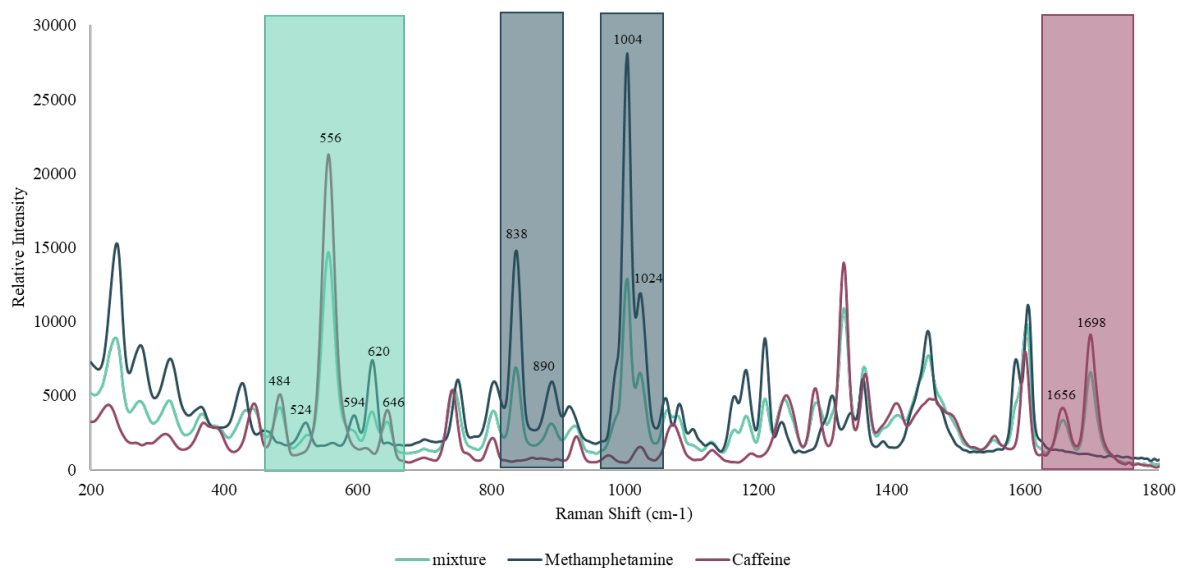
**Figure 29:** Example of a replicate spectrum of methamphetamine and caffeine at a 1:4 ratio. The two standards, caffeine and methamphetamine, are also present. Bands are present from both standards in the mixture spectrum. The bands highlighted in blue are present in methamphetamine and not caffeine. The bands present in purple are present in caffeine but not methamphetamine. The bands highlighted in green combine methamphetamine (524, 594, and 620) and caffeine (484, 556, and 646).

## 3.5 – Pharmaceutical Medicine Samples

Pseudoephedrine pills are one of the precursors used for clandestine methamphetamine production. In 2005, the United States created the Combat Methamphetamine Epidemic Act (CMEA). The CMEA restricted the sale of pseudoephedrine to limit the domestic manufacture of methamphetamine. Phenylephrine HCl has since been replaced as the over-the-counter sinus congestion medicine. Pseudoephedrine can still be purchased behind-the-counter. In pharmaceutical pills, the active ingredient is the compound(s) in the pharmaceutical pill that produces the desired effect, like pseudoephedrine in SUDAFED or acetaminophen in Tylenol. These pills contain other inactive ingredients: fillers, binders, flavorings, coatings, or preservatives. [78]

Two different pharmaceutical medicines, pseudoephedrine from Kroger and phenylephrine HCl from SUDAFED[PE], were analyzed by both the TacticID and the iRaman. The Mira analyzer was not utilized because it was unavailable. The TacticID did not have a phenylephrine HCl standard in the instruments' library. The iRaman had both standards present in the library.

However, the phenylephrine HCl medicine was still analyzed to see if the phenylephrine HCl would be misidentified as pseudoephedrine. Phenylephrine HCl is not a controlled substance; pseudoephedrine is a regulated drug used to make methamphetamine.

3.5.1 – Laser Effect

The TacticID has a 785 nm laser. The iRaman Prime has 1064 nm. As previously mentioned, longer wavelengths have lower energy, limiting the amount of fluorescence. This effect can be seen with pharmaceutical pills. **Figure 30** shows the pseudoephedrine pill analyzed by the iRaman and TacticID. Only the main band at around 1004 cm$^{-1}$ is visible for TacticID. However, the iRaman has more discernible bands.
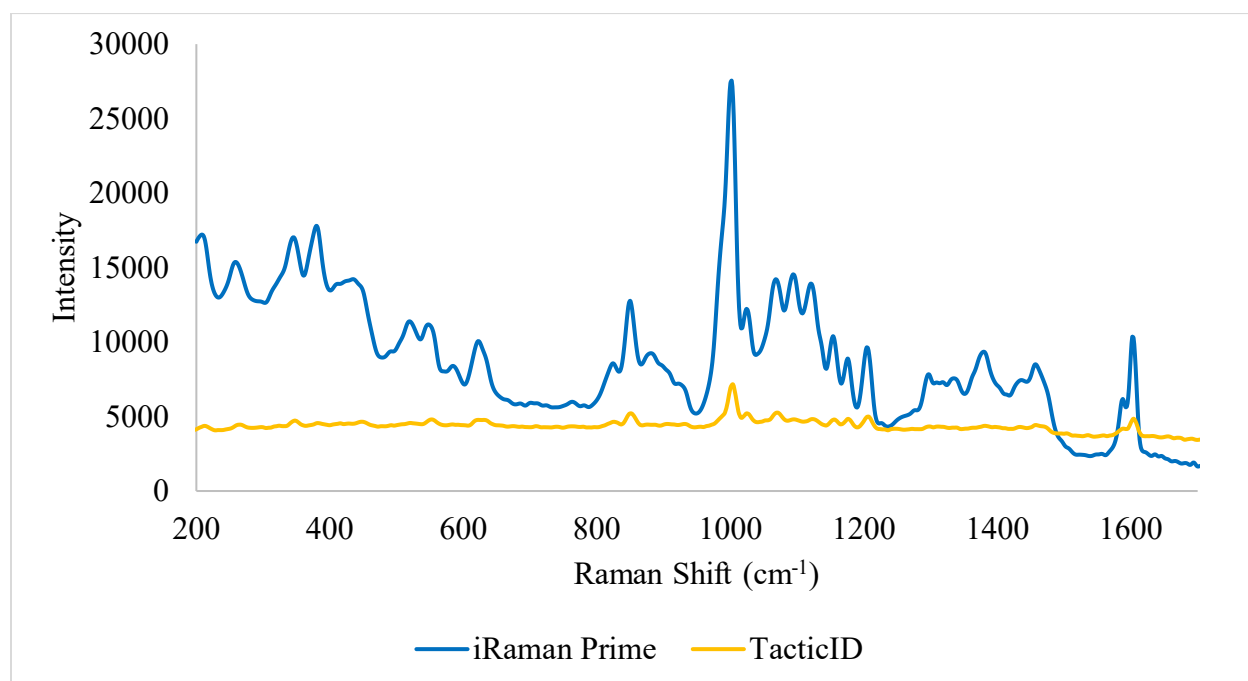


**Figure 30:** A spectra comparison showing the effect of the wavelength for the TacticID (785 nm) and iRaman (1064 nm).

3.5.2 – TacticID

**Table 6** shows the results for pseudoephedrine medicine using the mixture analysis function, which gives the spectral weight of the compound identified. The best results came from the inner portion containing the active ingredient in the highest concentration. When using only the HQI results, only one of the inner portion replicates had an HQI score above the threshold, with a score of 88.2 (* in **Table 6**). When using the mixture function, all but one mixture could identify pseudoephedrine. The replicate that did not identify pseudoephedrine was a replicate from

the outer coating. It identified calcium phosphate dibasic dihydrate, which is an inactive ingredient. Calcium phosphate is a compound used in coating pseudoephedrine pills and is listed as an inactive ingredient one the container. [79] The low HQI score is due to issues with fluorescence. The pills were red, and the outer and powder method would have had issues with the color. All the spectra have issues with fluorescence. The main band able to be seen that could be related to pseudoephedrine was 1000 cm$^{-1}$ from the aromatic CC stretching, as seen in **Figure 30**. No false positives were identified in the pseudoephedrine pills.

**Table 6:** TacticID mixture analysis results for the pseudoephedrine pharmaceutical medicine.

| Method | Replicate | Result | Spectral Weight % |
|---|---|---|---|
| Outer coating | 1 | Pseudoephedrine | 29.0 |
| | | calcium phosphate dibasic dihydrate | 23.9 |
| | 2 | calcium phosphate dibasic dihydrate | 16.1 |
| | 3 | Pseudoephedrine | 22.8 |
| Inner portion | 3 | Pseudoephedrine | 22.9 |
| | 2 | Pseudoephedrine | 36.2 |
| | | calcium phosphate dibasic dihydrate | 22.2 |
| | 3* | Pseudoephedrine | 55.2 |
| Powder | 1 | Pseudoephedrine | 25.2 |
| | | calcium phosphate dibasic dihydrate | 22.5 |
| | 2 | Pseudoephedrine | 40.3 |
| | 3 | Pseudoephedrine | 36.0 |
| | | calcium phosphate dibasic dihydrate | 22.3 |

* Gave an identification using the HQI. Replicate was correctly identified as pseudoephedrine with an HQI of 88.2

The phenylephrine was also analyzed, even though the TacticID did not have phenylephrine in the library, to see how the instrument identified the ingredients. **Table 7** shows the results using the mixture analysis function. No results for any of the replicates for the phenylephrine had an HQI score above the threshold. All the replicates identified cellulose using the mixture analysis function. Cellulose is a listed ingredient in the packaging and is used as a filler and suspending agent. [80] However, the TacticID identified potential compounds not listed in the ingredients section (false positives), including trenbolone acetate (CAS # 10161-34-9) and

hydrazine (CAS # 304-01-2). Trenbolone acetate is an anabolic steroid medication and a controlled III substance used in veterinary medicine. Hydrazine is a flammable liquid. This could be due to the fluorescence seen in the spectrum (**Figure 30**). Another explanation could be that some bands from the phenylephrine were present, but since the instrument does not have the phenylephrine standard, it tries to identify these bands with the compounds in the library. Just like the binary mixtures, none of the false positives were present in all three replicates.

**Table 7:** TacticID mixture analysis results for the phenylephrine pharmaceutical medicine.

| Method | Replicate | Result | Spectral Weight % |
|---|---|---|---|
| Outer coating | 1 | Cellulose | 26.5 |
| | 2 | Cellulose | 38.2 |
| | | trenbolone acetate | 16.6 |
| | 3 | Cellulose | 29.4 |
| | | trenbolone acetate | 22.9 |
| Inner portion | 3 | Cellulose | 53.3 |
| | | hydrazine | 25.1 |
| | 2 | Cellulose | 48.9 |
| | | hydrazine | 19.2 |
| | 3 | Cellulose | 65.2 |
| Powder | 1 | Cellulose | 59.8 |
| | 2 | Cellulose | 72.2 |
| | 3 | Cellulose | 52.0 |

3.5.3 – iRaman

The iRaman had both the phenylephrine HCl and pseudoephedrine standard for identification. As mentioned before, the iRaman does not have a mixture analysis function. **Table 8** shows the highest HQI result from the BWID software of the iRaman. None of the HQIs are above the 75 thresholds. However, every replicate for each method had the respective active ingredient as the highest HQI. The HQI for the pseudoephedrine pill was between 54.2 and 65.5. The HQI for the phenylephedrine HCl was between 9.6 and 20.7. The powdered pill, on average, gave the best HQI. This is most likely due to it being the easiest to analyze. The pills were harder to hold against the aperture for a good signal.

**Table 8:** iRaman highest HQI result for the pseudoephedrine and phenylephrine HCl pharmaceutical medicine.

| Method | Replicate | Pseudoephedrine | | Phenylephrine HCl | |
|---|---|---|---|---|---|
| | | First result | HQI | First result | HQI |
| Outer coating | 1 | Pseudoephedrine | 58.9 | Phenylephrine HCl | 10.7 |
| | 2 | Pseudoephedrine | 58.2 | Phenylephrine HCl | 9.6 |
| | 3 | Pseudoephedrine | 59.8 | Phenylephrine HCl | 11.5 |
| Inner portion | 1 | Pseudoephedrine | 59.7 | Phenylephrine HCl | 11.1 |
| | 2 | Pseudoephedrine | 61.5 | Phenylephrine HCl | 13.9 |
| | 3 | Pseudoephedrine | 65.5 | Phenylephrine HCl | 12.2 |
| Powder | 1 | Pseudoephedrine | 54.2 | Phenylephrine HCl | 17.0 |
| | 2 | Pseudoephedrine | 58.6 | Phenylephrine HCl | 17.4 |
| | 3 | Pseudoephedrine | 66.1 | Phenylephrine HCl | 20.7 |

*3.6 – Cosine Similarity*

The data from each instrument was also analyzed using cosine similarity. **Figure 31** shows a zoomed-in spectra comparison for the three Raman instruments. The iRaman provided the most intense signal; however, the bands are broader than the 785 nm laser, which decreases the resolution of the spectra. The Mira, which has the ORS optical element, provided a higher intensity signal than the TacticID, which does not have the ORS.
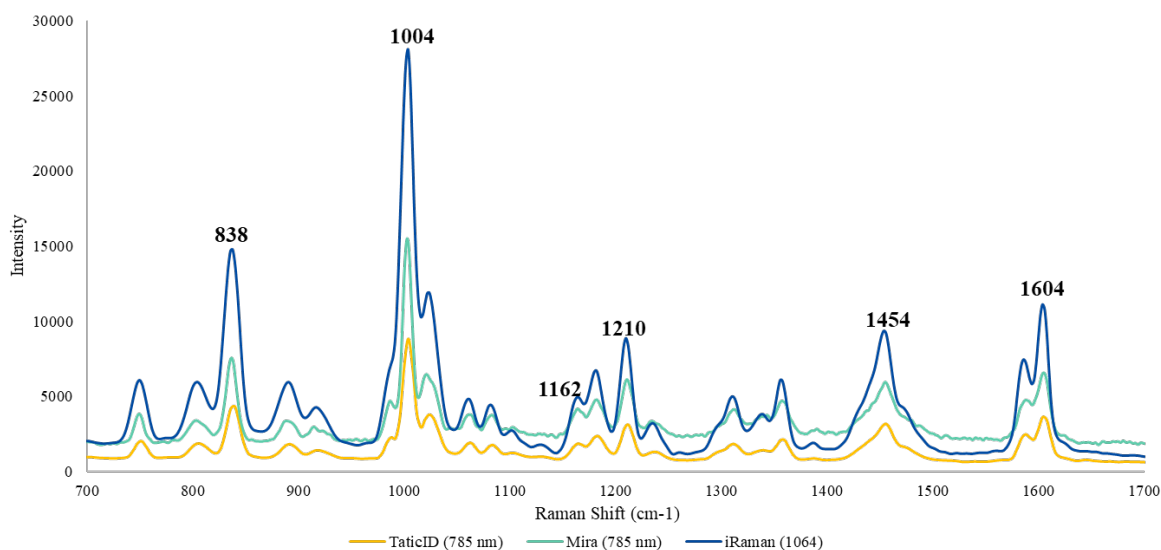


**Figure 31:** Spectra comparison for the three instruments using the methamphetamine standard.

When looking at the top three results of cosine similarity, the lowest score for the compounds present was 79 % for the iRaman, 75 % for the TacticID, and 74 % for the Mira. The

results for each replicate were combined to better represent the samples' variation. After combining the individual replicates, the percent identification was 67.9 % for the iRaman, 78.6 % for TacticID, and 84.5 % for the Mira.

While the iRaman had higher cosine scores, the percent identification was the lowest out of the three. This is because the spectra had the least resolution, as demonstrated in **Figure 31**. The Mira had the lowest cosine scores for the ground truth; However, the percent identification for the Mira was the highest at 84.5 %. The Mira provided the best percent identification because the ORS allowed for a more intense signal without decreasing the resolution, as demonstrated in **Figure 31**. The TacticID performed better than the iRaman because the 785 nm laser allowed for better resolution compared to the iRaman.

None of the binary mixtures had issues with fluorescence, as they were all white powders. The benefits of the iRaman are shown in the spectra collection for the pharmaceutical pills, as seen in **Figure 30**. The TacticID only showed 1004 cm$^{-1}$ as a visible peak, whereas the iRaman prime had many more bands visible in their spectra. The TacticID only achieved one score above the HQI, and the other replicates only identified compounds based on the mixture analysis function. The iRaman Prime did not identify any compounds in the pharmaceutical pills. This is primarily due to the software. Pharmaceutical pills are complex mixtures, and iRaman does not have a mixture analysis function.

The percent identification for cosine similarity is higher than the HQI scores. Cosine similarity and HQI are two similarity metrics and therefore compare the spectra differently. HQI is considered a correlation algorithm and uses dot products to calculate the similarity between two spectra. [49] Cosine similarity also uses dot products in the numerator. However, HQI considers the magnitude of the vectors from the dot product. Whereas cosine similarity accounts for the vectors' length, only considering the direction of the magnitude when calculating the similarity. It should be noted that the magnitude of the vectors is the same for each instrument. In this case, the difference in percent identification is because the spectra were truncated to include the critical bands. This allows for comparisons between prominent bands and reduces background noise contributions.
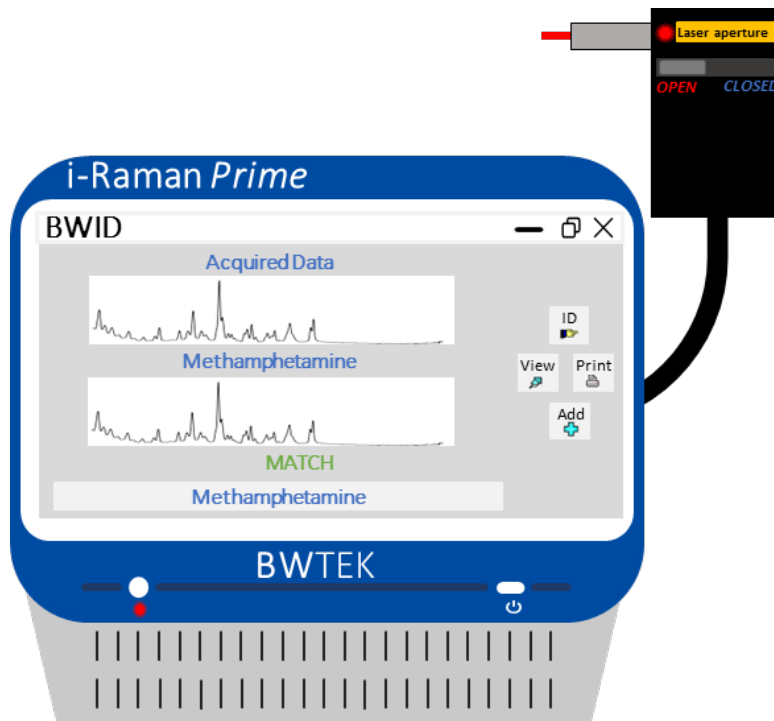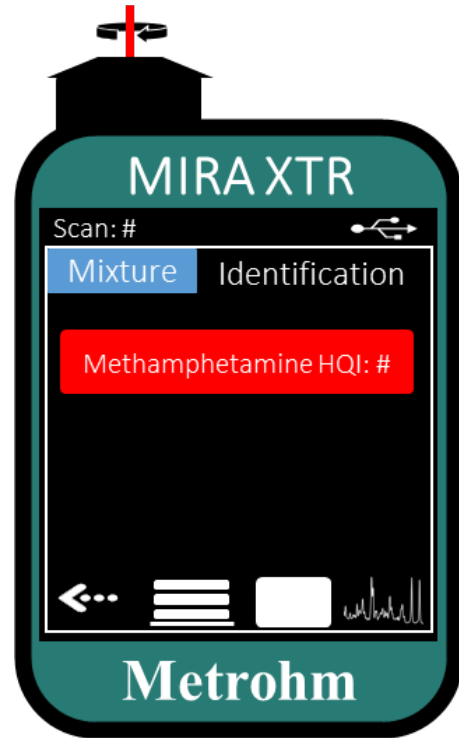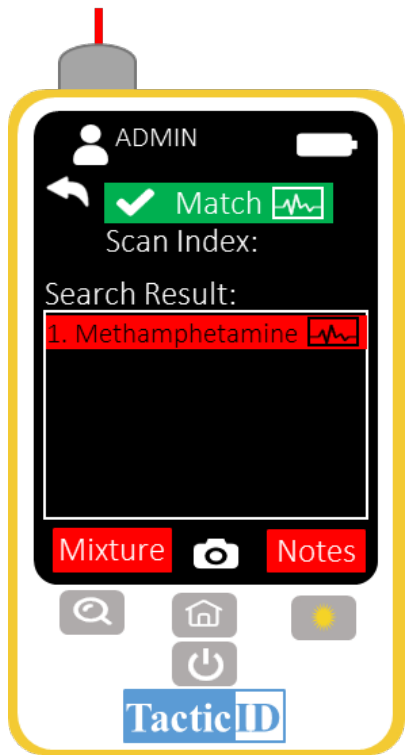
# Chapter 4: Conclusions

*4.1 – Portable Raman Comparison*

**Table 9** compares the instrument's ability to identify 0, 1, and 2 components in the mixture using the instrument's software and the binary mixtures. The most significant difference that affected the portable Raman's ability to identify mixtures was the software used by the instrument.

**Table 9:** Comparison of the three instruments' ability to identify the components of the binary mixtures.

| Instrument | Laser (nm) | %ID | Number of mixtures | | |
| | | | 0 Correct | 1 Correct | 2 Correct |
| --- | --- | --- | --- | --- | --- |
| TacticID | 785 | 66.6 % | 0 | 28 | 14 |
| Mira | 785 | 66.6 % | 0 | 28 | 14 |
| iRaman | 1064 | 53.6 % | 0 | 39 | 2 |

*%ID = percent identification using the instrument's software

**Figure 32** shows a 1:4 mixture of methamphetamine and caffeine analyzed by iRaman. When analyzed by the BWID software with the iRaman, the results were below the 75 % HQI threshold. After a manual comparison of the mixture to the standards, bands from both compounds are present in the mixture spectrum, as highlighted by the boxes. This can be compared directly to **Figure 33**, which shows the same mixture analyzed by the Mira. The bands highlighted in **Figure 32** are also present in this replicate. When analyzed by the Mira mixture analysis software for the iRaman, the software identified both compounds: caffeine with a spectral weight of 68 % and methamphetamine with a spectral weight of 23 %.
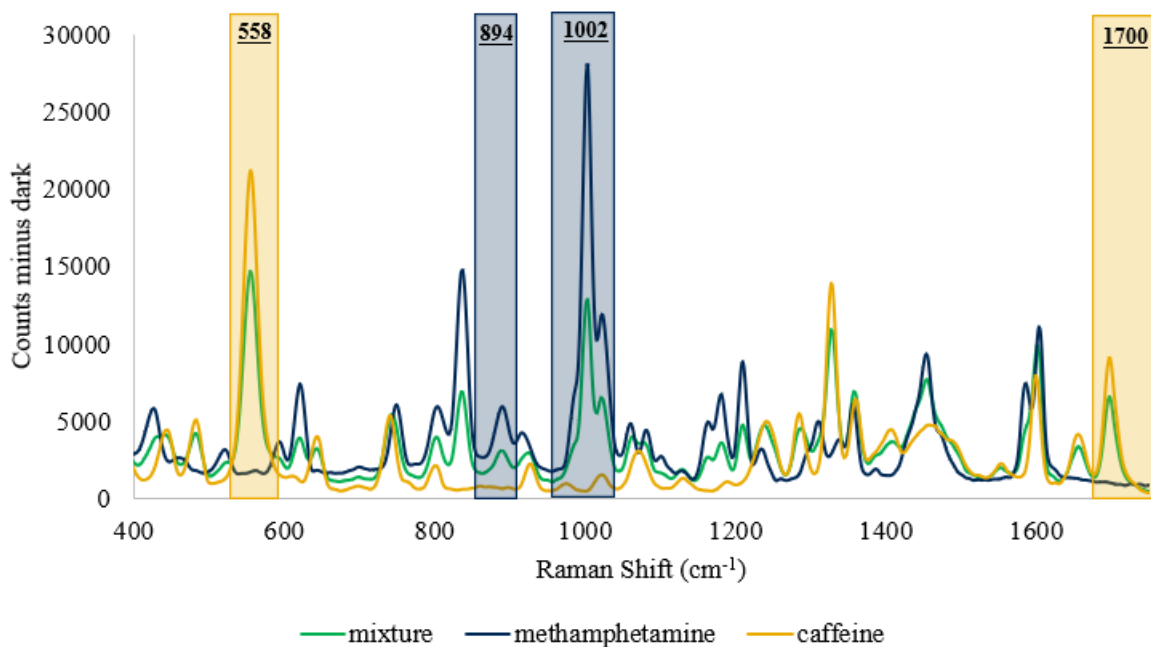
**Figure 32:** Manual comparison for one replicate of the 1:4 mixture of methamphetamine and caffeine using iRaman. The yellow boxes highlight two distinct areas where the mixture lines up with caffeine. The blue boxes highlight two distinct areas where the mixture lines up with methamphetamine.
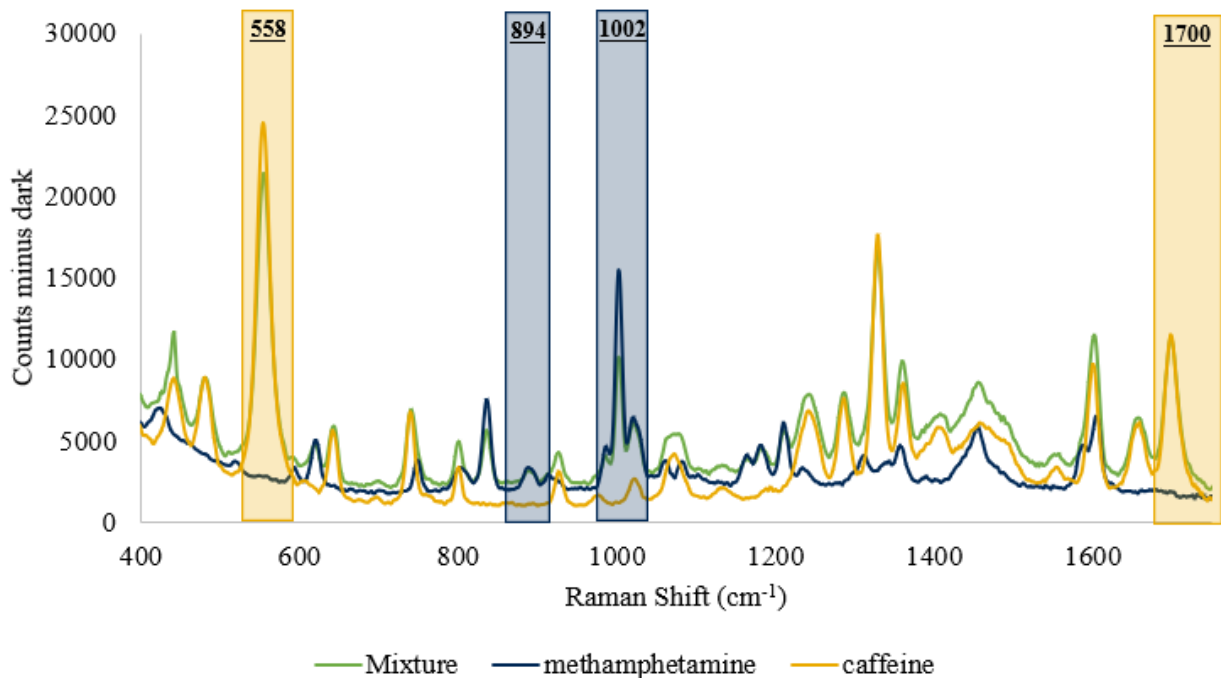


**Figure 33:** Manual comparison for one replicate of the 1:4 mixture of methamphetamine and caffeine using Mira. The yellow boxes highlight two distinct areas where the mixture lines up with caffeine. The blue boxes highlight two distinct areas where the mixture lines up with methamphetamine.

This study shows that the TacticID and the Mira XTR are more efficient for detecting mixtures due to their mixture analysis option. Both instruments got a percent identification of 66.6 %. Crime scene investigators or first responders could use these instruments as they are user-friendly with color coding to identify threat levels. The TacticID had no issues with false positives, whereas the Mira XTR had several false positives for both the pure standards and the binary mixtures. Most of the false positives from the mixtures were consistent with the false positives for the pure standards. The rest of the false positives had a low spectral weight score. By including a threshold for the spectral weight score, the analyst could limit the false positives.

The iRaman had better spectra quality when analyzing pharmaceutical pills, with more intense bands present, as seen in **Figure 30**. However, the software could not identify the pseudoephedrine from the set threshold. The HQI for the pseudoephedrine pills analyzed by iRaman was around 55, with the highest HQI out of the libraries. The phenylephedrine spectra were also better with the iRaman. The HQI for the phenylephrine HCl was around 10, but it was the highest HQI out of the library.

TacticID had fluorescence problems that blocked the Raman signal from the pills. The pseudoephedrine was identified using the HQI, with one replicate using the inner part of the pill. The mixture analysis function identified the active ingredient in all but one replicate. The replicate was analyzed using the outer coating. TacticID did not have a phenylephrine standard but correctly identified cellulose as an ingredient. The TacticID also identified other results not present in the ingredients section. However, the TacticID had problems with fluorescence, where most of the bands were hidden. These incorrect identifications could also result from the TacticID spectrum having bands from the phenylephrine. However, since no standard was present, TacticID attempted to identify the bands with the compounds in the library.

The iRaman using the BWID software had more issues with detecting mixtures. This was primarily attributed to the software not having the mixture analysis function. This instrument does have other software features that could benefit other purposes. For instance, there is BWIQ that allows for more advanced statistical processing. The BWIQ can perform both regression and classification models. However, this software only allows for six classes for a model. These additional statistical processing methods would have issues like the HQI and cosine similarity metrics because they do not account for complex spectra with bands from multiple components.

BWSpec is the software used in the next part of the thesis. This software allows for more advanced data acquisition.

The iRaman has a better laser and more features. This study shows it is not the best for complex mixtures, as the available software has no current mixture analysis. This instrument still has several features beneficial in a laboratory, like advanced multivariate analysis and data acquisition.

The two 785 nm instruments, Mira and TacticID, performed similarly in their ability to identify mixtures. It should be noted that Mira was not used to analyze the pills, where features like fluorescence rejection could be adequately tested. Our laboratory groups had more time with the TacticID, establishing bias, precision, reproducibility, and analyzing binary mixtures and authentic samples. [54,81] The Mira performed the same in terms of the percent identification but did have more issues with the false positives. The Mira would perform better if there were time to optimize the instrument and create in-house libraries.

*4.2 – Next Steps*

The highest percent identification calculated using the instruments library was 66.6 %. This value was lower than expected of a screening technique, which should be over 80 %. The cosine similarity had better percent identifications. The following section will compare cosine similarity to machine learning to further improve the detection of binary mixtures. The six standards were increased to include additional drugs and common cutting agents seen to make the algorithm more applicable to a forensic laboratory. A total of 100 binary mixtures were used to incorporate the new standards. Twelve authentic samples were also included as more complex mixtures to test these methods better.

# Part III: Improving Raman Spectroscopy Using Machine Learning
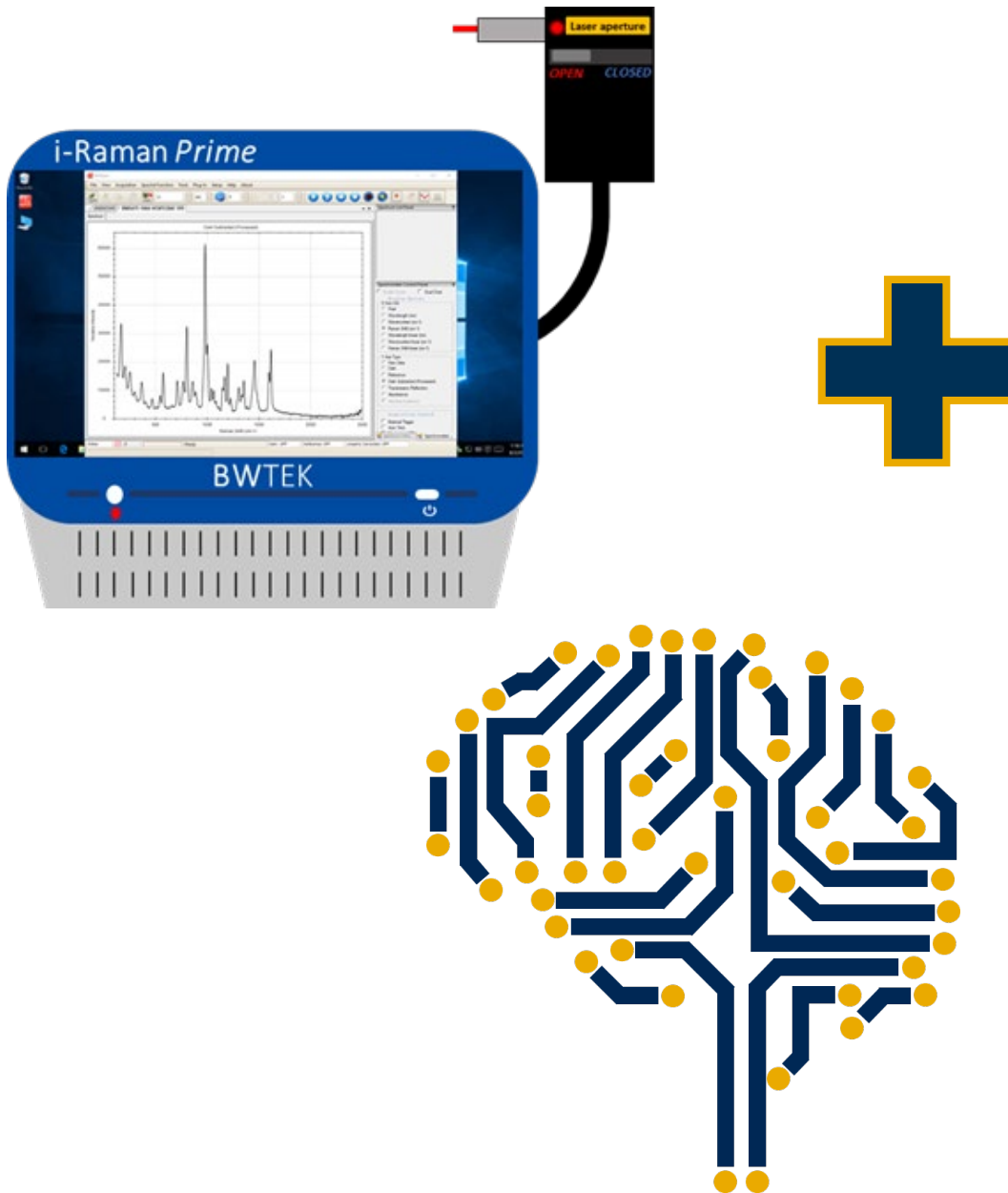


## Chapter 1: Relevant Literature Review

**Part III: Improving Raman Spectroscopy Using Machine Learning** from this thesis revolved around improving Raman's ability to identify multiple components in the mixture using machine learning. The standards and mixtures analyzed in this section were included along with many of the standards and mixtures used in conjunction with the NIJ grant: Award #2019-DU-BX-0030. This was done to have a more extensive library or database for machine learning and cosine similarity. Additional mixtures were also included to have a more diverse test set. Cosine similarity was used as a traditional similarity metric to compare machine learning.

*1.1 – Raman Mixture Analysis*

As discussed in **Part II: Comparison of Portable Raman Instruments**, one of the main limitations of Raman Spectroscopy is the analysis of mixtures. Complex samples are hard for Raman because bands from multiple components convolute the Raman spectra. Examples of complex samples can be seen in **Figure 32** and **Figure 33** on page 53. The mixture spectra in both figures have bands relating to methamphetamine and caffeine. In **Figure 32**, iRaman did not have a mixture analysis option to attempt to analyze the mixture. However, in **Figure 33**, the Mira did have a mixture analysis option and could identify both compounds.

*1.2 – Machine Learning*

One of the methods used to combat complex Raman spectra is machine learning. Machine learning uses experience, in the form of known data, to make predictions about new data. [82] There are many tasks of machine learning. **Figure 34** shows a Venn diagram with different subsets of machine learning with an example from each. [83] The artificial neural networks and deep learning are separated by a dashed line because there is no well-defined differentiation between the two in previous literature. The main task of machine learning is to develop algorithms that iteratively learn from data. The data allows the computer to find hidden insights and complex patterns without being programmed. The algorithm develops models that can then be used to predict new data. There is no universal algorithm for machine learning. The specific type of algorithm depends on the problem and the number of variables available. Therefore, the data used to train the algorithm needs to be specific to the problem being addressed.
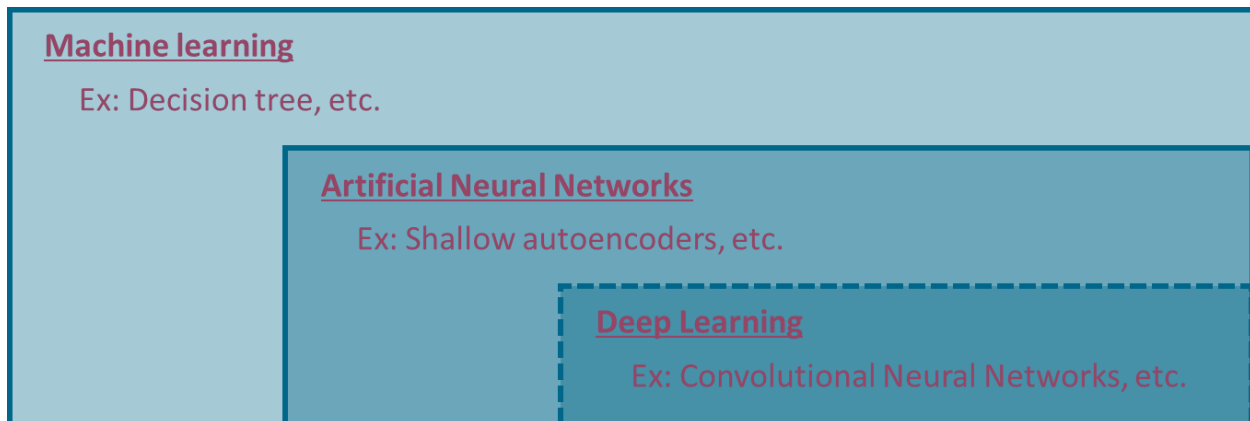
**Figure 34:** Venn diagram of machine learning concepts. Adapted from [83].

1.2.1 – Artificial Neural Networks

A subset of machine learning algorithms includes artificial neural networks or ANN. ANNs consist of mathematical representations of connecting processing units called artificial neurons. The neurons are modeled off the brain and are organized into networks. There is a minimum of two layers, an input and output layer. The input layer receives the data for the training, and the output provides the overall result or prediction. There can also be hidden layers responsible for non-linear mapping between the input and output layers. [84] The algorithm cannot learn the number of layers; these are considered hyperparameters and are set manually. These parameters can still be optimized through trial and error. Both machine learning and artificial neural networks are considered shallow machine learning. These algorithms do not need to be explicitly trained. However, the programmer needs to extract the features and classifiers for the algorithm. The quality of the algorithm depends heavily on feature extraction.

1.2.2 – Deep Learning

Deep learning is within the ANN subset of machine learning. The main difference between machine learning and deep learning is that deep learning contains advanced artificial neural networks. These neural networks are modeled after the brain. Just like the brain, the connections between the neurons transmit a signal depending on the thresholds set. [84] In deep learning, the neurons contain advanced operations. Advanced operations allow the neural network to be fed raw input data and determine relevant features for the required task. This allows deep learning to overstep the handcrafted feature design necessary for machine learning. A diagram of the differences between the two model builds can be seen in **Figure 35**.
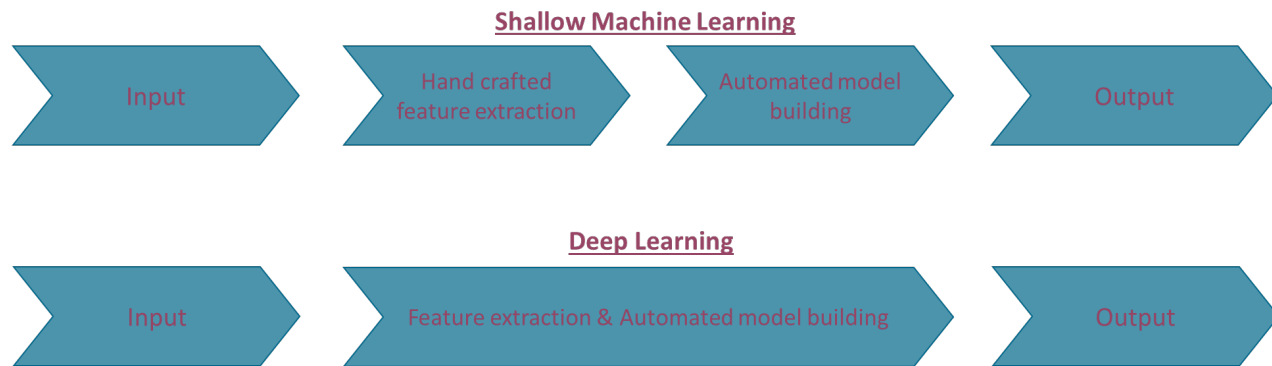
**Figure 35:** Process of model building for shallow machine learning and deep learning. Adapted from [84].

One of the main benefits of deep learning is that the algorithm automatically extracts the features and then learns from the errors. Due to the complex structure of the algorithms, deep learning algorithms require millions of different data points. The large datasets are to eliminate fluctuations and provide the best interpretations.

1.2.3 – Convolutional Neural Networks

The type of deep learning this thesis uses is called convolutional neural networks, or CNN. CNN uses convolutions to extract features. In simple terms, convolution is a function derived from two given functions by integration, which expresses how the shape of one is modified by the other. [85] This expression can be seen in **Equation 8**. Where x(a) is a weighted average operation at every datapoint, w(a) is a weighted function, and a is the age of measurement. The weighted function allows the analyst to average several measurements while giving more weight to recent measurements. [85]

$$\textbf{Equation 8:} \qquad (x * w)(t) = \int_{-\infty}^{\infty} x(a)w(t-a)da$$

*The function of x* in **Equation 8** is typically referred to as the input, and the *function of w* is referred to as the kernel. The kernels can be either one-dimensional or two-dimensional. This thesis uses one-dimensional kernels. The convolution output can be referred to as the output of the feature map. CNN is a type of supervised machine learning. [86] Supervised machine learning uses labeled input and output data to learn the algorithm. [87] In Raman spectroscopy the input is the spectra and the output is the spectrum's respective compound(s).

The activation function used for the convolution layer was the Rectified Linear Unit (ReLU). The ReLU function is a piecewise linear function that will output the input directly if it is positive; otherwise, it will output zero. ReLU is one of the simpler activation functions and therefore is one of the most used. [88]

Convolutions are not the only layers or neurons in CNN algorithms. This thesis uses other layers, including batch normalization, max pooling, flatten, and dense. **Figure 38** shows the complete architecture for the CNN used in this thesis. Normalization is a preprocessing technique used to standardize data. Batch normalization is a normalization technique that normalizes batches of data in the network, using **Equation 9**. [89]

$$\text{Equation 9:} \qquad x^N = \frac{Z - m_Z}{s_Z}$$

Where z is the neuron's output, $m_Z$ is the mean of the neuron's output, and $s_z$ is the mean of the neuron's output.

Pooling techniques provide summary statistics of the nearby outputs. Pooling is used to help make the algorithm invariant to small translations in input. For max pooling, the operation reports the maximum output within the rectangular neighborhood. [85] This reduces the dimensionality of the feature map or output. Another layer includes "flatten," which converts the two-dimensional arrays into a single continuous linear vector. [90] This step transitions the convolutional layer into a fully connected or dense layer. The dense layer is connected to all the neurons in the preceding layer and is used to classify the images.

1.2.3.1 – Prediction Coding

After the models are trained, the analyst can use the model to predict new data. There are three prediction/classification algorithm types: binary, multilabel, and multiclass. [91] The binary method only works when two mutually exclusive classes exist, like whether a patient has a disease. The algorithm is trained to look for features associated with the disease, and the other class is used if the algorithm does not see the identified features.

Multilabel and multiclass are both methods that use three or more classifications. The model is trained to identify important features associated with each class. Multiclass is used for mutually exclusive classes, like a type of animal. The important features identified are assumed to be unique to the class. The new data is only assigned to one label or class for multiclass.

In multilabel, multiple labels can be assigned to one set of data. Multilabel was used for this research since the Raman bands are CNN's important features. Even though the Raman spectra are unique to the compounds, the bands are based on the functional groups. Different compounds can have similar Raman Bands, like bands related to an aromatic ring or amine functional group. The algorithm was trained using simulated mixtures, where two pure spectra were combined to simulate binary mixtures. The simulated mixtures had features relating to two classes.

1.2.3.2 – Validating CNN Algorithms

It is essential to validate the CNN algorithm to ensure it works properly. The validation method used was a cross-method validation using *k-fold* in Python. The k refers to the number of groups the data will be split. This thesis used a 10-fold cross-validation, which has been found to have low bias and is recommended for machine learning. [92] A variation called stratified was used to ensure each fold has equal portions of observations for each class. The train-test-split function was also used, which splits the data from each fold into train and test sets. The train set is used to train the model. The test set is not used to train the model but instead evaluates the fit of the model. This thesis used 90 % for training and 10 % for testing.

1.2.3.3 – Evaluating Algorithms

There are several ways to evaluate an algorithm. The method used in this thesis is a classification report. Scikit-learn's classification report provides each class's precision, recall, f-1 score, and support. Precision quantifies the number of correct positive predictions or the accuracy. However, this metric does not include false negatives. The precision, recall, and f1-score formulas for binary classification can be seen in **Equation 10**, **Equation 11**, and **Equation 12**, respectively. Precision is best to minimize false positives, whereas recall is best to minimize false negatives. F1-score is used to combine precision and recall. For multi-classification, the values are the sum of the values across the classes. [93] For all these scores, 0 is poor, and 1 is perfect.

$$\textbf{Equation 10: } Precision = \frac{True\ Positives}{True\ Positives\ and\ False\ Positives}$$

$$\textbf{Equation 11}: Recall = \frac{True\ Positives}{True\ Positives\ and\ False\ Negatives}$$

$$\textbf{Equation 12: } f1\ score = \frac{2 * Precision * Recall}{Precision + Recall}$$
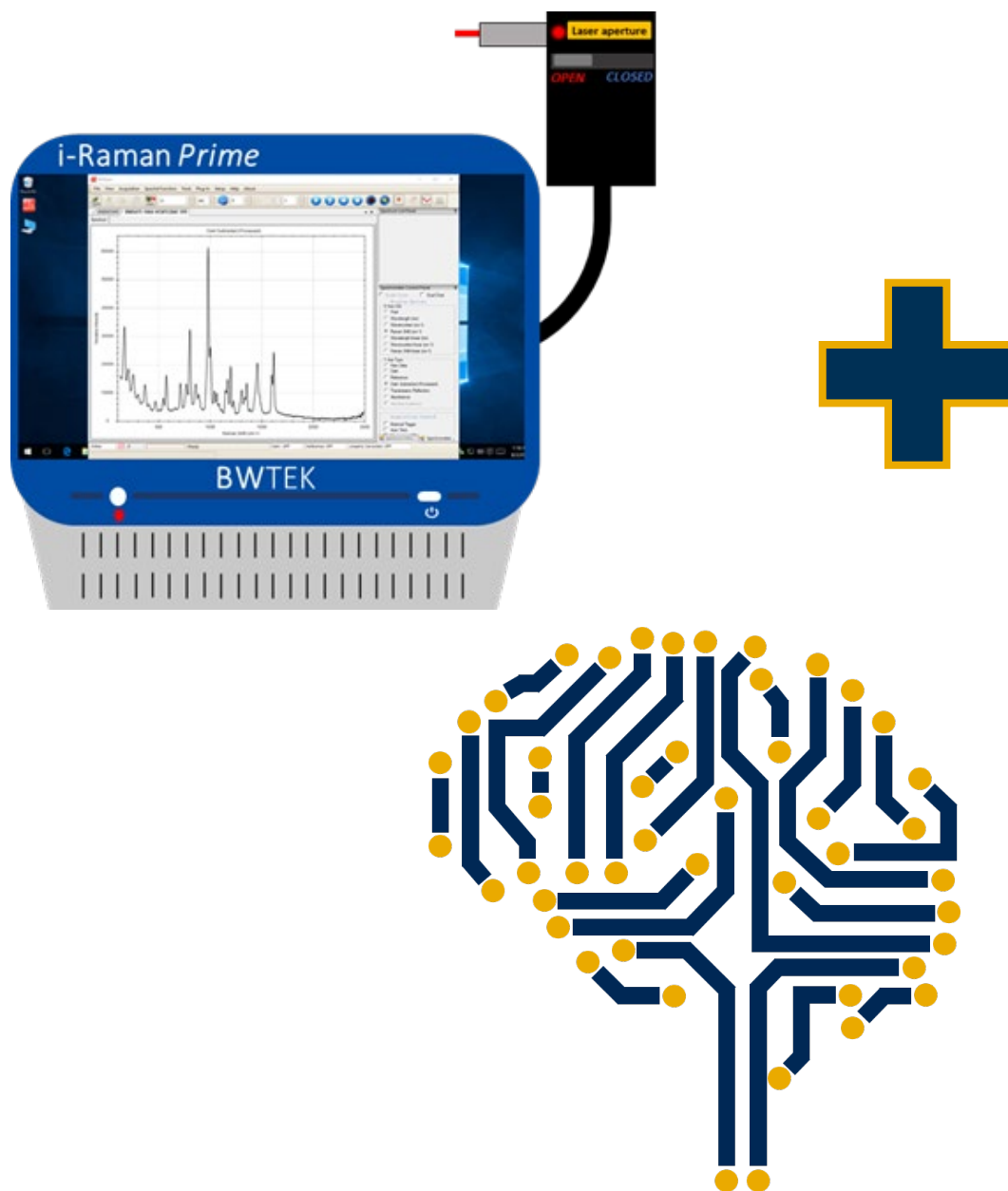
Chapter 2: Materials, Methods, and Experimental Design

Table 10 shows the 38 drugs used as standards for Raman data analysis. The CNN included an empty polyethylene baggie, the same kind used to hold the powders. The baggie class can identify potential interference from the baggie. The interference could result from poor Raman signal from the sample or positioning of the laser aperture. **Table 11** shows the 100 binary mixtures used to simulate real drug samples. Some binary mixtures were previously used in previous publications by our group [54,81]. The binary mixtures were created with different ratios to simulate authentic samples. Raman also analyzed twelve adjudicated samples from the Maryland State Police Forensic Sciences Division as more complex mixtures.

**Table 10:** List of standards used for Raman analysis.

| | | | | |
|---|---|---|---|---|
| 4-MEC[1] | Caffeine[3] | Ephedrine [2] | Maltose[6] | Procaine[4] |
| 4-MMC[2] | Carfentanil[1] | Eutylone[1] | Mannitol[2] | Pseudoephedrine[2] |
| Acetaminophen[2] | Cocaine[1] | Fentanyl[1] | Methamphetamine[1] | Quinine[1] |
| Amphetamine[1] | Codeine[1] | Heroin[1] | Mitragynine[1] | Sorbitol[5] |
| Alprazolam[1] | Dibutylone[1] | Hydroxyzine[5] | Myo-inositol[7] | Starch[10] |
| Aspirin[10] | Diltiazem[4] | Ketamine[2] | Naltrexone[1] | Δ9-THC[1] |
| Benzocaine[2] | Dimethyl Sulfone[1] | Levamisole[4] | Phenacetin[8] | |
| Boric Acid[3] | Diphenhydramine[2] | Lidocaine[2] | Phenolphthalein[9] | |

4-MEC = 4-Methylethcathinone, 4-MMC = 4-Methylmethcathinone, Δ9-THC = Delta-9-tetrahydrocannabinol [1] Cayman Chemical (Anne Arbor, MI), [2] Millipore-sigma (St. Louis, MO), [3] Acros Organics (Geel, Belgium), [4] Baker (Radnor, PA), [5] Spectrum Chemical MFG (New Brunswick, NJ), [6] MPBio (Salon, OH), [7] Alfa Aesar (Ward Hill, MA), [8] TCI Chemicals (Portland, OR), [9] Fisher Chemical (Fairlawn, NJ), [10] Kroger (Morgantown, WV)

**Table 11:** Binary mixtures analyzed by Raman.

| | Mass Ratio | | | |
|---|---|---|---|---|
| Mixture | 1:4 | 1:7 | 1:10 | 1:20 |
| 4-MEC : Benzocaine | | ✓ | ✓ | |
| 4-MEC : Maltose | ✓ | ✓ | | |
| 4-MMC: Lidocaine | | ✓ | ✓ | |
| 4-MMC : Maltose | ✓ | | | |
| Acetaminophen : Myo-inositol | | | ✓ | ✓ |
| Alprazolam : Caffeine | ✓ | ✓ | | |
| Alprazolam : Levamisole | ✓ | ✓ | | |
| Amphetamine : Acetaminophen | ✓ | | ✓ | ✓ |
| Amphetamine : Caffeine | | ✓ | | ✓ |
| Caffeine : Levamisole | ✓ | ✓ | | |
| Cocaine : Benzocaine | ✓ | | | |
| Cocaine : Boric acid | | | ✓ | |

| Mixture | | | | |
|---|:---:|:---:|:---:|:---:|
| Cocaine : Diltiazem | ✓ | ✓ | ✓ | ✓ |
| Cocaine : Levamisole | ✓ | | | |
| Cocaine : Caffeine | ✓ | ✓ | ✓ | ✓ |
| Cocaine : Hydroxyzine | ✓ | | ✓ | |
| Cocaine : Lidocaine | ✓ | ✓ | | ✓ |
| Cocaine : Maltose | | ✓ | | ✓ |
| Cocaine : Procaine | ✓ | ✓ | ✓ | |
| Codeine : Acetaminophen | ✓ | ✓ | ✓ | ✓ |
| Codeine : Maltose | ✓ | ✓ | ✓ | ✓ |
| Ephedrine : Acetaminophen | ✓ | | | ✓ |
| Ephedrine : Caffeine | | ✓ | ✓ | |
| Ephedrine : Levamisole | | ✓ | ✓ | |
| Fentanyl : Cocaine | ✓ | | | |
| Fentanyl : Methamphetamine | ✓ | | | |
| Fentanyl : Caffeine | | | | ✓ |
| Heroin : Acetaminophen | ✓ | ✓ | | ✓ |
| Heroin : Quinine | | | ✓ | |
| Hydroxyzine : Maltose | | ✓ | ✓ | |
| Methamphetamine : Acetaminophen | ✓ | ✓ | | ✓ |
| Methamphetamine : Amphetamine | ✓ | ✓ | | |
| Methamphetamine : Caffeine | ✓ | ✓ | ✓ | |
| Methamphetamine : Dimethyl Sulfone | ✓ | | | ✓ |
| Methamphetamine : Ephedrine | | ✓ | ✓ | ✓ |
| Methamphetamine : Maltose | | | | ✓ |
| Methamphetamine : Levamisole | ✓ | ✓ | ✓ | ✓ |
| Methamphetamine : Pseudoephedrine | ✓ | ✓ | ✓ | ✓ |
| Naltrexone : Maltose | ✓ | ✓ | ✓ | ✓ |
| Phenacetin : Sorbitol | | ✓ | | ✓ |
| Procaine : Starch | ✓ | | ✓ | |
| Pseudoephedrine : Acetaminophen | ✓ | | | ✓ |
| Pseudoephedrine : Caffeine | | ✓ | ✓ | |
| Pseudoephedrine : Levamisole | ✓ | | | ✓ |

4-MEC = 4-Methylethcathinone, 4-MMC = 4-Methylmethcathinone

*2.2 – Instrumentation and Data Collection*

Raman spectra were collected using a 1064 nm i-Raman Prime by B&W Tek (Newark, DE) and BWSpec (*v. 4.15_3*). The BWSpec software is not equipped with libraries for identifying samples; instead, the software is used for data acquisition. The BWSpec allows for easier instrument control, with the integration time and laser power able to be altered in between data collection for optimal spectrum resolution. The Raman instrument was operated at 80 % power. A

polystyrene standard ensured the instrument was working correctly. The integration time was varied to get a good spectrum with the highest intensity between 50,000 - 60,000 counts minus dark. The integration time was between 3 to 15 seconds. The Raman spectra were acquired from 96.82 cm$^{-1}$ to 2501.62 cm$^{-1}$. All standards and binary mixtures were analyzed in triplicate through a plastic bag.

*2.3 – Data Augmentation*

The collected pure Raman spectra were augmented to improve the data analysis. Each spectrum was multiplied by 500 random numbers between 0 and 1, which created 58,000 spectra. The random numbers were generated using *numpy v* 1.23.3. **Figure 36** shows the effect of random numbers used for data augmentation. The random numbers added variation to the intensity of the Raman bands, increasing the spectra in the database for pairwise comparisons and possible identification for cosine similarity while reducing the overfitting of the convolutional neural network (CNN).
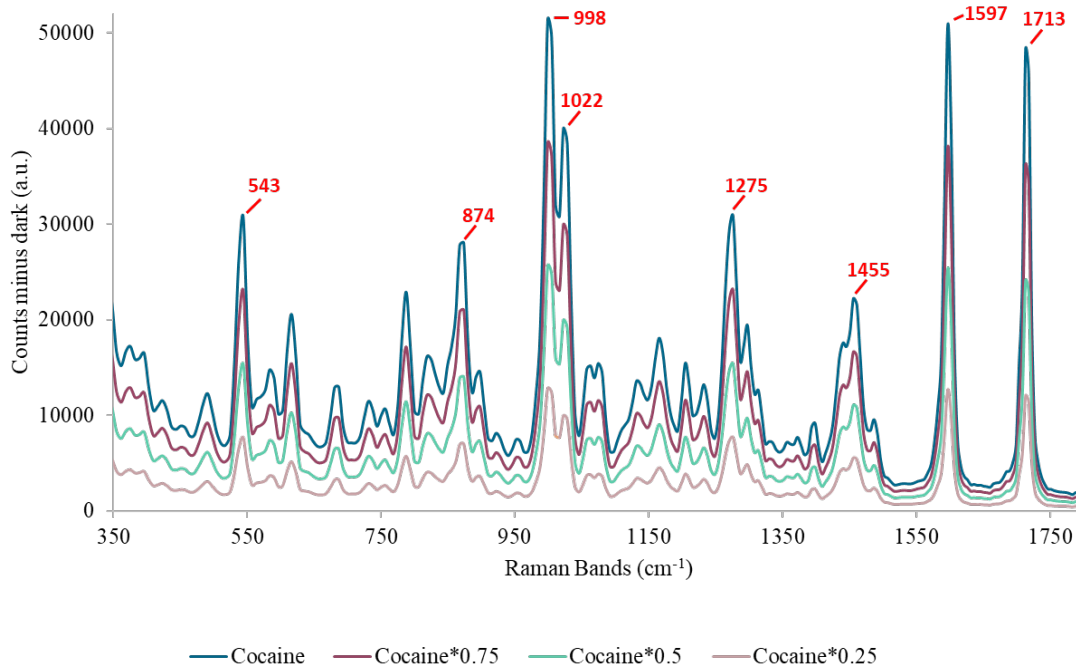
| Raman shift | | | |
|---|---|---|---|
| 543 cm$^{-1}$ | $\delta$ | 1275 cm$^{-1}$ | $\nu$ CN |
| 874 cm$^{-1}$ | $\nu$ CC (tropane ring) | 1455 cm$^{-1}$ | $\delta_{as}$ CH$_3$ |
| 998 cm$^{-1}$ | $\nu_s$ aromatic ring | 1597 cm$^{-1}$ | $\nu$ C=C aromatic ring |
| 1022 cm$^{-1}$ | $\nu_{as}$ -aromatic ring | 1713 cm$^{-1}$ | $\nu_s$ C=O Carbonyl stretch |

**Figure 36:** Effect of random numbers for data augmentation. The spectra shown is for Cocaine. The table provides some Raman shifts for the labeled Raman Bands [94]. $\nu$ = stretching $\delta$ = deformation, s = symmetric, as = asymmetric

The CNN also used mixture augmentation, combining spectra to simulate possible mixtures using **Equation 13**. A mixture augmentation example is shown in **Figure 37**. The mixture augmentation was done for every drug combination for each random number. Twenty random numbers were used, for a total of 262,200 simulated mixture spectra.

**Equation 13:** $Mixture = (drug1 * RN) + (drug2 * RN)$

Where RN = random number between 0 and 1, drug1 is one of the drugs listed in **Table 10**, drug2 is another drug listed in **Table 10** excluding drug1, and Mixture is the resulting simulated mixture.

| Raman shift | | | |
|---|---|---|---|
| 1547 cm$^{-1}$ | δ CNH and ν CN* | 1665 cm$^{-1}$ | ν C=O secondary amide |
| 1597 cm$^{-1}$ | ν C=C aromatic ring | 1713 cm$^{-1}$ | ν$_s$ C=O Carbonyl stretch |
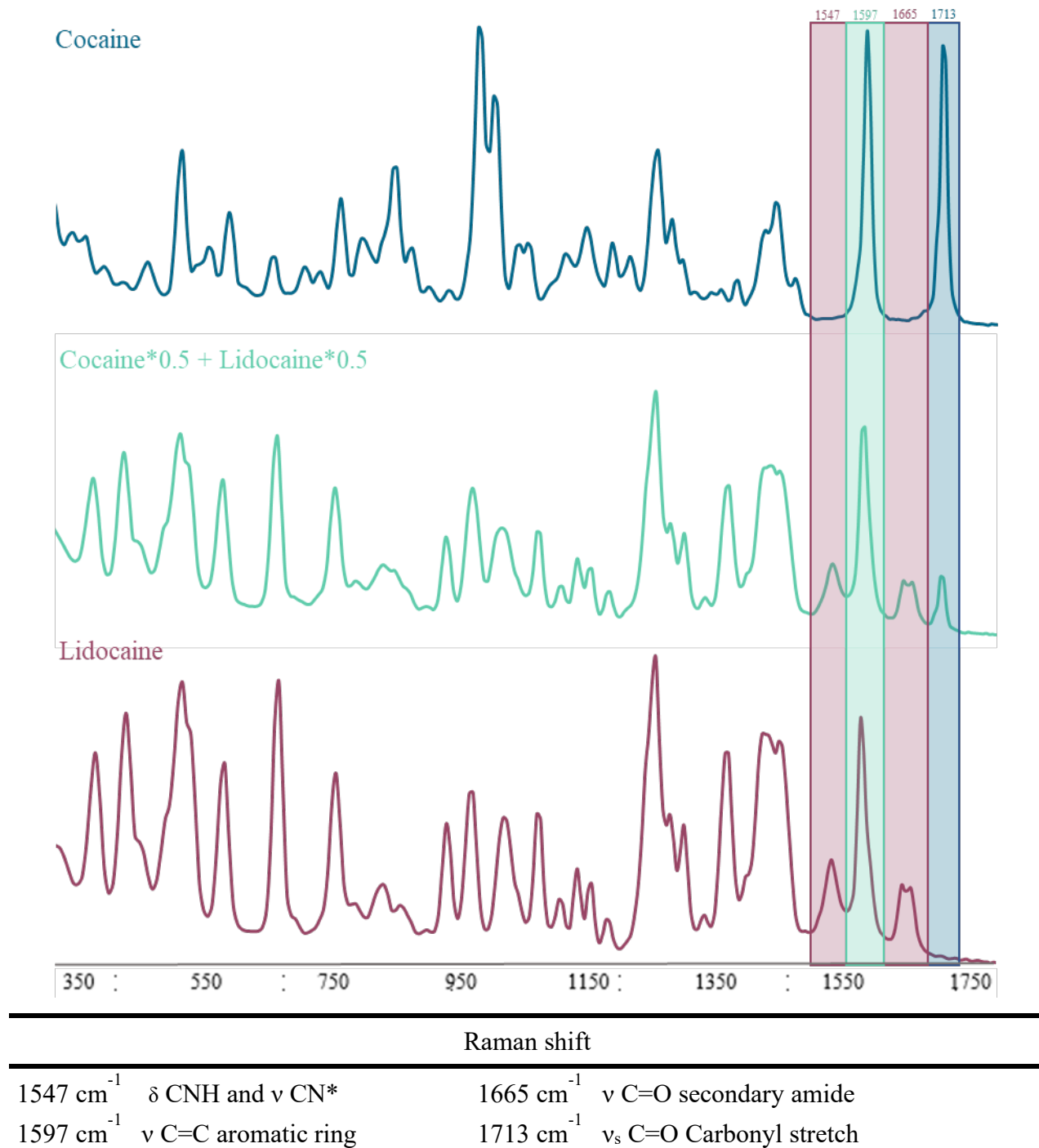
**Figure 37:** Example of how the spectra get combined for the mixture augmentation. Some bands are labeled to help show how the two pure spectra, cocaine (blue spectrum on top) and Lidocaine (purple spectrum on bottom) are combined into one simulated mixture spectrum (teal spectrum in middle). ν = stretching δ = deformation, s = symmetric. [94,95]

*2.4 – Cosine Similarity*

Cosine similarity was used to investigate how well Raman spectra identify multiple components in a mixture. The cosine similarity was performed with *sklearn v* 1.1.2. The database used included pure augmentation data. The mixture augmentation could not be used because it would convolute the differences between the standards` spectra. The vectors were created from the intensities (y-axis) of the Raman bands in each spectrum. The binary mixtures, shown in **Table 11**, were used to evaluate cosine similarity's ability to identify both components in the mixtures. The binary mixtures were truncated to 312.17 $cm^{-1}$ to 1802.35 $cm^{-1}$ to match the vector length of the augmented mixtures. The top 5 results for each binary mixture were provided as predictions. A percent identification was calculated using **Equation 7**, shown on page 29. The authentic samples were also analyzed using the same database and code.

*2.5 – Convolutional Neural Network*

Another analysis that investigated the detection of binary mixtures using Raman Data was CNN. CNN is a type of machine learning that can train algorithms. The CNN algorithm was based on *Keras v* 2.10.0 with a *Tensorflow v* 2.10.0 backend. Both pure augmentation and mixture augmentation were used to train the algorithm. **Figure 38** shows the architecture of the CNN used. CNN had two convolution layers to train the algorithm, with a 16 convolutional window (kernel). The batch normalization normalizes the layer contributions for each layer, which speeds up algorithm training. Max pooling helps with over-fitting by providing an abstracted form of the data in the training set. Flatten puts the output layer into a 1D vector. Dense classifies the spectra based on the output from the convolutional layers. The training was completed using 90 % of the data set. The other 10 % was split to validate and test the CNN algorithm. A 10-fold cross-validation was used to determine the best model.

| conv1d_input | input: | [(None, 262, 1)] |
|---|---|---|
| InputLayer | output: | [(None, 262, 1)] |

| conv1d | | input: | (None, 262, 1) |
|---|---|---|---|
| Conv1D | relu | output: | (None, 262, 128) |

| batch_normalization | input: | (None, 262, 128) |
|---|---|---|
| BatchNormalization | output: | (None, 262, 128) |

| max_pooling1d | input: | (None, 262, 128) |
|---|---|---|
| MaxPooling1D | output: | (None, 131, 128) |

| conv1d_1 | | input: | (None, 131, 128) |
|---|---|---|---|
| Conv1D | relu | output: | (None, 131, 64) |

| batch_normalization_1 | input: | (None, 131, 64) |
|---|---|---|
| BatchNormalization | output: | (None, 131, 64) |

| max_pooling1d_1 | input: | (None, 131, 64) |
|---|---|---|
| MaxPooling1D | output: | (None, 66, 64) |

| flatten | input: | (None, 66, 64) |
|---|---|---|
| Flatten | output: | (None, 4224) |

| dense | | input: | (None, 4224) |
|---|---|---|---|
| Dense | sigmoid | output: | (None, 39) |

**Figure 38:** The architecture for the CNN algorithm.

The same binary mixtures used for the cosine similarity were used as an additional test set for the individual models, using the same Raman shift range as the augmented samples. *MultiLabelBinarizer* encodes the database with augmented samples and pure and simulated mixtures.

The threshold for identification was set to 0.6 a.u. This threshold was selected to better compare the DART-MS in **Part IV** using a 0.6 a.u. threshold for predictions. The threshold is lower than other confirmatory techniques because these instruments are being used as screening methods, where the false negatives are more detrimental than the false positives. Crime scene laboratories require confirmatory techniques. The false positives will be corrected using a confirmatory technique. However, false negatives will prevent the controlled substance from being identified, as many crime laboratories stop analysis if nothing is found. A percent identification was calculated using **Equation 7** (page 29) for each model. The model with the best percent identification was also used to analyze the Maryland State Police Forensic Science Division (MSP FSD) authentic samples with the same Raman shift range.
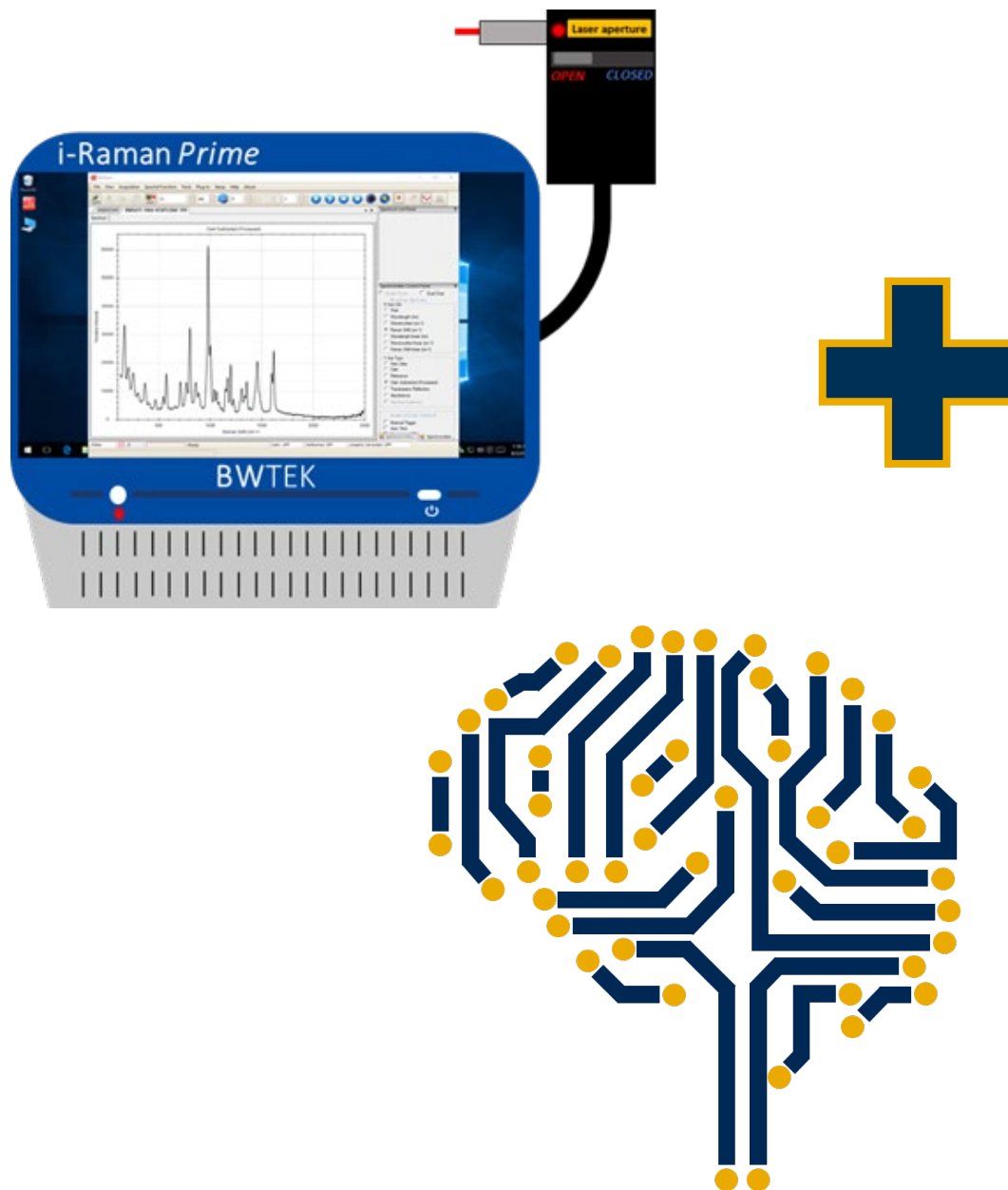
Chapter 3: Results and Discussion

Two methods were used to analyze Raman spectra, cosine similarity, and CNN. Cosine similarity was used as a regular similarity metric to better compare the results from machine learning. **Figure 39** compares a mixture spectrum of cocaine and lidocaine (1:4) and a spectrum of the standards. The same bands are highlighted in **Figure 37** to show the similarity between the simulated and collected binary mixtures. The band at 1713 cm$^{-1}$, from the carbonyl group in cocaine, is less intense in the binary mixture than in the simulated mixture. This is because the simulated mixture was at a 1:1 ratio, whereas the collected binary mixture was at a 1:4 ratio.
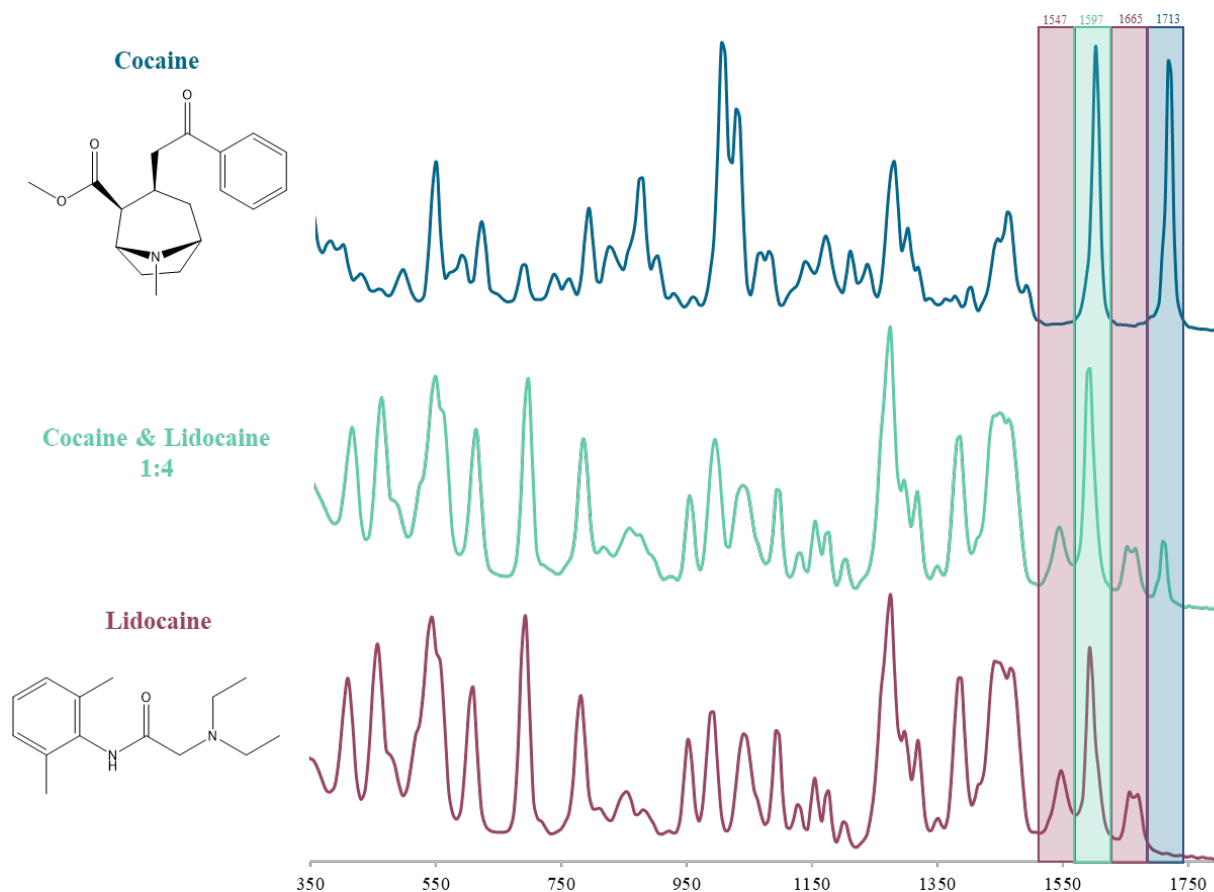


**Figure 39:** An example of a binary mixture where there are Raman bands in the mixture spectrum correlates to both standards. The purple highlighted section shows where the mixture, lidocaine, and cocaine all have the same peak at the same location. The green highlighted sections show a location where the mixture spectrum correlates to lidocaine. The blue highlighted section shows a location where the mixture spectrum correlates to cocaine.

*3.1 – Cosine Similarity*

3.1.1 – Binary mixtures

       The top five results from the cosine similarity were used to predict the compounds in the binary mixtures. **Figure 40** shows a histogram of the cosine similarity scores for each replicate of the binary mixtures. The lowest cosine similarity score was 0.65 a.u., and the average score was 0.96 a.u.
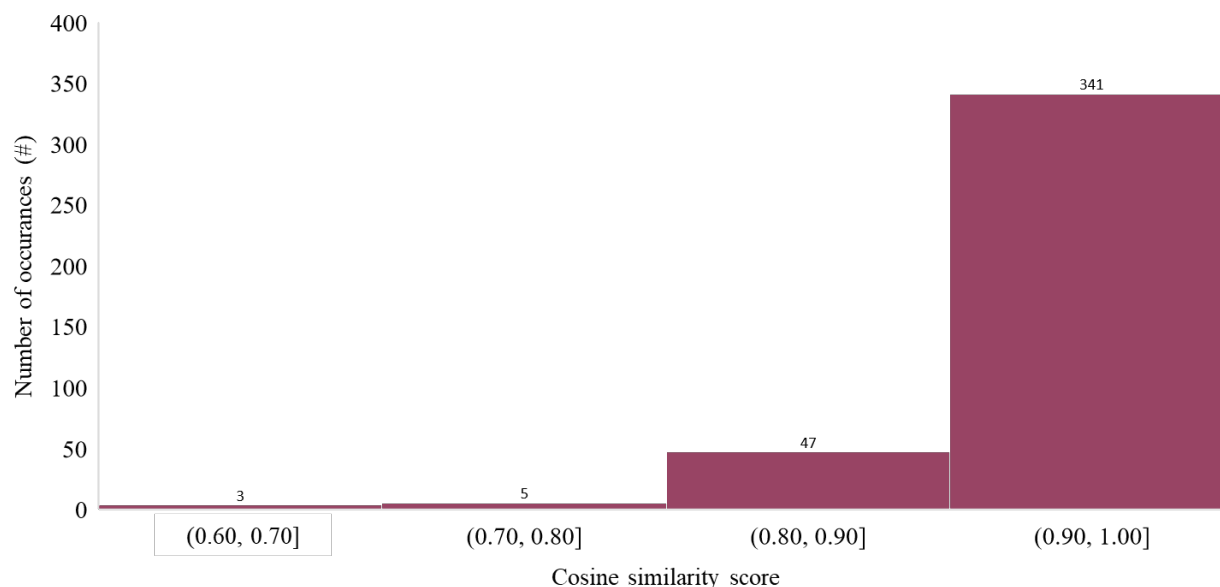


**Figure 40:** Histogram of the cosine similarity scores for the ground truth of the binary mixtures.

       **Figure 41** compares using the replicates as individual samples and combining three replicates for one overall sample. The percent identification for the individual replicates was 66 %. When the results of the three replicates are combined to identify each mixture, the percent identification increases to 72.0%. The percentage increases because the replicates allow for a more representative mixture sample. Since the top five scores were used for the results, there were false positives in all the results. However, all the individual replicates did successfully identify at least one compound. For example, in a mixture of methamphetamine and amphetamine at a 1:4 ratio, amphetamine had a score of 0.99, and methamphetamine had a score of 0.92. However, ephedrine also had a score of 0.92 and pseudoephedrine had a score of 0.89. The false positives present in the results could be minimized with a scoring threshold or by limiting the top scores used for the percent identification. The TacticID and the Mira portable Raman instruments from Part II used a HQI threshold of 85% and made the top three scores visible. There would still be false positives

using these parameters, like the above example. Many of the compounds that had similar spectra tended to have similar scores, which created several false positives.

The mixtures were separated into ratios to assess their effect on cosine similarity's ability to identify both compounds. **Figure 42** shows the number of mixtures that identified either 0, 1, or 2 compounds separated by each ratio. For the same graph but using replicates as individual samples, see **Figure A - 3** in the **Appendix**. As the samples get more diluted in both instances, the algorithm's ability to identify both compounds decrease.
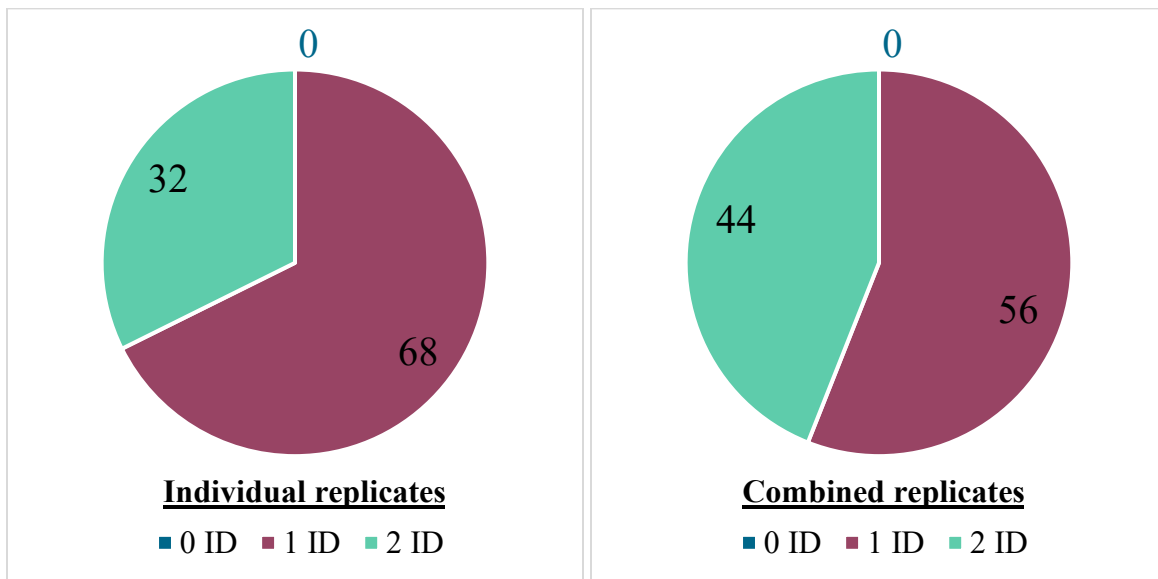


**Figure 41:** Two pie charts comparing the percentage of mixtures able to identify either 0, 1, or 2 compounds in the binary mixtures. The one on the left uses the replicates as individual samples. The one on the right combined the replicates into one overall result for each mixture. All samples identified at least one compound.
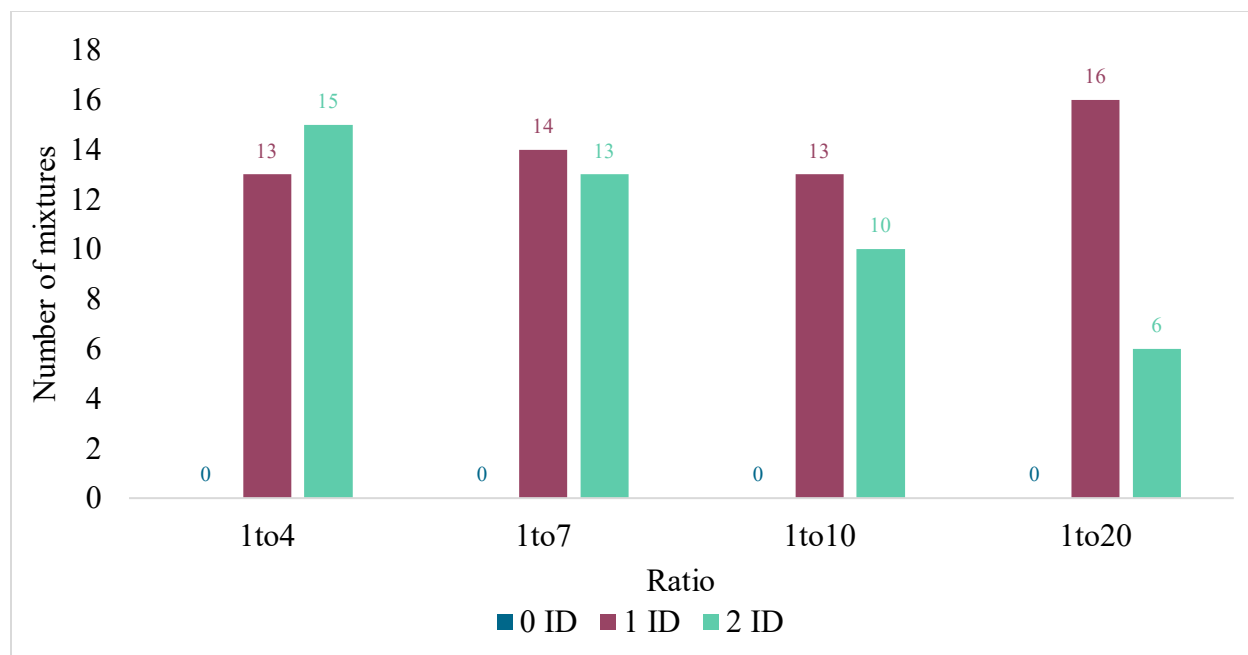
**Figure 42:** Number of each mixture for each ratio of the binary mixtures when using the combined results. The "0 ID", "1 ID", "2 ID" is the number of mixtures that identified either 0, 1, or 2 compounds respectively.

3.1.2 – Authentic samples

The 12 authentic samples from the MSP FSD were analyzed using cosine similarity with the same approach. The percent identification for the authentic samples was 36.4 %. The authentic samples had more issues than the binary mixtures because the authentic samples consisted of more complex samples. Some of the components in the authentic samples were not included in the 38 standards.

*3.2 – Convolutional Neural Network*

3.2.1 – Binary mixtures

The second data analysis tool used for Raman analysis included CNN. The average classification report for each compound across the 10-fold cross-validation can be found in **Table 12**. **Figure 43** shows the classification report micro-averages for the ten models and the percent identification for the binary mixtures for each model. **Table A - 1** in the **Appendix** shows the precision, recall, and f1-scores values for all the folds. The micro-average was used so that all drug samples were treated equally. When looking at the micro-averages, fold 8 gave the best precision, fold 2 gave the best recall, and fold 3 gave the best f1-score. Typically, the f1-score is the best metric because it considers precision and recall. However, precision is the best metric for a forensic

screening test because it is more important to identify the drug present. The false positives can be corrected during the confirmatory analysis. If a screening analysis does not identify the controlled substance, giving a false negative result, the analysis will most likely be stopped, and the drug will not be identified. The binary mixtures were used as an additional test set for each model. Fold 6 gave the best percent identification, with 82.3 % using the replicates as individual samples. However, Fold 3 gave the best percent identification with 94.0 % when the replicates were combined into one result. The best fold differs based on the metric and test set used because each fold uses a different training and testing set from the data provided. Therefore, there will be differences in the features extracted for each fold.

**Table 12:** Score average ± standard error of the 10-fold cross validation classification report.

| | Precision ± σ | Recall ± σ | f1-score ± σ |
|---|---|---|---|
| 4-MEC | 99.82 ±0.04 | 98.71 ±0.12 | 99.26 ± 0.07 |
| 4-MMC | 99.54 ± 0.11 | 97.57 ± 0.18 | 98.55 ± 0.12 |
| Acetaminophen | 99.65 ±0.35 | 99.09 ±0.05 | 99.37 ± 0.18 |
| Alprazolam | 99.67 ±0.18 | 98.76 ±0.13 | 99.21 ± 0.18 |
| Amphetamine | 99.87 ±0.09 | 98.63 ±0.12 | 99.25 ± 0.08 |
| Aspirin | 99.75 ±0.21 | 98.88 ±0.13 | 99.31 ± 0.12 |
| Benzocaine | 99.94 ±0.03 | 98.80 ± 0.14 | 99.36 ± 0.07 |
| Boric Acid | 99.51 ±0.30 | 98.36 ±0.18 | 98.93 ± 0.14 |
| Caffeine | 99.66 ±0.24 | 98.92 ±0.09 | 99.29 ± 0.13 |
| Carfentanil | 99.66 ±0.22 | 97.87 ±0.18 | 98.75 ± 0.15 |
| Cocaine | 99.97 ±0.03 | 99.21 ±0.10 | 99.59 ± 0.06 |
| Codeine | 99.97 ±0.03 | 98.86 ±0.09 | 99.41 ± 0.05 |
| Dibutylone | 100.00 ± 0.00 | 99.02 ±0.05 | 99.51 ± 0.03 |
| Diltiazem | 99.95 ± 0.05 | 99.33 ± 0.11 | 99.64 ± 0.07 |
| Dimethyl Sulfone | 99.94 ± 0.06 | 98.99 ± 0.06 | 99.46 ± 0.04 |
| Diphenhydramine | 99.63 ± 0.22 | 97.94 ± 0.12 | 98.77 ± 0.09 |
| Ephedrine HCl | 99.70 ± 0.13 | 97.95 ± 0.17 | 98.81 ± 0.11 |
| Eutylone | 99.02 ± 0.36 | 96.86 ± 0.21 | 97.93 ± 0.26 |
| Fentanyl | 99.87 ± 0.08 | 97.93 ± 0.18 | 98.89 ± 0.09 |

| | | | |
|---|---|---|---|
| Heroin | 99.71 ± 0.20 | 98.72 ± 0.12 | 99.21 ± 0.12 |
| Hydroxyzine | 99.80 ± 0.20 | 98.92 ± 0.10 | 99.35 ± 0.11 |
| Ketamine | 99.99 ± 0.01 | 98.98 ± 0.11 | 99.48 ± 0.06 |
| Levamisole | 99.74 ± 0.18 | 98.27 ± 0.11 | 99.00 ± 0.08 |
| Lidocaine | 99.61 ± 0.27 | 99.28 ± 0.07 | 99.44 ± 0.14 |
| Maltose | 99.81 ± 0.15 | 98.88 ± 0.07 | 99.34 ± 0.08 |
| Mannitol | 99.55 ± 0.40 | 98.55 ± 0.08 | 99.04 ± 0.18 |
| Methamphetamine | 99.95 ± 0.04 | 98.01 ± 0.07 | 98.97 ± 0.05 |
| Mitragynine | 99.79 ± 0.10 | 95.95 ± 0.22 | 97.83 ± 0.13 |
| Myo-inositol | 99.97 ± 0.02 | 98.67 ± 0.10 | 99.32 ± 0.05 |
| Naltrexone | 99.87 ± 0.06 | 98.82 ± 0.12 | 99.34 ± 0.06 |
| Phenacetin | 99.91 ± 0.09 | 98.89 ± 0.10 | 99.39 ± 0.05 |
| Phenolphthalein | 100.00 ± 0.00 | 99.44 ± 0.05 | 99.72 ± 0.03 |
| Polyethylene Baggie** | 99.85 ±0.08 | 93.58 ±0.31 | 96.61 ± 0.15 |
| Procaine | 99.94 ± 0.05 | 98.86 ± 0.13 | 99.40 ± 0.09 |
| Pseudoephedrine | 99.99 ± 0.013 | 98.60 ± 0.12 | 99.28 ± 0.06 |
| Quinine | 99.91 ± 0.09 | 98.97 ±0 .08 | 99.44 ± 0.05 |
| Sorbitol | 99.60 ± 0.18 | 98.53 ± 0.04 | 99.06 ± 0.09 |
| Starch | 98.50 ± 0.66 | 98.83 ± 0.10 | 98.66 ± 0.32 |
| Δ9-THC | 99.41 ± 0.43 | 97.70 ± 0.11 | 98.54 ± 0.22 |

σ = standard error, 4-MEC = 4-Methylethcathinone, 4-MMC = 4-Methylmethcathinone, Δ9-THC = Delta-9-tetrahydrocannabinol
** empty plastic bag was used to identify possible interference from the baggie.
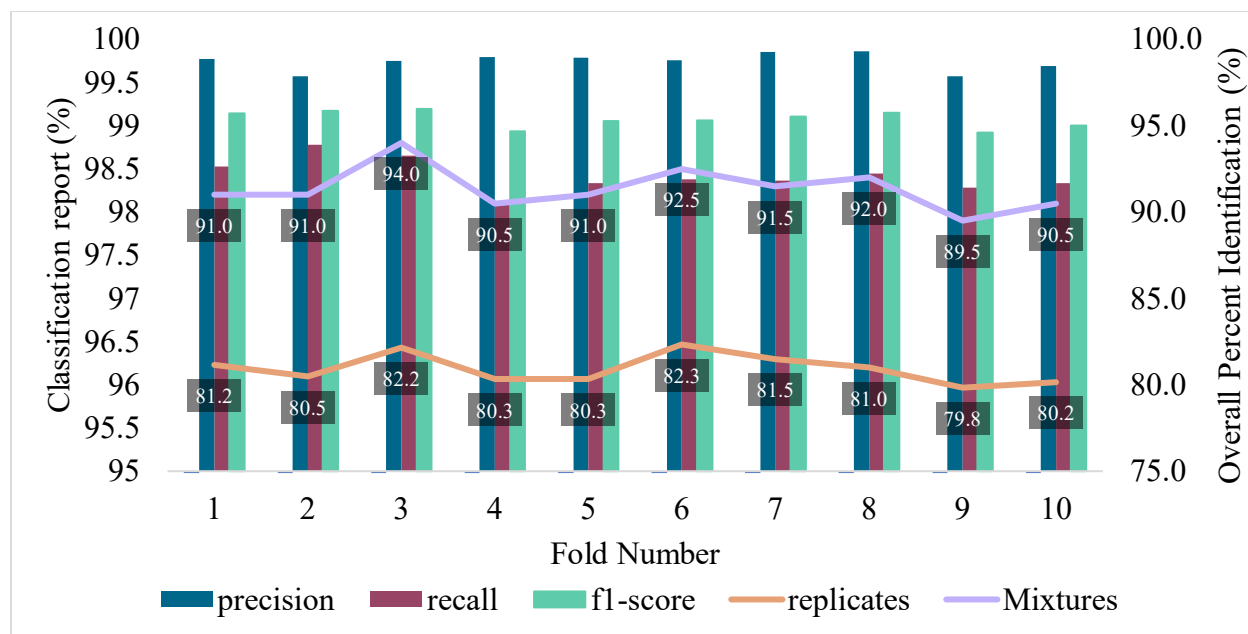
**Figure 43:** Micro-average for the CNN precision, recall, and f1-score across a 10-fold cross-validation. The peach line displays the percent identification for each of the folds using replicates of the binary mixtures. The light purple line combines the triplicate results into one result for each mixture.

Like cosine similarity, all compounds listed as a potential match were listed in the results. This also created several false positives. Looking at the results from the binary mixtures using fold 3, each compound had on average 8-9 potential compounds above the 0.60 threshold. The false positives could be decreased by using a higher threshold. A 0.60 threshold was used to better compare CNN to the DIT software, which will be discussed in **Part III**. Only looking at the top 3-5 results would also limit the false positives. CNN reports the top results in alphabetical order, so the programmer/analyst will have to update the code to report the similarity score and sort the score in descending order, reporting only the top 3-5 results above the threshold. However, just like cosine similarity all replicates had at least one true positive result.

The mixtures were separated by their respective ratios to see how the ratios affected CNN's ability to detect mixtures. Fold 3 was used to show the effect because it gave the highest percent identification for the combined results. **Figure 44** shows the trend in CNN's ability to detect binary mixtures. Like cosine similarity, the algorithm's ability to identify both compounds decreases as the samples get more diluted.
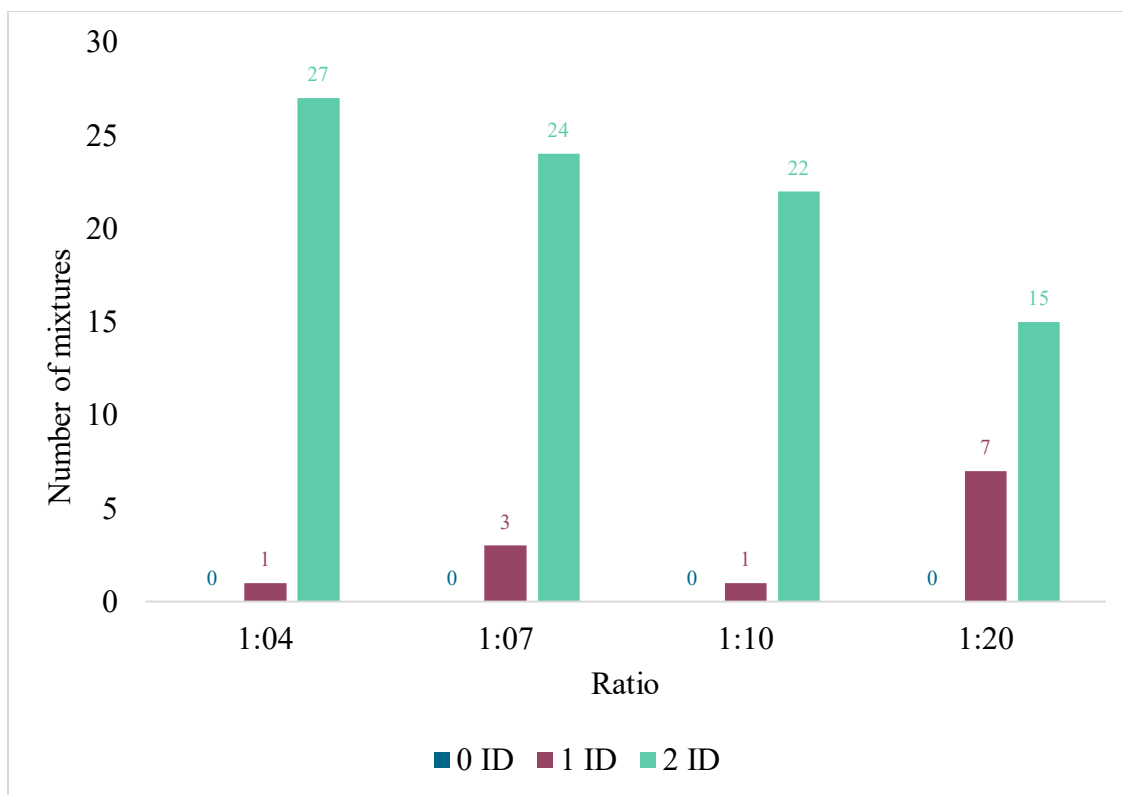
**Figure 44:** Effect of the ratios on the CNN'S ability to detect mixtures, using the combined results. The "0 ID", "1 ID", "2 ID" is the number of mixtures that identified either 0, 1, or 2 compounds respectively.

3.2.2 – Authentic Samples from MSP

Authentic samples from the Maryland State Police Forensic Sciences Division (MSP FSD) were analyzed on Folds 3 and 6 as they provided the best percent identification for the binary mixtures. The replicates were combined to have better variability of each sample. Fold 3 gave the better percent identification for the authentic samples at 41.2 %. The drop in percent identification is because CNN was trained with binary mixtures, whereas many authentic samples were more complex. This number can be further improved using more complex mixture augmentation for the training set.
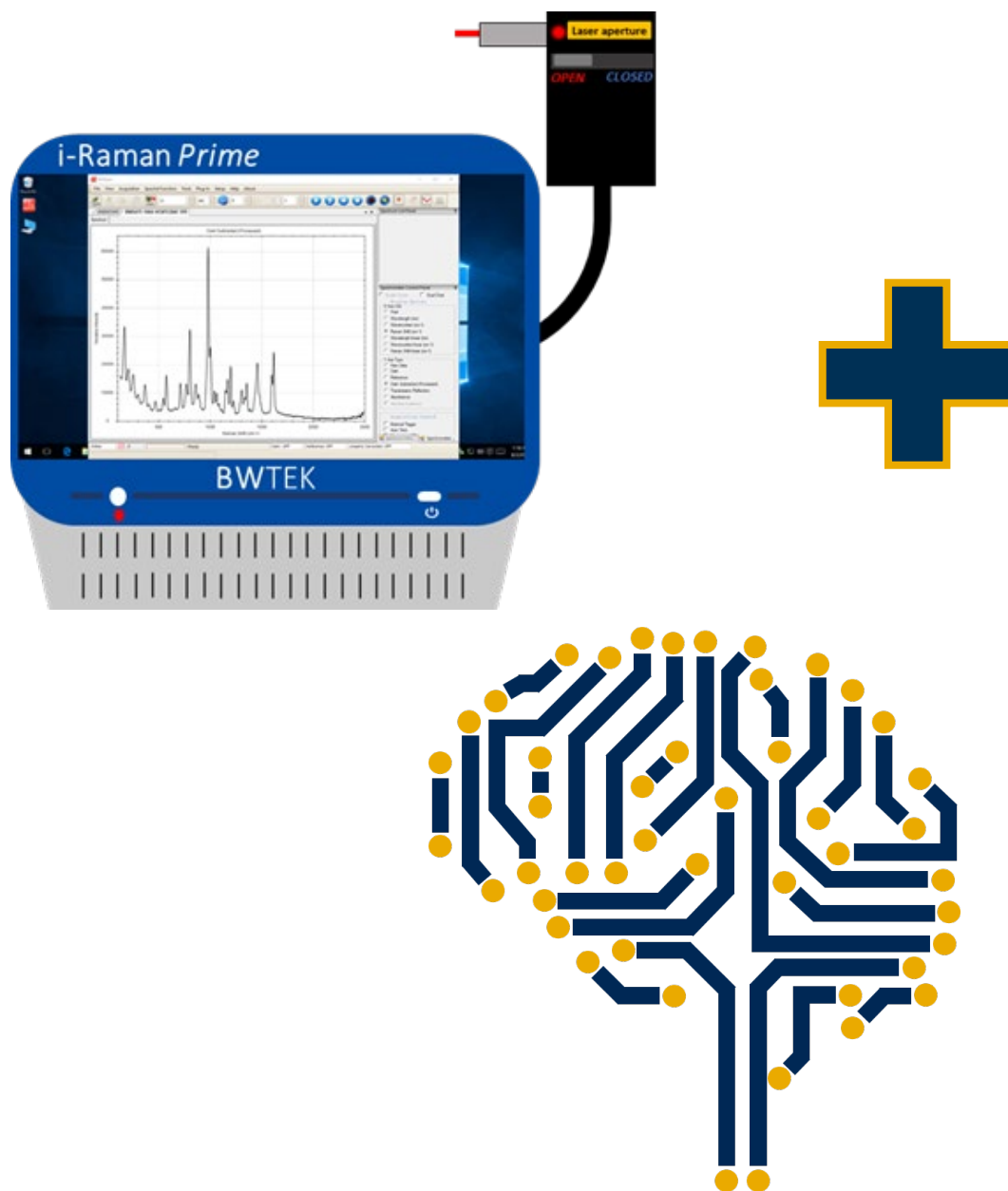
Chapter 4: Conclusions

**Figure 45** compares the cosine similarity and CNN's ability to identify 0, 1, or 2 compounds in the mixtures. Cosine similarity was used as a traditional similarity metric to compare against CNN. The Cosine similarity identified at least one compound for every replicate. Cosine similarity gave a percent identification of 71.5 % when using the combined replicates. It was more difficult for CNN to identify the more diluted sample, as seen in **Figure 42**. For the 1:4 ratio, out of 28 samples, 13 identified one component, and 6 identified both components. For the 1:20 ratio, out of 22 samples, 16 identified one component, and 15 identified both components. The authentic samples from the MSP FSD gave a percent identification of 36.4 %.

The CNN algorithm performed better than cosine similarity. Ten different models were trained to predict compounds present in complex samples. Fold 2 had the best precision, and Fold 6 had the best recall and f1-score. Fold 3 gave the best percent identification for binary results at 94.0 % using the combined results. CNN also had a trend where it had more difficulty identifying both components, as seen in **Figure 44**. For the 1:4 ratio, out of 28 samples, all but one could identify both components. For the 1:20 ratio, out of 22 samples, 7 identified one component, and 15 identified both components. This trend is less significant than in the cosine similarity results. Fold 3 also gave the best percent identification for authentic samples from the MSP FSD at 41.2 %.
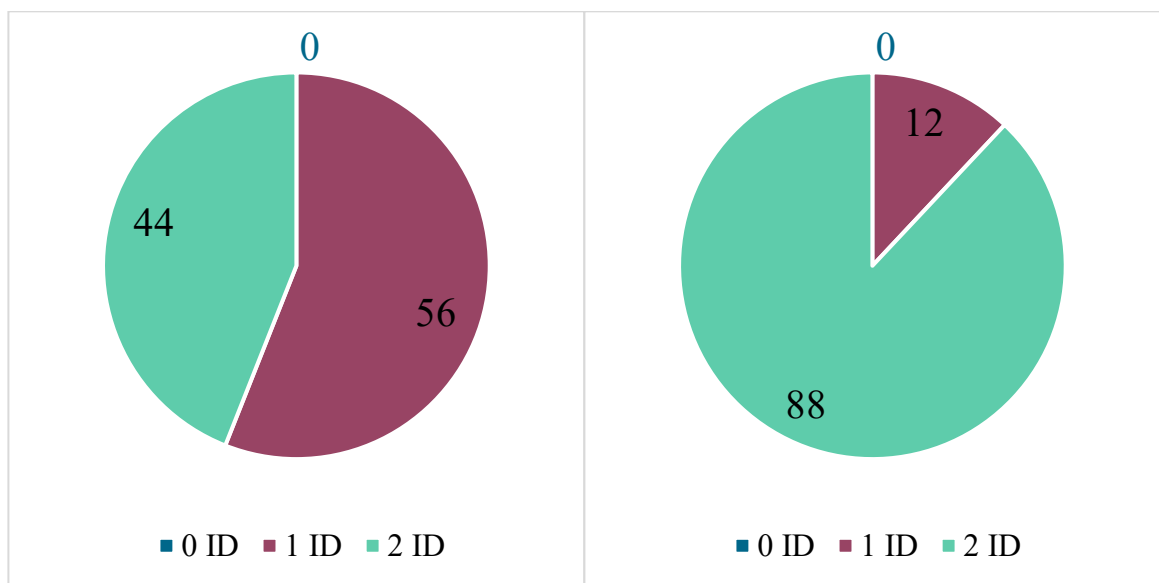


**Figure 45:** Two pie charts comparing the percentage of mixtures that identified either 0, 1, or 2 compounds in the binary mixtures using the combined results. The one on the left is from the cosine similarity. The one on the right is from CNN. All samples identified at least one compound.

Overall, the CNN was better capable of identifying complex samples. The CNN had over 20 % higher percent identification when compared to the cosine similarity. CNN also had a higher percent identification for authentic samples. However, both methods had difficulty analyzing the more complex samples. Both cosine similarity and CNN had issues with false positives due to the methods/parameters used for analysis. Cosine similarity looked at the top 5 results and CNN listed all compounds above a 0.60 a.u. threshold. By limiting the number of potential results and by minor adjustments to the CNN, the false positives could be limited. However, it should be noted that these are being used as a screening technique, and therefore the false positives are not as problematic as they are for confirmatory testing.

The CNN worked well analyzing the binary mixtures but had difficulty analyzing authentic samples. This is likely because the algorithm was only trained on binary mixtures. Only three authentic samples were similar to the augmented mixtures used to train the CNN algorithm. The other samples were either more complex having up to eight compounds present or had compounds present not included in the training set, like 6-monoacetylmorphine (6-MAM). If bands were present from 6-MAM, the CNN would not be able to identify the 6-MAM and would try to match the bands to a compound with a similar band in the training set.

# Part IV: Direct Analysis in Real-Time Mass Spectrometry
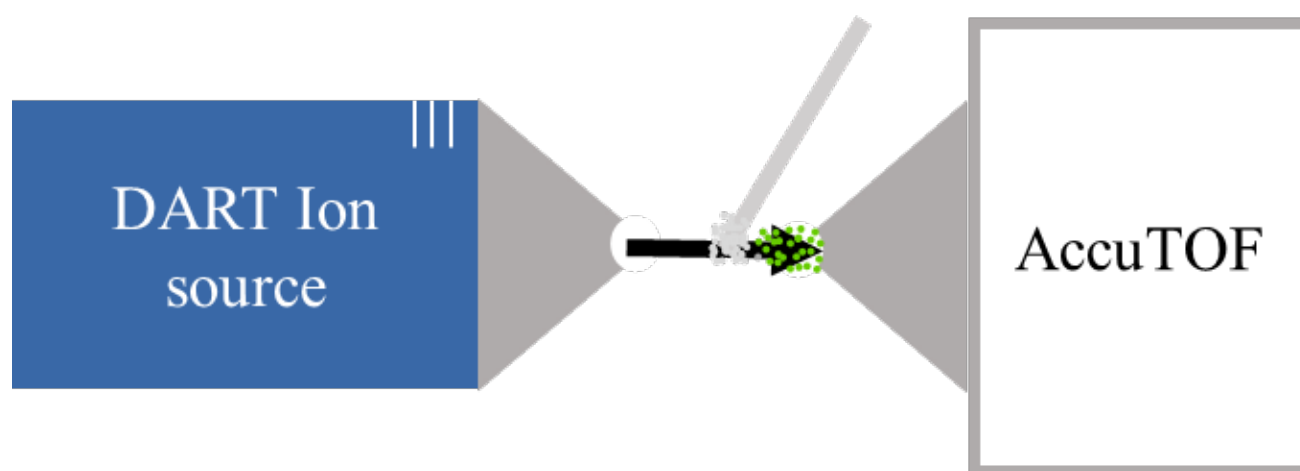


Chapter 1: Relevant Literature Review

*1.1 – Theory of DART-MS*

Investigation into ambient ionization techniques has led to many different forms of ionization over the years. An ambient ionization technique called direct analysis in real-time mass spectrometry (DART-MS) was developed in 2003 by Dr. Robert Cody [96] and commercialized in 2005. [97] In ambient ionization, a sample is analyzed/ionized in the open atmosphere. DART-MS provides a sensitive and near-complete mass spectrum in a matter of seconds. [98] DART-MS uses metastable gas to ionize the analytes of interest, where the ions can then be analyzed via mass spectrometry (MS).

DART-MS passes a gas, usually helium, through a needle electrode with a high voltage, creating a corona discharge. [99] This produces ions, electrons, and excited-state atoms. The ions and electrons are neutralized, and the excited-state neutral species (metastable gas) exits the ionization source into the sample interface, where the sample gets ionized. DART-MS uses Penning ionization to ionize the sample. [99] Penning ionization occurs when a metastable molecule collides with another molecule to ionize it. The most common gas used is helium because its excited electronic state has an energy of 19.8 eV and can ionize atmospheric water and oxygen. [100] There are two potential ionization methods: positive and negative. In positive ionization, the metastable helium molecules ($He^*$) react with atmospheric water to create water clusters which are then used to protonate the sample. These reactions can be seen in **Equation 14** through **Equation 17**.

| | |
|---|---|
| **Equation 14:** | $He^* + H_2O \rightarrow H_2O^{+\bullet} + He + e^-$ |
| **Equation 15:** | $H_2O^{+\bullet} + H_2O \rightarrow H_3O^+ + OH^-$ |
| **Equation 16:** | $H_3O^+ + nH_2O \rightarrow [(H_2O)_n + H]^+$ |
| **Equation 17:** | $M + [(H_2O)_n + H]^+ \rightarrow [M + H]^+ + nH_2O$ |
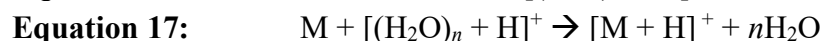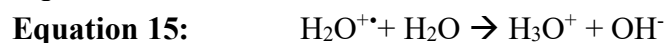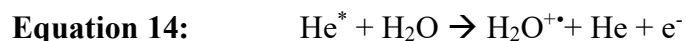
In negative ionization, the metastable helium gets thermalized to release electrons which react with atmospheric oxygen, which then react with the analyte to deprotonate the sample. These reactions can be seen in **Equation 18** and **Equation 19**.

| | |
|---|---|
| **Equation 18:** | $O_2 + e^- \rightarrow O_2^{-\bullet}$ |
| **Equation 19:** | $O_2^{-\bullet} + M \rightarrow [M - H]^- + OOH^\bullet$ |
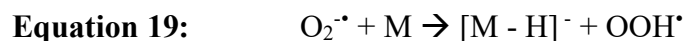
*1.2 – Accurate Time-of-flight Mass Spectrometer*

This project will use an accurate time-of-flight mass spectrometer or AccuTOF, which provides high-resolution data for the entire spectrum with no sensitivity loss. [100] There is an atmospheric pressure interface (API) where the ions enter the AccuTOF and are guided

electrostatically through two off-center orifices to an ion guide/transport. The off-center orifices are set at different potentials. Orifice 1 is the difference between the orifices. The difference allows in-source collision-induced dissociation (is-CID) to provide both the protonated or deprotonated molecule and the fragmentation pattern. The ion guide/transport is a quadrupole with only radio frequencies to focus the ion lens and bring the ions into a high vacuum region. The ions then travel to the analyzer, where a 2-step acceleration occurs to separate the ions based on their mass. Orthogonal acceleration (OA) gives the ions equal kinetic energy. Assuming the ions have the same kinetic energy, the smaller ions will travel faster than the larger ions. A reflectron accounts for possible kinetic energy variations, making higher energies travel faster. After the separation, the ions are detected with a micro-channel plate, an electron multiplier. Several parameters can be optimized. Orifice 1 is the difference between the two orifices. The difference will change the amount of fragmentation. The peak voltage, or RF ion guide voltage, determines the smallest m/z detected. Finally, the multiplier voltage controls the signal and the spectra noise. [101]

*1.3 – Previous Applications*

DART-MS has been used in security applications [102], fieldwork [103], distinguishing plant material [104], and identifying possible drugs in drinks. [105,106] In 2010, Steiner used DART coupled with a high-resolution time-of-flight mass spectrometer (AccuTOF-MS) as a confirmatory technique for the identification of iodine and red phosphorous, which are two chemicals used in the manufacture of methamphetamine. [107] In 2015, Gwak et al. used DART and a portable ion trap mass spectrometer to analyze common and designer drugs, including methamphetamine and amphetamine. The ion trap enabled the mass spectrometer to be completely field accessible. [108] In 2017, Lian et al. combined a DART time-of-flight mass spectrometer (DART-TOF-MS) with ion mobility spectrometry (IMS) for rapid screening of 53 drugs of abuse, including ephedrine, pseudoephedrine, methamphetamine, and amphetamine. Both amphetamine and methamphetamine had a LOD of 0.05 µg, and ephedrine and pseudoephedrine had a LOD of 0.2 µg. [109] Also, in 2017, Sisco et al. used Thermal Desorption DART-MS (TD-DART-MS) to detect fentanyl, fentanyl analogs, and opioids as a screening technique. [110] In 2019, Sisco et al. analyzed the drug packaging of evidence bags and the inner drug packaging as a screening test to determine the bag's contents. An estimated 1-10µg was found on the inner drug packaging, resulting in a 91 % accuracy. [111]

*1.3 – Data Interpretation Tool*

In 2021, NIST and NIJ developed the DART-MS Data Interpretation Tool (DIT) to help analyze complex DART-MS data [112]. The DIT identifies potential fragments from a complex spectrum that could be related to a pure standard in a library by identifying partial patterns. This thesis used three in-source collision-induced dissociation (is-CID) energies to vary the sample fragmentation amount. Low energy (~30 V) have little to no fragmentation, where the mass spectrum can give the molecule analyzed. The medium (~ 60 V) and high (~ 90 V) increase the fragmentation of the molecules. Using all three levels, the DIT can compare the collected sample more accurately to the library by comparing the molecular ion and its fragmentation pattern.

The first step the DIT performs is target selection, where the DIT will select the fragments above a user-defined relative intensity or target threshold using the low fragmentation mass spectrum. [113] Then DIT will identify potential compounds in the library based on the identified targets, and the user sets mass tolerance, usually 5 mDa. In this step, the DIT classifies the targets in the collected spectrum that have a potential match in the library spectrum. The targets include Protonated molecule, +1 Isotope of the protonated molecule, base peak, +1 isotope of the base peak, and major fragment ion. [113] The last set in the DIT compares the targets from the collected mass spectrum and the identified potential compound spectrum. This step is performed using all the mass spectra included in the search. So if the user only includes the low-fragmentation spectrum, only the low-fragmentation of the library spectrum will be compared. By including the higher fragmentation mass spectra from the sample, the DIT can better compare the mass spectra by comparing the fragmentation patterns.

Three similarity scores are visible on the latest version of the DIT, fraction of library peak intensity explained (FPIE), reverse match factor (RevMF), and low-fragmentation mass spectrum protonated molecule Isotope ratio difference (LFPM IRD) [113]. FPIE uses the total peak intensity that can be related to the pure spectrum in the library. The RevMF is a cosine similarity score between the related fragments between the mixture spectrum and the pure spectrum in the library. LFPM IRD is the difference between the protonated molecule and its major isotope. No value is reported if the protonated molecule and its major isotope are absent. The DIT has been used in previous publications to detect seized drugs.

DIT has previously been used in seized drug analysis. Sisco et al. [114] performed qualitative analysis using the DIT to assess the target results of the DIT using the scheme shown

in **Figure 46**. The scheme ranks the target results based on whether the expected compounds are present and if there are other compounds present above the threshold. The assessment considers both the same class as the expected compound and if it is a different class from the expected compound.
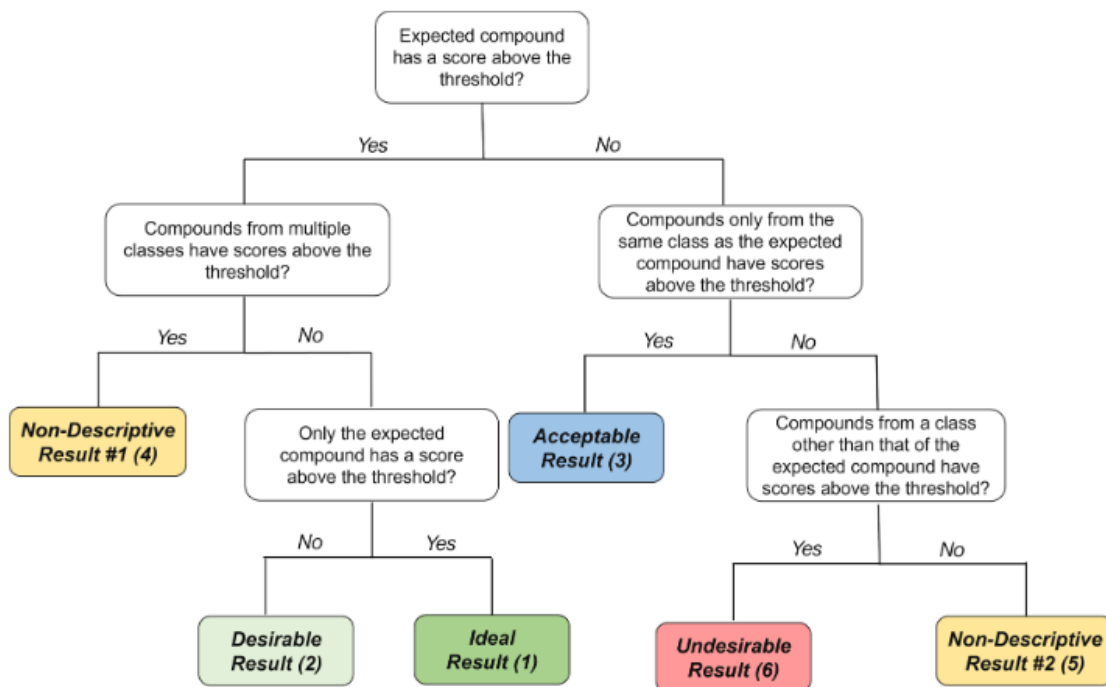


**Figure 46:** Assessment scheme for the target results using the DIT. [114]

Appleya et al. [115] ed DART-AccuTOF and the DIT to develop an analytical platform that provides comprehensive and real-time drug and cutting agent information for most samples. The authors analyzed paraphernalia residues to provide near complete chemical profiles of the drug and cutting agents in the illicit substance and found that the DART-AccuTOF detected a wide range of drugs and cutting agents, with only occasionally needing additional methods, like tandem mass spectrometry. Couch et al. [116] assessed the DIT's ability to use different ionization sources. The authors compared DART-is-CIS and ESI-is-CID. They found that the ESI-is-CID and the DART-is-CID provided comparable mass spectra and had near identical results when using the DIT.
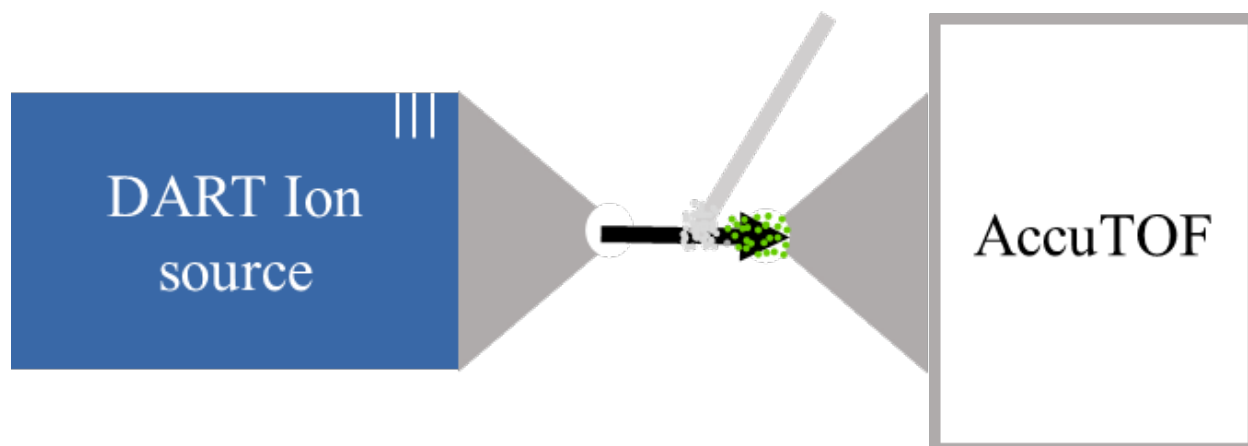
# Chapter 2: Materials, Methods, and Experimental Design

*2.1 – Materials*

**Table 13** shows the 60 binary mixtures analyzed by DART-MS (✱). The mixtures analyzed by Raman from the previous section are also included to show the similarity. The mixtures not analyzed with DART-MS for this section were already analyzed in another publication by a previous group member. The same twelve adjudicated samples from **Part III** and the two pharmaceutical drugs from **Part II** were also analyzed by the DART-MS and DIT.

**Table 13:** The binary mixtures analyzed by Raman (✓) and DART-MS (✱). The differences in the mixtures were due to the libraries available for each technique.

| Mixture | Mass Ratio | | | |
|---|---|---|---|---|
| | 1:4 | 1:7 | 1:10 | 1:20 |
| 4-MEC : Benzocaine | | ✓ | ✓✱ | |
| 4-MEC : Maltose | ✓ | ✓ | | |
| 4-MMC: Lidocaine | ✱ | ✓ | ✓ | |
| 4-MMC : Maltose | ✓ | | | |
| Acetaminophen : Myo-inositol | | | ✓ | ✓ |
| Alprazolam : Caffeine | ✓ | ✓ | | |
| Alprazolam : Levamisole | ✓✱ | ✓✱ | | |
| Amphetamine : Acetaminophen | ✓✱ | | ✓✱ | ✓✱ |
| Amphetamine : Caffeine | | ✓✱ | | ✓✱ |
| Caffeine : Levamisole | ✓ | ✓ | | |
| Cocaine : Benzocaine | ✓ | | | |
| Cocaine : Boric acid | | | ✓ | |
| Cocaine : Diltiazem | ✓✱ | ✓✱ | ✓✱ | ✓✱ |
| Cocaine : Levamisole | ✓ | | | |
| Cocaine : Caffeine | ✓✱ | ✓✱ | ✓✱ | ✓✱ |
| Cocaine : Hydroxyzine | ✓✱ | | ✓✱ | |
| Cocaine : Lidocaine | ✓✱ | ✓✱ | | ✓✱ |
| Cocaine : Maltose | | ✓ | | ✓ |
| Cocaine : Procaine | ✓✱ | ✓✱ | ✓✱ | |
| Codeine : Acetaminophen | ✓✱ | ✓✱ | ✓✱ | ✓✱ |

| | 4-MEC | 4-MMC | | |
|---|---|---|---|---|
| Codeine : Maltose | ✓ | ✓ | ✓ | ✓ |
| Ephedrine : Acetaminophen | ✓✹ | | | ✓✹ |
| Ephedrine : Caffeine | | ✓✹ | ✓✹ | |
| Ephedrine : Levamisole | | ✓ | ✓ | |
| Fentanyl : Cocaine | ✓✹ | | | |
| Fentanyl : Methamphetamine | ✓✹ | | | |
| Fentanyl : Caffeine | | | | ✓✹ |
| Heroin : Acetaminophen | ✓ | ✓✹ | | ✓✹ |
| Heroin : Quinine | | | ✓ | |
| Hydroxyzine : Maltose | | ✓ | ✓ | |
| Methamphetamine : Acetaminophen | ✓✹ | ✓✹ | | ✓✹ |
| Methamphetamine : Amphetamine | ✓✹ | ✓✹ | | |
| Methamphetamine : Caffeine | ✓✹ | ✓✹ | ✓✹ | |
| Methamphetamine : Dimethyl Sulfone | ✓ | | | ✓ |
| Methamphetamine : Ephedrine | ✹ | ✓✹ | ✓✹ | ✓✹ |
| Methamphetamine : Maltose | | | | ✓ |
| Methamphetamine : Levamisole | ✓ | ✓✹ | ✓ | ✓ |
| Methamphetamine : Pseudoephedrine | ✓✹ | ✓✹ | ✓✹ | ✓✹ |
| Naltrexone : Maltose | ✓ | ✓ | ✓ | ✓ |
| Phenacetin : Sorbitol | | ✓ | | ✓ |
| Procaine : Starch | ✓ | | ✓ | |
| Pseudoephedrine : Acetaminophen | ✓✹ | | | ✓✹ |
| Pseudoephedrine : Caffeine | | ✓✹ | ✓✹ | |
| Pseudoephedrine : Levamisole | ✓ | | | ✓ |
| Sufentanil : caffeine | ✹ | | | |

4-MEC = 4-Methylethcathinone, 4-MMC = 4-Methylmethcathinone

*2.2 – Instrumentation and Data Collection*

DART-MS spectra were acquired in positive ionization mode with an IonSense DART-SPV ion source (Saugus, MA) and a JEOL AccuTOF 4G-LC-plus mass spectrometer (Peabody, MA). Data collection used the parameters outlined in **Table 14**. The DART-MS was calibrated using polyethylene glycol (PEG). Data collection was performed by first dipping the end of a capillary tube in the gas stream to remove any byproducts from the manufacturing process of the capillary tubes. The cleaned capillary tubes were cooled to room temperature and put directly into the binary mixture powder. The dipped capillary tubes were reinserted into the gas stream, and the time was recorded on a run sequence for future reference. The AB-FUBINACA was analyzed first and reanalyzed throughout the run to account for mass drift during the run. The 60 binary mixtures in **Table 11** were analyzed in triplicate to account for the variation in the mixture. A time sequence was created, including the mixture analyzed and the analysis time.

**Table 14:** DART-MS parameters

| | |
|---|---|
| DART Temperature | 400 °C |
| DART gas | Helium |
| Orifice 1 voltage | 30 V, 60 V, 90 V, switching as 0.2 s/scan |
| Ring voltage | 5 V |
| Orifice 2 voltage | 20 V |
| Ion guide | 500 V |
| m/z scan range | m/z 50 – m/z 800 |

*2.3 – MsAxel*

DART analysis was performed using msAxel Data Processing LP by JEOL (Peabody, MA). Drift compensation was performed using m/z 352.14558 from AB-FUBINACA. One mass spectrum for each mixture was extracted for each in-source collision-induced dissociation (is-CID) voltage. The mass spectrum gave the average mass fragments across all three replicates.

*2.4 – NIJ/NIST Data Interpretation Tool*

The extracted mass spectra were analyzed using NIJ and NIST's DART-MS Data Interpretation Tool (DIT). The targeting threshold used 4 % relative intensity. The DIT m/z tolerance was set to $\pm$ 0.005 Da. The three mass spectra for each mixture were uploaded and target fragments were identified. A score for the LFPM IRD was required for the result to be correct. This metric requires at least two fragments related to the result, the protonated molecule and its major isotope. Therefore, without an LFPM IRD score, the DIT did not find a protonated molecule

as a target fragment. Two arbitrary thresholds, 0.60 a.u. and 0.70 a.u., were selected for the spectral similarity scores. The scoring metrics included a fraction of library peak intensity explained (FPIE) and reverse match factor (RevMF). These thresholds were used to determine what threshold and similarity metric works better. A percent identification (**Equation 7** on page 29) was also calculated for each threshold and similarity metric. Spectra with a compound without a target fragment identified using FPIE were reanalyzed with a lower target threshold to see how it affected the identification. The metric and ratio with the best percent identification were used for the pharmaceutical pills and authentic samples.
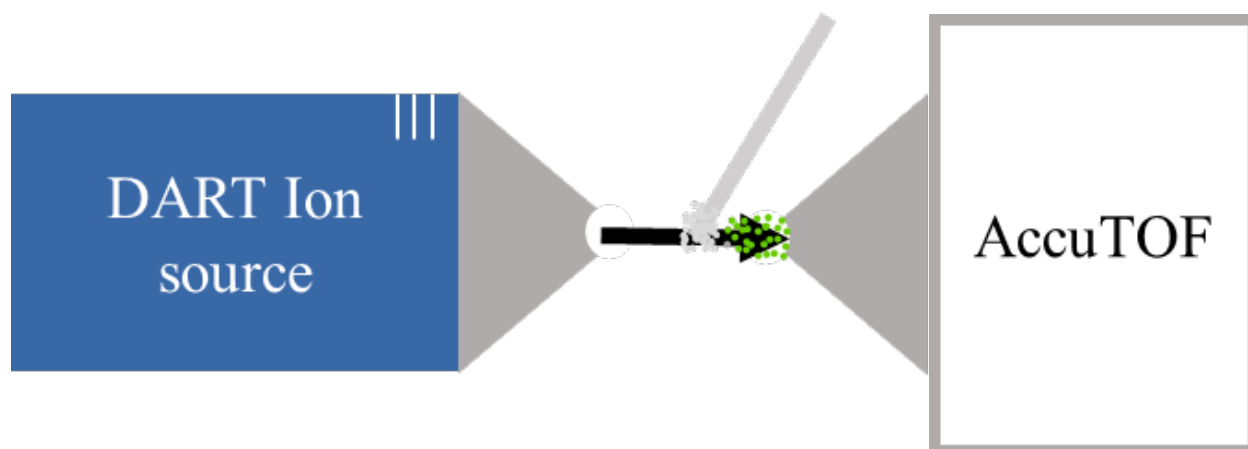
# Chapter 3: Results and Discussion

*3.1 – DIT*

The data analysis tool used for DART-MS analysis was the DIT. **Figure 47** shows an example of the results from a DIT library search of a mixture of cocaine and caffeine. Targets 2 and 4 were identified as caffeine, with no other results. Targets 1, 3, and 5 identified potential compounds within the 0.005 Da m/z tolerance for the target fragments. However, only the scores for cocaine are above the threshold used in this study, with an FPIE score of 0.727 and a RevMF score of 0.669. This means that when using a threshold of 0.60, both scoring metrics can identify cocaine as a potential compound. However, if the threshold was 0.70, RevMF would not identify cocaine.



**Target 1:**

| | Compound | Δ m/z | FPIE | RevMF | IRD | Match Type |
|---|---|---|---|---|---|---|
| 1 | Cocaine | -0.0001 | 0.727 | 0.669 | 0.003 | Protonated Molecule |
| 2 | Scopolamine | -0.0001 | 0.237 | 0.320 | 0.003 | Protonated Molecule |

**Target 2:**

| | Compound | Δ m/z | FPIE | RevMF | IRD | Match Type |
|---|---|---|---|---|---|---|
| 1 | Caffeine | -0.0009 | 0.698 | 0.691 | 0.024 | Protonated Molecule |

**Target 3:**

| | Compound | Δ m/z | FPIE | RevMF | IRD | Match Type |
|---|---|---|---|---|---|---|
| 1 | Cocaine | -0.0001 | 0.727 | 0.669 | 0.003 | +1 Isotope (PM) |
| 2 | Scopolamine | -0.0001 | 0.237 | 0.320 | 0.003 | +1 Isotope (PM) |

**Target 4:**

| | Compound | Δ m/z | FPIE | RevMF | IRD | Match Type |
|---|---|---|---|---|---|---|
| 1 | Caffeine | -0.0015 | 0.698 | 0.691 | 0.024 | +1 Isotope (PM) |

**Target 5:**

| | Compound | Δ m/z | FPIE | RevMF | IRD | Match Type |
|---|---|---|---|---|---|---|
| 1 | 2C-H | -0.0013 | 0.184 | 0.424 | -0.108 | Protonated Molecule |
| 2 | 3,4-Dimethoxyphenethylamine | -0.0013 | 0.248 | 0.425 | -0.108 | Protonated Molecule |
| 3 | Cocaine | -0.0013 | 0.727 | 0.669 | 0.003 | Base Peak |

| Target | Compound | Match type | Measured m/z | Δ m/z | Relative intensity |
|---|---|---|---|---|---|
| T1 | Cocaine | Protonated molecule | 304.1547 | -0.0001 | 100% |
| T2 | Caffeine | Protonated molecule | 195.0880 | -0.0009 | 76.4% |
| T3 | Cocaine | +1 Isotope (PM) | 305.1592 | 0.0003 | 18.7% |
| T4 | Caffeine | +1 Isotope (PM) | 196.0909 | -0.0015 | 8.5% |
| T5 | Cocaine | Base peak | 182.1168 | -0.0013 | 6.8% |

**Figure 47:** The results for cocaine using a 1 to 4 mixture of cocaine and caffeine using a threshold of 0.60 a.u. Targets 1 and 2 were identified as protonated cocaine and caffeine, respectively. Target 3 and 4 can be identified as the isotopes of the protonated cocaine and caffeine, respectively. Target 5 is identified as a base peak of cocaine.

A value for LFPM IRD was required for results to be considered possibilities. This scoring metric tells the analyst that a protonated molecule was found in the complex spectrum. An example of how the FLPM IRD affects the decision threshold can be seen in **Figure 48**.

| Legend | |
|---|---|
| — Non-target ion | — Target ion w/ possible matches |
| — Target ion w/o match | ···· Targetting Threshold |

**Target 3:**

| | Compound | Δ m/z | FPIE | RevMF | IRD | Match Type |
|---|---|---|---|---|---|---|
| 1 | Methamphetamine | -0.0003 | 0.668 | 0.838 | 0.005 | Protonated Molecule |
| 2 | Phentermine | -0.0003 | 0.645 | 0.598 | 0.005 | Protonated Molecule |

**Target 5:**

| | Compound | Δ m/z | FPIE | RevMF | IRD | Match Type |
|---|---|---|---|---|---|---|
| 1 | 1-Benzylpiperazine | -0.0013 | 0.366 | 0.482 | NA | Base Peak |
| 2 | 4-Dimethylamino-N-benzylcathinone | -0.0013 | 0.482 | 0.750 | NA | Base Peak |
| 3 | 4-Methylthio-N-benzylcathinone | -0.0013 | 0.498 | 0.647 | NA | Base Peak |
| 4 | Amphetamine | -0.0013 | 0.805 | 0.909 | NA | Base Peak |
| 5 | Benzedrone | -0.0013 | 0.495 | 0.555 | NA | Base Peak |
| 6 | BMDB | -0.0013 | 0.390 | 0.620 | NA | Base Peak |
| 7 | Mephentermine | -0.0013 | 0.632 | 0.698 | NA | Base Peak |
| 8 | Methamphetamine | -0.0013 | 0.668 | 0.838 | 0.005 | Base Peak |
| 9 | Methamphetamine Methyl Carbamate | -0.0013 | 0.560 | 0.819 | NA | Base Peak |
| 10 | N,N-Dimethylamphetamine | -0.0013 | 0.518 | 0.704 | NA | Base Peak |

| Target | Compound | Match type | Measured m/z | Δ m/z | Relative intensity |
|---|---|---|---|---|---|
| T1 | Fentanyl* | Protonated molecule | 337.2276 | 0.0000 | 100% |
| T2 | Fentanyl* | Protonated molecule | 338.2310 | -0.0003 | 24.4 % |
| T3 | Methamphetamine | +1 Isotope (PM) | 150.1278 | N/A | 18.3% |
| T4 | N/A* | N/A | 119.0860 | -N/A | 25.4% |
| T5 | Methamphetamine | Base Peak | 91.0534 | -0.0013 | 18.3% |

**Figure 48:** The results for methamphetamine using a 1 to 4 mixture of fentanyl and methamphetamine. Target 5 gives 10 different results as potential compounds in the mixture. All results are from the base peak of several compounds. However, only methamphetamine has a value for the IRD because methamphetamine was the only compound that had a protonated molecule in the complex spectrum. * The fentanyl results are not shown for simplicity.

*3.2 – Ground Truth Scores*

The spread of the scores was investigated for the ground truth of the binary samples. **Figure 49** and **Figure 50** shows a histogram of the scores from the results using DIT. **Figure 49** used each replicate peak as an individual sample. **Figure 50** used the average of the three replicates for each mixture as one sample. The scoring was better overall when using the average of the three replicates, as seen in **Figure 49**. Thirteen compounds did not receive any target identification from the DIT library search when using a target threshold of 4 %. In comparison, in **Figure 50**, all compounds in the binary samples had at least one target fragment when using the average of the three replicate peaks. Two scoring thresholds, 0.6 and 0.7, were arbitrarily chosen to identify the binary mixtures, accounting for most of the samples while limiting the risk of false positives.
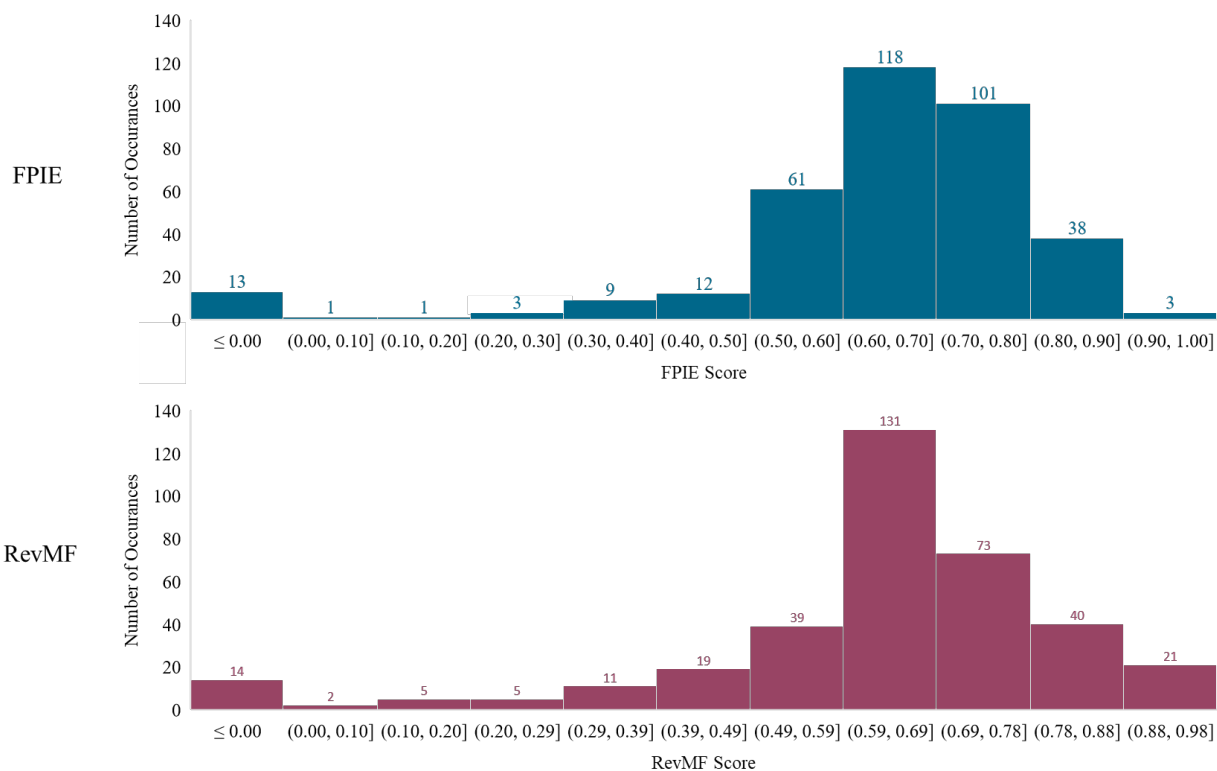
**Figure 49:** Histogram of the scores from the two scoring metrics, fraction of library peak intensity explained (FPIE) (top) and reverse match factor (RevMF) (bottom) using the replicates as individual samples. A total of 13 of the compounds did not receive any target fragments using DIT with a target threshold of 4 % and m/z tolerance of ±0.005 Da.
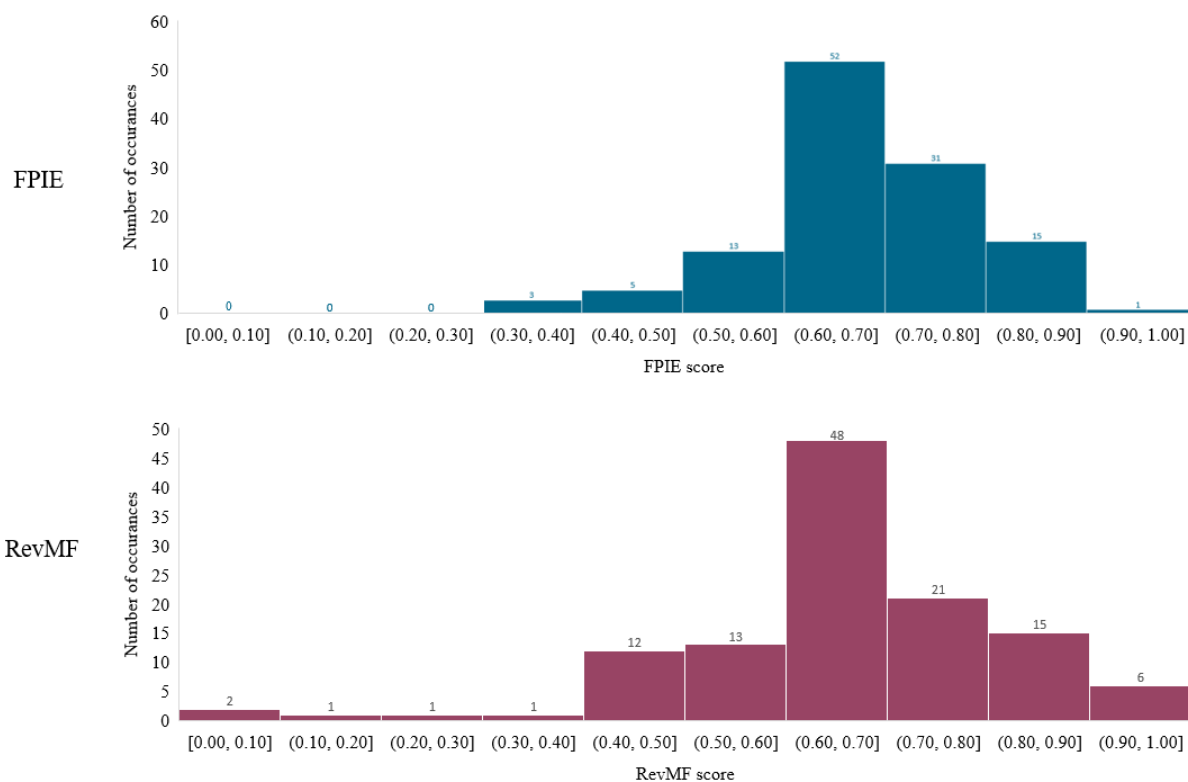
**Figure 50:** Histogram of the scores from the two scoring metrics, FPIE (top) and RevMF (bottom) using the average of the three replicates for one sample. All of the samples received a score.

*3.3 – Score Threshold and Metric Comparison*

Percent identification was used to see how the threshold affects the ability to identify compounds. **Figure 51** shows how many compounds were identified in the binary compounds using the two different similarity metrics and the two thresholds. The 0.60 a.u. threshold using FPIE gave the best percent identification at 82.5 %. One of the reasons why RevMF tends to have a lower threshold is because it includes relative abundance in the calculation. When mixtures are analyzed, competitive ionization affects the compounds' ability to get ionized, which affects the relative intensity of the fragments in the mass spectra. A total of 21 compounds had an FPIE score below the 0.60 a.u. threshold and were therefore not detected. Out of these 21 compounds, 9 were cutting agents and 12 were controlled substances. The cutting agents included (number occurrence): acetaminophen (2x), caffeine (3x), lidocaine (1x), and procaine (3x). The controlled substances included: 4-MMC (1x), cocaine (2x), codeine (4x), heroin (1x), ephedrine (2x), and pseudoephedrine (2x). It should be noted that the 4 times the codeine was not identified, there were other results that could be used to infer that a codeine type compound is present. An example can

be seen in **Figure A - 4**a in the Appendix. Both hydrocodone and pseudocodeine are present above the thresholds.

| FPIE | | RevMF | |
|---|---|---|---|
| **0.70 a.u.** | **0.60 a.u.** | **0.70 a.u.** | **0.60 a.u.** |
| | | | |
| **Percent ID:** 40.0 % | **Percent ID:** 82.5 % | **Percent ID:** 35.0 % | **Percent ID:** 79.8 |

0 ID  1 ID  2 ID
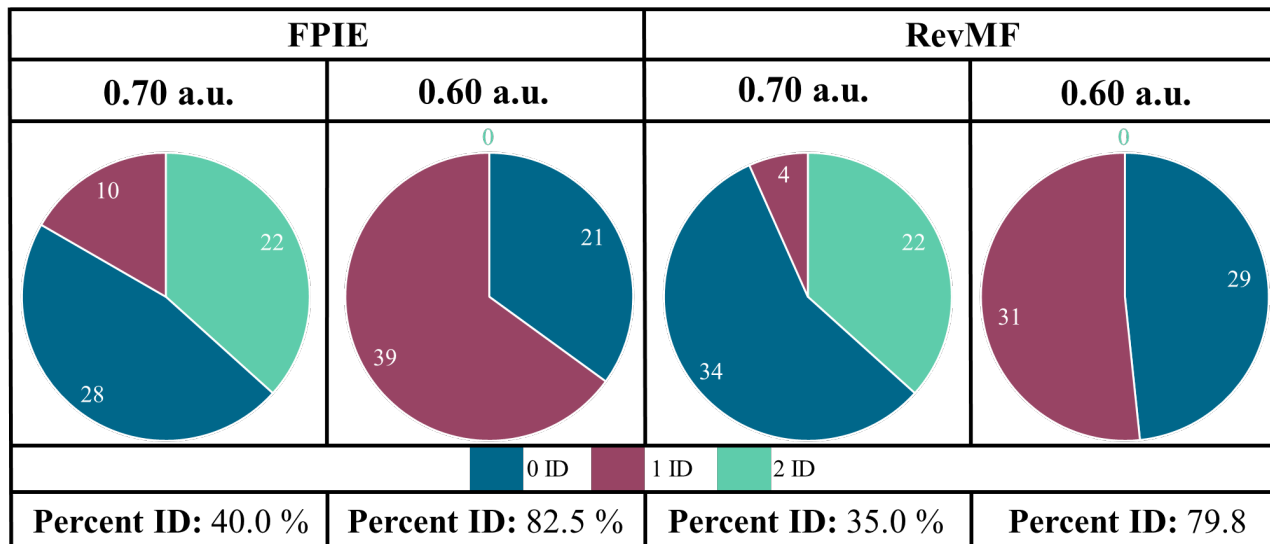
**Figure 51:** Percent identification of the binary mixtures using FPIE (left) and RevMF (right) using the two different thresholds. The pie charts show the percentage of mixtures able to identify either 0 (blue), 1 (purple), or two (green) compounds. The numbers on the pie chart are the number of mixtures included in each section. The percentage at the bottom is the overall calculated percent identification.

Some false positives were identified. Most of the false positives were from compounds with similar masses to the compound present. For example, 4-methylethcathinone has the same mass as ten other compounds (**Figure A - 5** in the Appendix). Seven of the compounds are present above the 0.60 a.u. threshold. All results were cathinones. Some targets identified were not from the compounds present in the binary mixtures. Most of them were below the 0.60 a.u. threshold or did not have an IRD value present, and therefore were not considered as false positives. Three false positives were found that did have an FPIE score above 0.60 a.u. They were all protonated molecules, which gave them an IRD value. One false positive could be eliminated looking at the difference between the *m/z* values. This result can be seen in **Figure A - 6** in the Appendix. The Δ*m/z* value for this false positive was positive. The Δ*m/z* for the m/z ranges trended negative for the true positives in the mixtures. Previous publications have determined that the Δ*m/z* value trends in one direction. [114] The two other false positives were less than 5% relative intensity.

The binary samples used for analysis were created at 1:4, 1:7, 1:10, and 1:20. The ratios were investigated to see how it affects DIT's ability to identify both compounds in the mixture.

**Figure 52** shows the percent identification across the different ratios. Unlike Raman spectroscopy, the ratios do not have as much of an effect for the detection of both compounds. This is most likely because the DART-AccuTOF is a highly sensitive instrument.
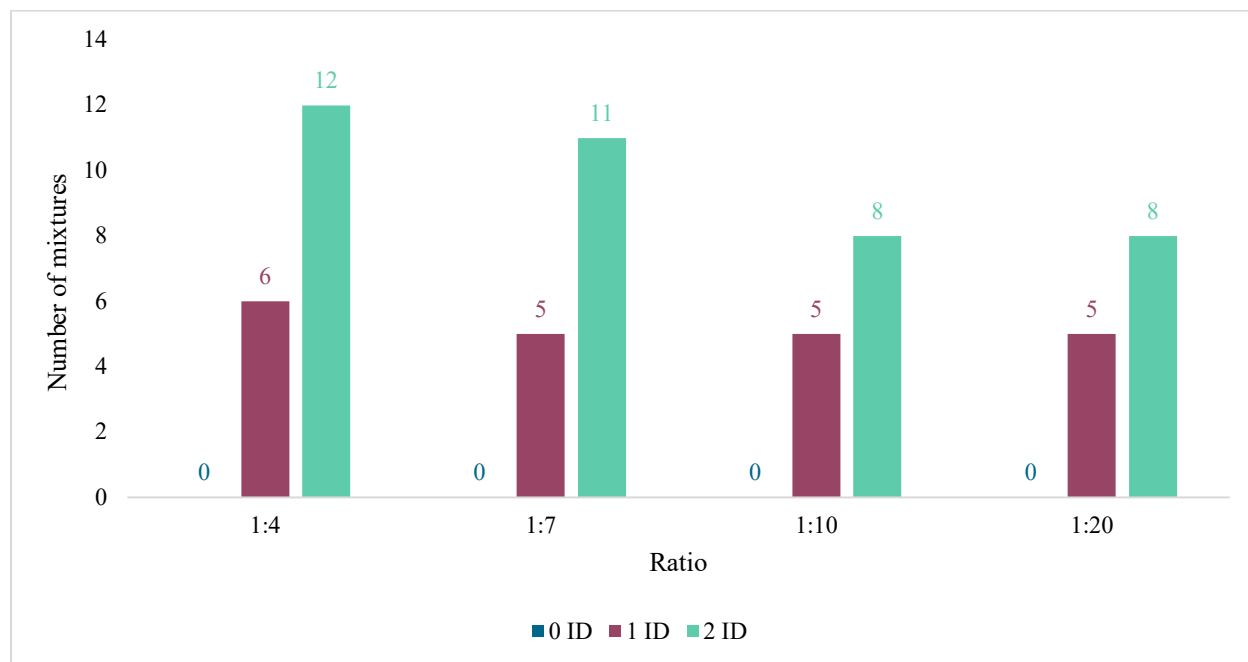


**Figure 52:** Effect of ratio on DIT's ability to identify both compounds in the binary samples using FPIE with a threshold of 0.60 a.u.

*3.4 – Target Threshold Effect*

Further investigation was done for the 13 mass spectra replicate with no targets from one of the compounds identified using DIT. The target threshold was lowered to see if the compounds were present but not identified as targets due to the 4 % relative intensity threshold. **Table 15** shows the target results from the 13 mixture replicate spectra using no target threshold. One mixture spectra replicate did not have a target for cocaine identified in the 30 V mass spectra even when the target threshold was set to 0 %. Regarding the FPIE scores, two methamphetamine compounds not initially identified scored above the 0.60 a.u. threshold. Three of the compounds not initially identified had a score above 0.60 a.u. when using RevMF.

While a lower target threshold would identify additional components, a relative intensity threshold too low would allow additional background target compounds to be identified. It is crucial to be aware that lowering the target and scoring threshold increases the likelihood of false positives. By requiring the LFPM IRD value, the analyst limits the number of false positives but

requires the protonated molecule and its main isotope to be present. It should be noted that three pseudoephedrine mixtures did not have an IRD value, as shown in **Table 15**. These two compounds were below the had a relative intensity of 3.9 and 2.1 %. These replicates were combined with caffeine, and the pseudoephedrine had a lower ratio. **Figure 53** shows the library low-fragmentation of pseudoephedrine. In a pure sample of pseudoephedrine, the protonated molecule is roughly 50 % relative intensity to the base peak. Therefore, it is understandable that the protonated molecule is not seen in the two replicates since the base peak is less than 4 % for the three replicates.

**Table 15:** Results of the mixtures that had a compound not identified in the binary mixtures. The compounds with (*) had a relative intensity below the target threshold, 4 %. The relative intensity uses the most abundant fragment for each compound. PM stands for protonated molecule and BP stands for base peak. The (**) identifies the compounds that did not have an IRD value associated with the base peak values.

| Mixture (ratio) | Replicate | Compound | FPIE score | RevMF score | Relative Intensity |
|---|---|---|---|---|---|
| 4-MMC : Lid 1:10 | 2 | 4-MMC * | 0.447 | 0.597 | PM: 2.8 % |
| | | Lidocaine | 0.656 | 0.696 | PM: 100 % |
| 4-MMC : Lid 1:10 | 3 | 4-MMC * | 0.447 | 0.611 | PM: 3.5 % |
| | | Lidocaine | 0.641 | 0.703 | PM: 100 % |
| Amp : Acet 1:20 | 1 | Amphetamine | 0.868 | 0.929 | BP: 100% |
| | | Acetaminophen* | 0.247 | 0.182 | PM: 1.4 % |
| Amp : Caf 1:7 | 1 | Amphetamine | 0.807 | 0.936 | BP: 100 % |
| | | Caffeine* | 0.130 | 0.021 | PM: 3.9 % |
| Coc : Lid 1:20 | 1 | Cocaine * | ---- | ---- | ---- |
| | | Lidocaine | 0.587 | 0.679 | PM: 100 % |
| Meth : Acet 1:20 | 1 | Methamphetamine* | 0.383 | 0.377 | PM: 1.9 % |
| | | Acetaminophen | 0.657 | 0.624 | PM: 100 % |
| Meth : Eph 1:4 | 3 | Methamphetamine* | 0.611 | 0.592 | PM: 3.4 % |
| | | Ephedrine | 0.646 | 0.552 | BP: 100 % |
| Meth : Eph 1:10 | 3 | Methamphetamine* | 0.677 | 0.452 | PM: 3.4 % |
| | | Ephedrine | 0.697 | 0.729 | BP: 100 % |
| Meth : Lev 1:7 | 3 | Methamphetamine * | 0.560 | 0.851 | PM: 2.5 % |
| | | Levamisole | 0.765 | 0.724 | PM: 100 % |
| Pse : Acet 1:4 | 1 | Pseudoephedrine* | 0.209 | 0.251 | BP: 1.9 % ** |
| | | Acetaminophen | 0.640 | 0.627 | PM: 100 % |
| Pse : Caf 1:7 | 2 | Pseudoephedrine* | 0.335 | 0.539 | BP: 3.9 % ** |
| | | Caffeine | 0.745 | 0.712 | PM: 100 % |
| Pse : Caf 1:10 | 2 | Pseudoephedrine* | 0.388 | 0.670 | BP: 2.1 % ** |
| | | Caffeine | 0.727 | 0.725 | PM: 100 % |
| Pse : Caf 1:10 | 3 | Pseudoephedrine* | 0.523 | 0.567 | BP: 3.4 % ** |
| | | Caffeine | 0.730 | 0.692 | PM: 100 % |

4-MMC = 4-Methylmethcathinone, Acet = acetaminophen, Amp = amphetamine, Caf = caffeine, Coc = cocaine, Eph = ephedrine, Lev = levamisole,  Lid = lidocaine, Meth = methamphetamine, Pse = pseudoephedrine
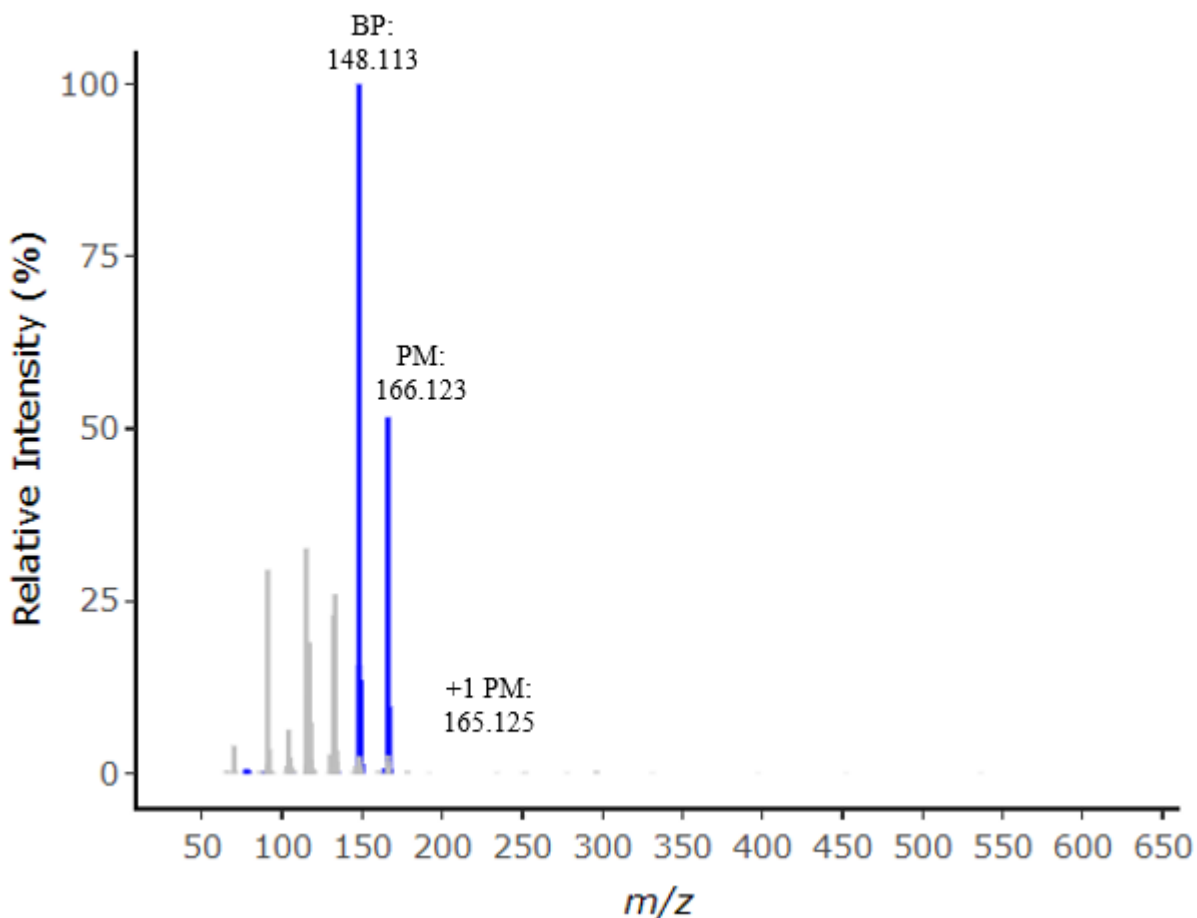


**Figure 53:** Library low-fragmentation (30 V) mass spectrum of pseudoephedrine. The base peak (BP), Protonated molecule (PM), and +1 Isotope of the Protonated molecule (+1 PM)

*3.5 – Pharmaceutical Pills*

The two pharmaceutical pills from Part **II: Comparison of Portable Raman Instruments** were also analyzed by the DART-MS and DIT using the same three methods, outer coating, inner portion, and powder. **Table 16** shows the DIT results for the pseudoephedrine and phenylephrine pills using the average across the three replicates for each method. All the collection methods had FPIE scores above 0.7 a.u. for pseudoephedrine. The RevMF scores were above the 0.6 threshold for the pseudoephedrine.   All the FPIE scores were above 0.9 for phenylephrine HCl. The

powdered average was below 0.6 a.u. for the average across the replicates. The powdered RevMF scores were also below the threshold for all individual replicates. The outer and inner methods were above the 0.6 threshold. When using FPIE with a threshold of 0.6 or 0.7, the percent identification for the pseudoephedrine and phenylephrine pills is 100 % when using FPIE.

**Table 16:** Results from the Pharmaceutical Pills using the DIT.

| Pill | Method | FPIE score | RevMF score | Targets Identified |
|---|---|---|---|---|
| Pseudoephedrine | Outer Coating | 0.808 | 0.677 | Base peak Protonated molecule +1 Isotope (base peak) |
| | Inner Portion | 0.721 | 0.628 | Base peak Protonated molecule +1 Isotope (base peak) |
| | Powder | 0.736 | 0.623 | Base peak Protonated molecule +1 Isotope (base peak) |
| Phenylephrine HCl | Outer Coating | 0.963 | 0.709 | Base peak Protonated molecule +1 Isotope (base peak) |
| | Inner Portion | 0.963 | 0.612 | Base peak Protonated molecule +1 Isotope (base peak) |
| | Powder | 0.962 | 0.570* | Base peak Protonated molecule +1 Isotope (base peak) |

* Below the 0.6 a.u. threshold.

*3.6 – Authentic Samples*

Twelve authentic samples for the Maryland State Police Forensic Sciences Division were used to test the DIT software using more complex samples. Based on the results from the binary mixtures, a 4 % relative intensity was used with a score threshold of 0.60 a.u. **Table 17** shows the compounds identified by the Maryland State Police Forensic Sciences Division. The overall percent identification using FPIE was 71.4 %. Unlike the binary mixtures, where the RevMF had a lower percent identification, the RevMF had a higher percent identification with a score of 74.3 %. In case #1, the 6-MAM was not identified when using FPIE, with a score of 0.428. The 6-MAM was identified using RevMF, with a score of 0.720.

It should be noted that even though the percent identification was below the preferred 80 %, the compounds not identified were mostly the cutting agents. The DIT successfully identified

at least one controlled substance for each authentic sample, as seen in **Table 17**. Out of the 9 compounds not identified (red compounds), two were controlled substances, including methamphetamine and 6-MAM. The compounds in blue were not in the library and were cutting agents except for benzoylecgonine and acetylcodeine.

**Table 17:** Table with the ground truth of the authentic samples from the Maryland State Police Forensic Sciences Division. The green drugs were identified when using RevMF with a threshold of 0.60 a.u. The red drugs are present in DIT library but were not identified above the threshold. The * identifies drugs that had target compounds present but the scores were below the threshold. The drugs in blue are not present in the DIT library and therefore the DIT would not be able to identify the compounds if present. ** 6-MAM was identified using the RevMF but not using FPIE.

|      | Drug #1       | Drug #2         | Drug #3    | Drug #4         | Drug #5   | Drug #6          | Drug #7         | Drug #8           |
|------|---------------|-----------------|------------|-----------------|-----------|------------------|-----------------|-------------------|
| #1   | heroin        | quinine         | 6-MAM**    | mannitol*       |           |                  |                 |                   |
| #2   | cocaine       | levamisole      |            |                 |           |                  |                 |                   |
| #3   | caffeine      | fentanyl        | quinine    | diphenhydramine |           |                  |                 |                   |
| #4   | acetaminophen | fentanyl        |            |                 |           |                  |                 |                   |
| #5   | cocaine       | phenacetin*     | levamisole |                 |           |                  |                 |                   |
| #6   | caffeine      |                 |            |                 |           |                  |                 |                   |
| #7   | caffeine      | quinine         | mannitol*  |                 |           |                  |                 |                   |
| #8   | aspirin       | caffeine        | fentanyl   | quinine         | benzocaine | methyl salicylate | salicylic acid | N-phenylpropamide |
| #9   | cocaine       | levamisole      | phenacetin | myo-inositol    |           |                  |                 |                   |
| #10  | ketamine      | methamphetamine | phenacetin |                 |           |                  |                 |                   |
| #11  | heroin        | quinine         | 6-MAM*     | Mannitol*       | acetylcodeine |              |                 |                   |
| #12  | cocaine       | benzoylecgonine |            |                 |           |                  |                 |                   |
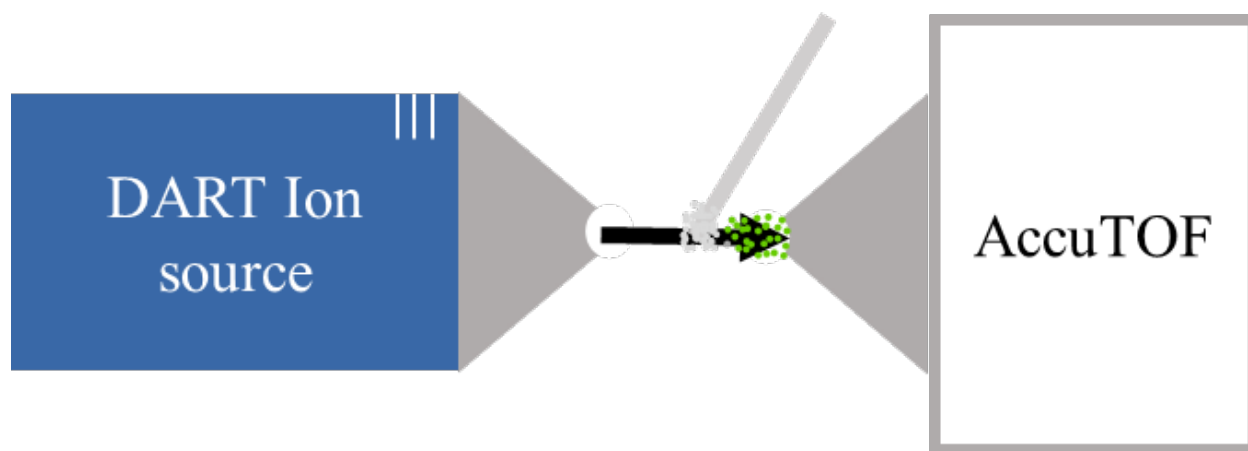
Chapter 4: Conclusions

When using the average across three replicates, DART-MS provided percent identification at 82.5 % using a fraction of library peak intensity explained (FPIE) with a score threshold of 0.60 a.u. Using FPIE with a threshold of 0.60 a.u., the DIT had a 100 % identification for the pseudoephedrine and phenylephrine pills. The authentic samples gave a percent identification of 74.3 %, using RevMF with the 0.60 a.u. threshold. The decrease in identification is due to competitive ionization and the proton affinity of the compounds analyzed. However, it should be noted that all twelve samples had at least one compound identified, which is sufficient for the purposes of a forensic screening technique. The majority of missed compounds were cutting agents.

The thirteen compounds from the individual replicates that did not have a target from the DIT were investigated further to see if the target threshold was causing the targets to be included as noise. While the targets were present when the target threshold was lowered, the scores given to the threshold were mostly below the threshold. Therefore, even if the analyst lowered the threshold, the scores would prevent the compounds from being identified. The analyst would also have to lower the score threshold. By lowering both thresholds, the chance of a false positive would increase. As mentioned in **Part III: Improving Raman Spectroscopy Using Machine Learning**, this could be acceptable if it were being used as a screening technique. However, it would be up to the analyst to decide if it is worth the risk. Requiring the protonated molecule to be present is one way to limit the false positives.

The DIT is a relatively new software developed in 2021. Future work involves using the software in additional samples with more variety of sample types and compounds present to truly identify the parameters that would work best in a crime laboratory. Like most of the instrumentation, these parameters will not be the same for everything. However, by analyzing different samples on the DART-MS, there will be a better understanding of the advantages and limitations of DART-MS.

# Part V: Comparison of Raman and DART-MS for the analysis of mixtures
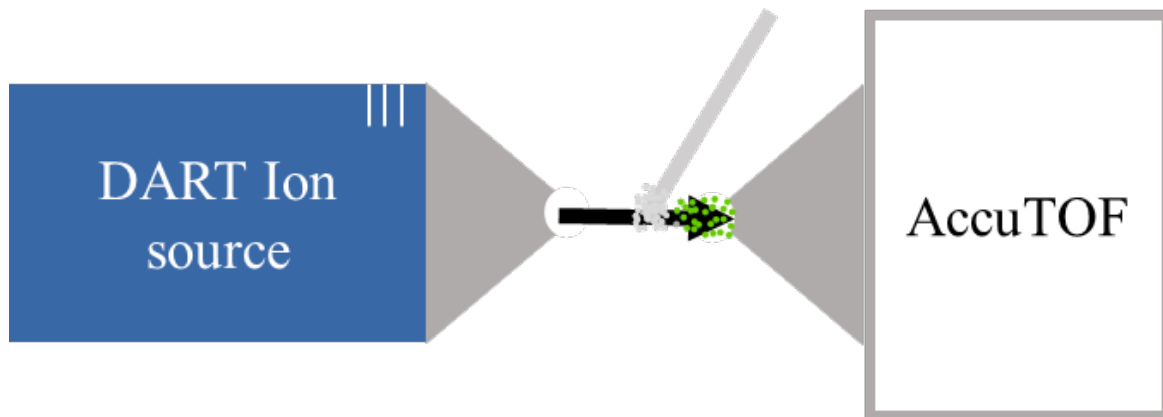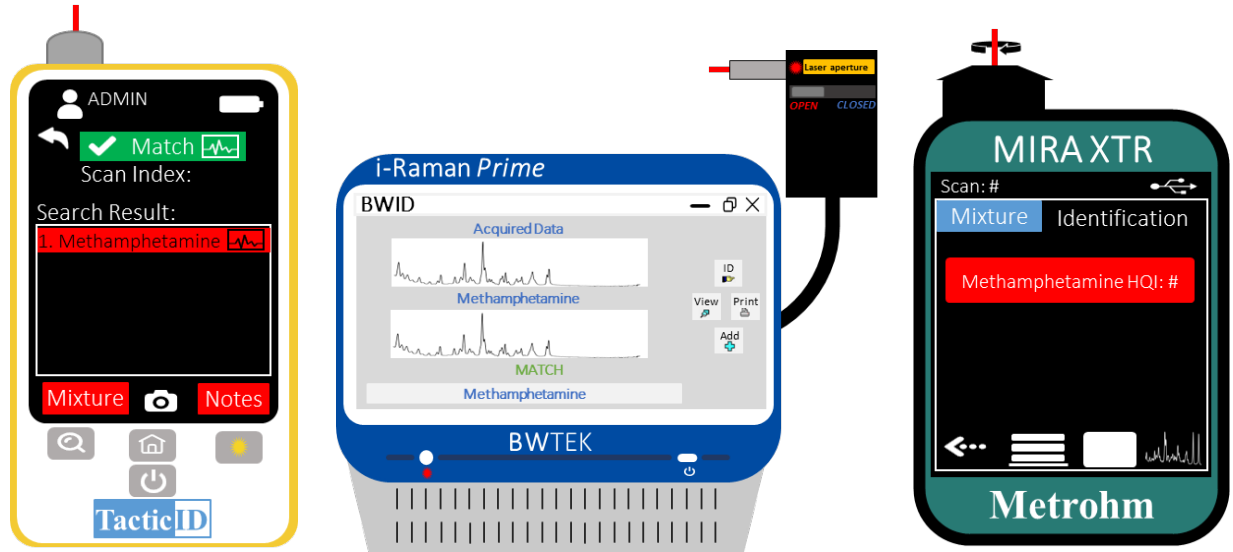


## Chapter 1: Comparison of Results

*1.1 – Portable Raman Instruments*

The most important aspect of portable Raman instruments is the software used to identify the compounds. The TacticID and Mira had a mixture analysis function in the instruments, allowing for a more complex identification using spectral weight. Both the TacticID and the Mira had a percent identification of 66.6 %. The iRaman, which did not have a mixture analysis function, had a much lower percent identification at 53.6 %.

The pharmaceutical pills had more issues with fluorescence. The iRaman provided better spectra because the 1064 nm laser has lower energy than the 785 nm in the TacticID. However, the software still had issues identifying the mixtures in the pharmaceutical pill. The TacticID could differentiate between pseudoephedrine and phenylephrine, even though the library did not include phenylephrine standards.

The Mira and the TacticID are both suited for the on-site detection of methamphetamine and its precursors that could be found in clandestine methamphetamine laboratories. The iRaman requires a more advanced understanding of Raman, and more advanced statistical methods may be required to get more accurate results.

*1.2 – Improving Raman with Machine Learning*

The iRaman was used to try and improve instrument results using machine learning. CNN compared cosine similarity to a traditional similarity metric. A total of 38 standards were used as a library/database for the predictions. A total of 100 binary mixtures and 12 authentic samples from the MSP FSD were used as a test set for the comparison. Cosine similarity had a percent identification of 71.5 %, while CNN had a percent identification of 94 % for the binary mixtures. The authentic samples were more difficult for the two metrics. CNN had a slightly higher percent identification at 41.2 % vs. 36.4 %. The authentic samples were more difficult because CNN was not trained with more complex samples.

*1.3 – DART-MS*

The DIT was used to identify 60 mixtures, two pharmaceutical pills, and the same 12 authentic samples from the MSP FSD. Using the FPIE with a threshold of 0.60 a.u., the DIT had a percent identification of 82.5 % for the binary mixtures, 100 % for the authentic samples, and 74.28 % for the authentic samples. The percent identification decrease for the authentic samples could be due to competitive ionization and each compound's proton affinity.
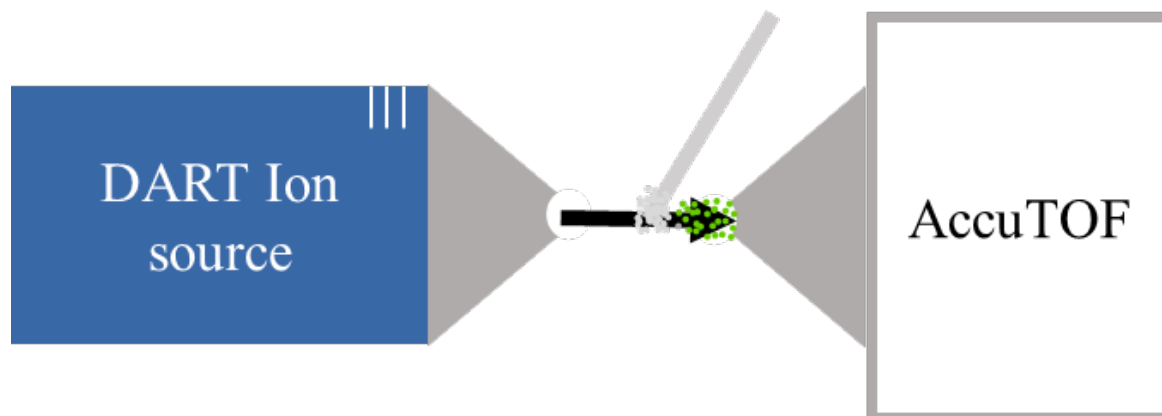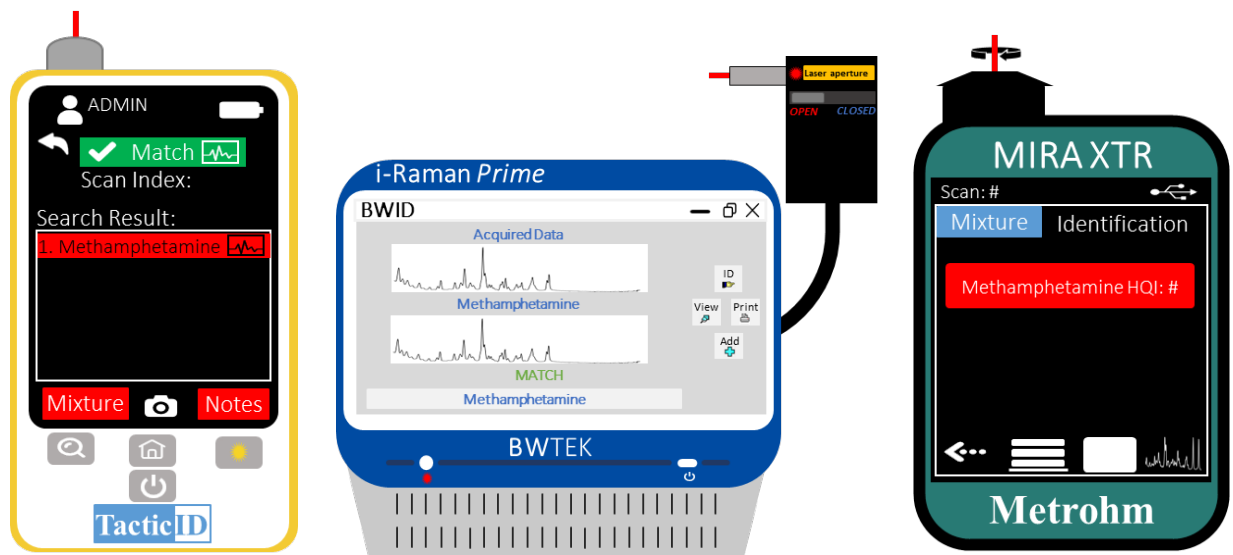
# **Chapter 2:** Other Factors to Consider

It is not enough for crime laboratories to only consider the ability of instruments to detect the components in seized drug samples. Crime laboratories must also consider other factors like applicability, portability, and instrument cost.

*2.1 – Applicability/portability*

One of the main benefits of Raman spectroscopy is that portable instruments can be used for on-site analysis. While, laboratory benchtop Raman spectroscopy is considered a category A technique, or confirmatory, as it provides structural information about the molecule. [44] Portable Raman instruments are considered a category B technique due to their low sensitivity and issues with complex samples. [117] Depending on the need for a forensic laboratory, they may instead have a portable Raman instrument to perform quick screening methods. A forensic laboratory needing multivariate analysis may prefer the iRaman Prime with the BWSpec software. A forensic laboratory needing mixture analysis may prefer the TacticID or the Mira XTR. A police department may choose a handheld Raman based on its simplicity and straightforward interpretation, like the TacticID or Mira XTR.

DART is not generally considered a portable instrument, though researchers are trying to make it portable using other detection methods. One benefit of DART-AccuTOF is that it is highly sensitive and better detects minor components in mixtures. DART-AccuTOF also demonstrated better detection of authentic samples, which may make it more beneficial to a forensic laboratory. This is because the seized drugs getting detected are becoming more complex, with more compounds added to the substance to change or enhance the effects of the drug. The DEA has a campaign called "One Pill Can Kill," explaining that six out of ten fentanyl-laced fake prescription pills contain lethal fentanyl [118]. Drugs like fentanyl are added to other controlled substances to make the drug cheaper and more potent, making it more addictive and dangerous [119]. Xylazine has also been reported to be included in fentanyl and heroin seized drugs [120]. The FDA has reported that naloxone may respond to xylazine, making opioids mixed with opioids like heroin or fentanyl more dangerous [121]. Canada has reported benzodiazepine-laced opioids. [122] Portable Raman instruments may not be sensitive enough to detect these laced components.

*2.2 – Instrument Cost*

One of the most important factors that the supervisors at a forensic laboratory need to consider is the cost. Does the laboratory have enough to afford the instrument the section would like? In an ideal world, forensic laboratories would have an unlimited budget to get the most

advanced equipment as needed. However, this is not realistic. Therefore, the forensic laboratory must budget its finances to get the instruments they need to complete its requirements successfully.

According to a JEOL sales manager, the standard configuration of an AccuTOF-DART instrument costs between $210,000 – $230,000. There are other additional purchases that the laboratory would need to consider, like the gas needed and the standards used for calibration and drift compensation. There is also the method of sampling. For this research, the mixtures were sampled using the closed end of microcapillary tubes. A pack of 250 can be found at Signal Aldrich for $92. (Product number: P0674) Some sample introduction methods include dissolving the power into a solvent to help homogenize the mixture. Other methods include thermal desorption, which would be an additional purchase.

According to a sales representative from Metrohm, the TacticID cost around $30,000 at the time of purchase for our research group. The Mira XTR DS is an upgraded version of the TacticID. The basic package for the Mira XTR DS includes the calibration standard, intelligent universal adapter (iUA), and USB cable, costing around $31,400. The advanced package includes everything in the basic package and a right-angle attachment, vial holder, SERS adapter, KnowItAll complete library, Mira Cal DS software, carrying case, protective laser glasses, Set of four lithium batteries, USB 5V 1A power supply, microfiber cleaning cloth and a blackout sampling cloth. The advanced package costs around $48,500.

The iRaman Prime instrument costs around $58,500. This price does not come with the software. The software is available for additional purchase. The BWSpec (used in the next section) costs around $1,400, with an available upgrade for an additional $715. The BWID standard (used in this section) costs around $3,600, with an available upgrade for an additional $1,183. The BWIQ costs around $6,800, with an available upgrade for an additional $1,030.

The Raman instruments do not have consumables for regular use. However, to use the SERS attachment, the analyst would have to purchase SERS strips and a solvent to dissolve the powder to get the SERS effect.

The DART-MS is almost four times as expensive as the iRaman Prime and over four times as expensive as the Mira XTR DS. However, the DART-MS was better equipped to handle the binary mixtures than the instrument's HQI. The DART-MS provided a percent identification of 82.5 % using a fraction of library peak intensity explained (FPIE) with a score threshold of 0.60 a.u. In comparison, The Mira and Tactic provided a percent identification of 66.6 % using the

instrument's library, and the iRaman gave 53.6 %. While machine learning improved the iRaman prime's percent identification to 94.0 %, CNN had issues with the more complex samples, which are more realistic to the samples that a forensic laboratory would encounter.

ADMIN

✔ Match

Scan Index:

Search Result:

1. Methamphetamine

Mixture    Notes

TacticID

i-Raman *Prime*

BWID

Acquired Data

Methamphetamine

View    Print

ID

Add

MATCH

Methamphetamine

BWTEK

Laser aperture

OPEN    CLOSED

MIRA XTR

Scan: #

Mixture    Identification

Methamphetamine HQI: #

Metrohm

DART Ion source

AccuTOF
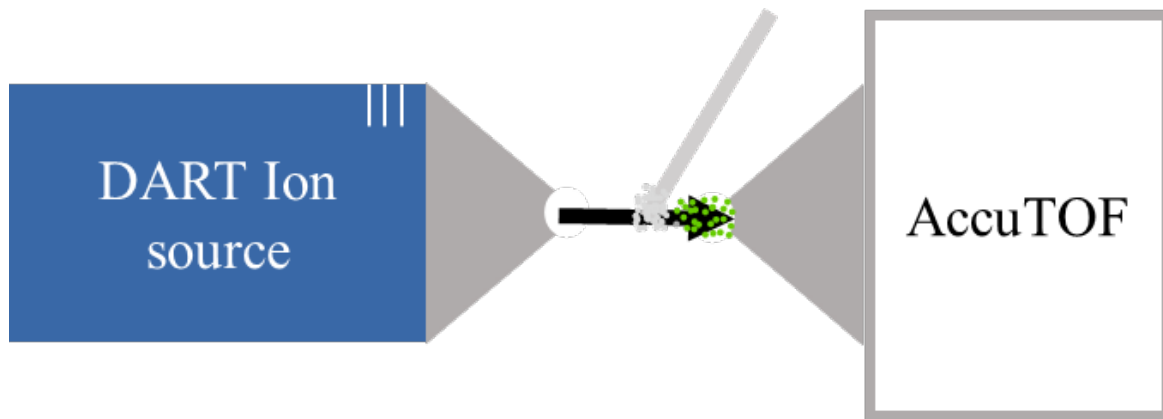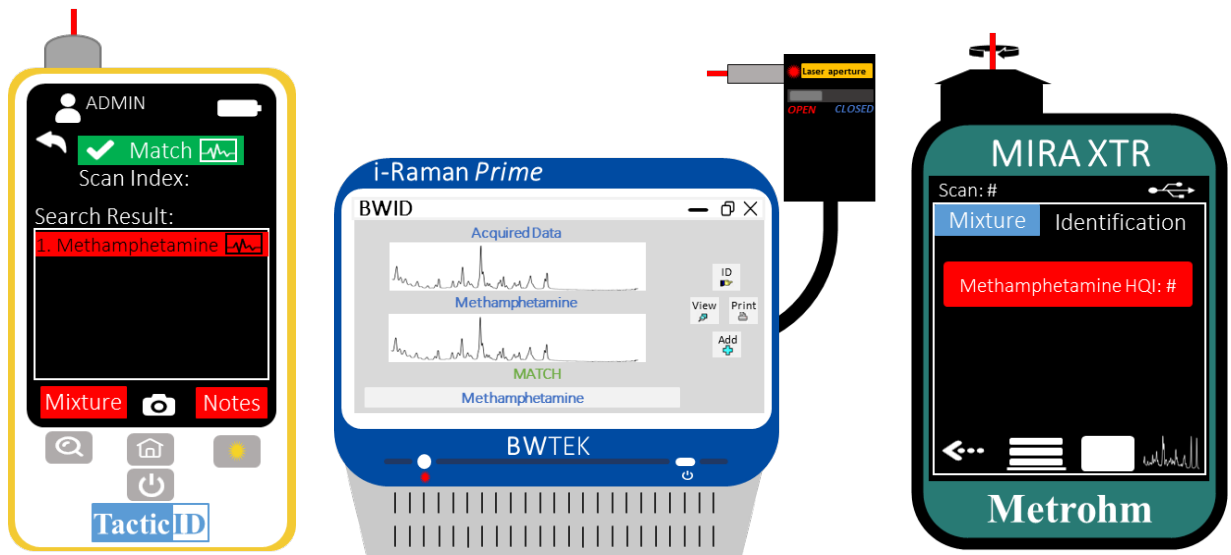
# **Chapter 3:** Conclusion

*3.1 – Conclusion*

This thesis looked at two ways to improve the detection of mixtures in clandestine methamphetamine laboratories: on-site, using portable Raman, and at the laboratory, using DART-MS. **Part II** focused on Portable Raman instruments. The portable Raman instruments with the mixture analysis function were the best for first responders to use in the field. The mixture analysis function allows for identifying multiple components in the sample below the HQI threshold. However, the mixture analysis function and other traditional similarity metrics do not consider complex spectra where bonds from multiple components convolute the data.

**Figure A - 7** in the Appendix shows an example of the implementation of a portable Raman instrument to a crime scene investigation for seized drug evidence. After the calibration of the instrument, each piece of evidence should be analyzed three times. Each analysis should be performed at different locations of the evidence to better account for variability in the sample. If there is a large seizure, use a large sampling procedure to determine how many samples should be analyzed. Each sample analyzed should be done in triplicate. If no controlled substance is detected with either the HQI or the mixture analysis function, then the analyst should report the result, including the scan index. The scan index is the instrument's numbering system to record and remember each analysis. If the instrument reported a controlled substance above the HQI threshold, the analyst should report the result, including the scan index. The officer can arrest the suspect and submit the evidence for further testing if possible. If a controlled substance is found using the mixture analysis function, discretion should be made for the results. The mixture analysis function has a higher risk of false positives. This is because the mixture analysis function allows for lower HQI scores to be used. If the mixture results are consistent, it increases the likelihood that the controlled substance is present. If the results change in between the replicate, it is likely that there could be an issue with fluorescence or interferences with a compound that is not present in the library. If this is the case, it is recommended that the analyst submits the evidence to a laboratory for further analysis. The officer should get the suspect's information, but not arrest to limit the risk of a false imprisonment.

**Figure A - 8** in the Appendix shows an example for implementation of a portable Raman instrument for a potential clandestine methamphetamine laboratory. In many cases a forensic chemist will be present to assist with the crime scene. In a clandestine operation, there will be other chemicals that are not controlled but are used to make the controlled substance. This can include

precursors and other reagents needed for the synthesis. The chemical present will be different depending on the method used for synthesis. One of the main benefits to using Raman spectroscopy is that it can identify many other chemicals, including solvents and reagents used in the manufacture. If there are no indications of a clandestine laboratory, there is no need for arrest or further analysis. If a clandestine laboratory is found, all chemicals present should be taken to a laboratory for further analysis even if it is not a known controlled substance, precursor, or reagent. The equipment should also be taken for further analysis.

In **Part III**, this research addressed Raman's mixture limitation by combining portable Raman with machine learning. The CNN training set included simulated mixtures where the algorithm could be trained to identify binary mixtures by combining bands from complex samples. The convolutional neural network successfully improved the mixture analysis results for the iRaman, from 71.5% using cosine similarity to 94.0 % using CNN. CNN had issues with the authentic samples. This can be attributed to the sample's complexity. Only three of the twelve samples were like the augmented mixtures used to train the algorithm. The rest were either more complicated, some having up to eight compounds present or had other compounds present not included in the training set like benzoylecgonine and 6-monoacetylmorphine (6-MAM). The ground truth of the authentic samples was qualitative and therefore did not identify the quantity of the compounds for the authentic sample. Raman scattering is weak compared to other spectroscopic techniques. Any component that had a smaller quantity had a smaller chance of getting detected. It is possible to include a trained CNN algorithm into the portable Raman instrument, which would be another search option like the HQI and the mixture analysis function. However, more work needs to be done to improve the CNN algorithm for more complex samples and decrease the false positives.

In **Part IV**, DART-MS was explored as a screening technique for the detection of mixtures using the DIT. The DART-MS performed better than the traditional Raman similarity metrics, like cosine similarity and HQI, with a percent identification of 82.5 %. The DART-MS provided the best percent identification for the authentic samples at 74.5 %. It should be noted that most compounds not identified were cutting agents, which are not necessary for a forensic laboratory. All twelve authentic samples identified at least one controlled substance. In most forensic laboratories, this is sufficient to move onto confirmatory testing.

**Figure A - 9** in the Appendix shows an example for implementation of a DART-AccuTOF as a screening technique for a forensic laboratory. The DART-AccuTOF should be calibrated before any analysis. During the analysis of the evidence, the samples should be analyzed in triplicate, sandwiched between two standards for drift compensation. The standard and samples analyzed can be repeated as necessary for all of the evidence. After data collection, drift compensation should be performed and then the mass spectra for the three is-CID voltages should be extracted. These extracted mass spectra can be analyzed with the DIT. Using the parameters set by the laboratory the analyst should determine if there is a controlled substance identified. It is not recommended to only use the FPIE/RevMF scoring metrics. The analyst should also consider other factors, like if an IRD value is present. If the analyst determines a controlled substance is present, the sample should continue to a confirmatory technique.

Since DART-MS is sensitive, it is recommended to use a sensitive confirmatory technique like a LC-MS/MS. A GCMS could be used but it should be noted that due to the lower sensitivity of a GCMS, some compounds identified in the DART-MS may not be detected using a GC-MS. One benefit to using a DART-AccuTOF for a clandestine laboratory case is that it is a highly sensitive instrument. Therefore, it is possible for residues found on the equipment of a clandestine laboratory to be analyzed using the DART-AccuTOF.

Overall Raman with CNN and DART-AccuTOF with the DIT software provide improved mixture analysis capabilities. The DIT can identify patterns in complex spectra related to the pure spectrum in the library. Due to the sensitivity of DART-AccuTOF, future work could involve using DART-AccuTOF to detect clandestine laboratory equipment. CNN can identify important features in the training set that allow for complex sample identification. CNN needs some improvements to the identification of more complex samples and decrease the number of false positives. This could be done by training the algorithm with more complex samples or exploring alternative model architectures with additional layers. However, training the model is computationally expensive when using large datasets. Portable Raman instruments can be used in the field, providing quick results.

**References**

[1]     L.N. Sacco, Drug Enforcement in the United States: History, Policy, and Trends, 2014.

[2]     DEA, 2020 National Drug Threat Assessment, Journal of Electronics and Informatics. 3 (2021). https://doi.org/10.36548/jei.2021.1.

[3]     United Nations Office on Drugs and Crime, Global Smart Update: Methamphetamine continues to dominate synthetic drug markets, 2018.

[4]     UNODC, Statistical Annex, UNODC. (n.d.). https://www.unodc.org/unodc/en/data-and-analysis/wdr2022_annex.html.

[5]     UNODC, Main methamphetamine trafficking routes, UNODC. (n.d.).

[6]     Recommended Methods for the Identification and Analysis of Amphetamine, Methamphetamine and their Ring-substituted Analogues in Seized Materials, New York, 2006.

[7]     Global Illicit Drug Trends: Understanding clandestine synthetic drugs, (2001) 11–28.

[8]     2020 Drug Enforcement Administration National Drug Threat Assessment, 2021.

[9]     I. Narcotics Control Board, Precursors and chemicals frequently used in the illicit manufacture of narcotic drugs and psychotropic substances, n.d. www.incb.org.

[10]    UNODC, Identification and analysis of amphetamine, methamphetamine and their ring-substituted analogues in seized materials, n.d.

[11]    J.K. Cunningham, J.C. Maxwell, O. Campollo, L.-M. Liu, W.J. Lattyak, R.C. Callaghan, Mexico's precursor chemical controls: Emergence of less potent types of methamphetamine in the United States, Drug Alcohol Depend. 129 (2013) 125–136.

[12]    J.K. Cunningham, L. Liu, R.C. Callaghan, Essential/precursor chemicals and drug consumption: impacts of US sodium permanganate and Mexico pseudoephedrine controls on the numbers of US cocaine and methamphetamine users, Addiction. 111 (2016) 1999–2009.

[13]    Global Synthetic Drugs Assessment 2020, Vienna, 2020. https://doi.org/10.18356/19d5a8d1-en.

[14]    K. Dobšíková, P. Michal, D. Spálovská, M. Kuchař, N. Paškanová, R. Jurok, J. Kapitán, V. Setnička, Conformational analysis of amphetamine and methamphetamine: a comprehensive approach by vibrational and chiroptical spectroscopy, Analyst. (2023) 1337–1348. https://doi.org/10.1039/d2an02014a.

[15] H.J. Yvon, Raman Spectroscopy for Analysis and Monitoring, Horiba Jobin Yvon, Raman Application Note. (2017) 1–2. http://www.horiba.com/fileadmin/uploads/Scientific/Documents/Raman/bands.pdf.

[16] Methamphetamine (Desoxyn), GoodRx. (n.d.). https://www.goodrx.com/methamphetamine/what-is.

[17] Controlled Substances in alphabetical order, DEA. (2023) 12.

[18] Drug Scheduling, DEA. (n.d.). https://www.dea.gov/drug-information/drug-scheduling.

[19] Desoxyn - Uses, Side Effects, and More, WebMD. (n.d.). https://www.webmd.com/drugs/2/drug-9124/desoxyn-oral/details.

[20] Desoxyn®, n.d.

[21] C. Staff, Drug Use: What is meth?, Caron. (n.d.). https://www.caron.org/addiction-101/drug-use/what-is-crystal-meth-and-meth.

[22] Clandestine synthetic drug labs, (n.d.). https://www.rcmp-grc.gc.ca/drugs-drogues/msdi-ilcmds/lab-eng.htm (accessed May 16, 2022).

[23] K. Norman, A.L. Ciesielski, J.R. Wagner, Identification and associated hazards of clandestine drug laboratories, WIREs Forensic Science. 3 (2021). https://doi.org/10.1002/wfs2.1393.

[24] M. Cameron, Health and safety concerns for law enforcement personnel investigating clandestine drug labs, Chem Health Saf. 9 (2002) 6–9. https://doi.org/10.1016/S1074-9098(01)00288-X.

[25] A.L. Ciesielski, J.R. Wagner, M. Alexander-Scott, J. Smith, J. Snawder, Surface Contamination Generated by "one-Pot" Methamphetamine Production, J Chem Health Saf. 28 (2021). https://doi.org/10.1021/acs.chas.0c00078.

[26] I. Onoka, A.T. Banyika, P.N. Banerjee, J.J. Makangara, L. Dujourdy, A review of the newly identified impurity profiles in methamphetamine seizures, Forensic Sci Int. 2 (2020) 194–205. https://doi.org/10.1016/j.fsisyn.2020.06.004.

[27] V. Lekskulchai, K. Carter, A. Poklis, W. Soine, GC-MS Analysis of Methamphetamine Impurities :, 24 (2000) 602–605.

[28] V. Kunalan, N.N. Daéid, W.J. Kerr, H.A.S. Buchanan, A.R. McPherson, Characterization of route specific impurities found in methamphetamine synthesized by the Leuckart and

reductive amination methods, Anal Chem. 81 (2009) 7342–7348. https://doi.org/10.1021/ac9005588.

[29] H. Copes, A. Hochstetler, The social organization of methamphetamine manufacturing: Roles, identities and persistence, J Crim Justice. (2021). https://doi.org/10.1016/j.jcrimjus.2021.101795.

[30] J.W. Martyny, S.L. Arbuckle, C.S. McCammon, E.J. Esswein, N. Erb, M. Van Dyke, Chemical concentrations and contamination associated with clandestine methamphetamine laboratories, J Chem Health Saf. 14 (2007) 40–52. https://doi.org/10.1016/j.jchas.2007.01.012.

[31] E.J. Kuhn, G.S. Walker, H. Whiley, J. Wright, K.E. Ross, Household contamination with methamphetamine: Knowledge and uncertainties, Int J Environ Res Public Health. 16 (2019). https://doi.org/10.3390/ijerph16234676.

[32] J. Wright, G.S. Walker, K.E. Ross, Contamination of homes with methamphetamine: Is wipe sampling adequate to determine risk?, Int J Environ Res Public Health. 16 (2019) 1–8. https://doi.org/10.3390/ijerph16193568.

[33] A.L. Ciesielski, environmental contamination from clandestine drug manufacture, (2015) 264.

[34] B.C. Dealy, B.P. Horn, R.P. Berrens, The impact of clandestine methamphetamine labs on property values: Discovery, decontamination and stigma, J Urban Econ. 99 (2017) 161–172. https://doi.org/10.1016/j.jue.2017.03.002.

[35] J.K. Cunningham, L.M. Liu, R.C. Callaghan, Essential/precursor chemicals and drug consumption: impacts of US sodium permanganate and Mexico pseudoephedrine controls on the numbers of US cocaine and methamphetamine users, Addiction. 111 (2016) 1999–2009. https://doi.org/10.1111/add.13480.

[36] V. Puthaviriyakorn, N. Siriviriyasomboon, J. Phorachata, W. Pan-ox, T. Sasaki, K. Tanaka, Identification of impurities and statistical classification of methamphetamine tablets (Ya-Ba) seized in Thailand, Forensic Sci Int. 126 (2002) 105–113. https://doi.org/10.1016/S0379-0738(02)00018-X.

[37] and X.G.H. Jian Xin Zhang, Da Ming Zhang, Identification of impurities and statistical classification of methamphetamine hydrochloride drugs seized in the China, Bone. 23 (2008) 1–7. https://doi.org/10.1016/j.forsciint.2008.09.012.

[38] L. Li, J.L. Brown, S.G. Toske, Simultaneous detection and quantitation of organic impurities in methamphetamine by ultra-high-performance liquid chromatography–tandem mass spectrometry, a complementary technique for methamphetamine profiling, Drug Test Anal. 10 (2018) 1209–1219. https://doi.org/10.1002/dta.2388.

[39] V. Kunalan, N.N. Daéid, W.J. Kerr, H.A.S. Buchanan, A.R. McPherson, Characterization of route specific impurities found in methamphetamine synthesized by the Leuckart and reductive amination methods, Anal Chem. 81 (2009) 7342–7348. https://doi.org/10.1021/ac9005588.

[40] B. Presley, B. Bianchi, J. Coleman, F. Diamond, G. McNally, Efficiency of extraction and conversion of pseudoephedrine to methamphetamine from tamper-resistant and non-tamper-resistant formulations, J Pharm Biomed Anal. 156 (2018) 16–22. https://doi.org/10.1016/j.jpba.2018.04.016.

[41] R. Reiss, F. Hauser, S. Ehlert, M. Pütz, R. Zimmermann, Comparison of different analytical methods for the on-site analysis of traces at clandestine drug laboratories, Applied Sciences (Switzerland). 11 (2021). https://doi.org/10.3390/app11093754.

[42] History of Raman spectroscopy | Nanophoton, (n.d.). https://www.nanophoton.net/lecture-room/raman-spectroscopy/lesson-1-4 (accessed May 16, 2022).

[43] G.S. Bumbrah, R.M. Sharma, Raman spectroscopy – Basic principle, instrumentation and selected applications for the characterization of drugs of abuse, Egypt J Forensic Sci. 6 (2016) 209–215. https://doi.org/10.1016/j.ejfs.2015.06.001.

[44] SWGDrug, Scientific Working Group for the Analysis of Seized Drugs recommendations, 2014. http://www.swgdam.org/.

[45] C.E. Ott, L.E. Arroyo, Transitioning surface-enhanced Raman spectroscopy (SERS) into the forensic drug chemistry and toxicology laboratory: Current and future perspectives, WIREs Forensic Science. (2023). https://doi.org/10.1002/wfs2.1483.

[46] S. Fedchak, Presumptive Field Testing Using Portable Raman Spectroscopy, (2014) 100.

[47] A. Geravand, S. Mohammad Hashemi Nezhad, Simulation study of the Orbital Raster Scan (ORS) on the Raman spectroscopy, Optik (Stuttg). 178C (2018) 83–89. https://doi.org/10.1016/j.ijleo.2018.09.090.

[48] Metrohm AG, Improving Verification with Orbital Raster Scan Technology, AZO Materials . (2019) 1–6. https://www.azom.com/article.aspx?ArticleID=17677.

[49]   Introduction to Interpretation of Raman Spectra Using Database Searching and Functional Group Detection and Identification, Spectroscopy. 31 (2016) 16–23. https://www.spectroscopyonline.com/.

[50]   BWID, B&W Tek. (2019). https://bwtek.com/products/bwid/.

[51]   BWIQ, B&W Tek. (2018). https://bwtek.com/products/bwiq/.

[52]   BWIQ – Software Overview Tutorial, B&W Tek. (2018). https://bwtek.com/videos/bwiq-software-overview-tutorial/.

[53]   BWSpec Software, B&W Tek. (2020). https://bwtek.com/products/bwspec/.

[54]   T. Cooman, C.E. Ott, K.A. Dalzell, A. Burns, E. Sisco, L.E. Arroyo, Screening of seized drugs utilizing portable Raman spectroscopy and direct analysis in real time-mass spectrometry (DART-MS), Forensic Chemistry. 25 (2021) 100352. https://doi.org/10.1016/j.forc.2021.100352.

[55]   P.H. Ciza, P.-Y. Sacre, C. Waffo, L. Coïc, H. Avohou, J.K. Mbinze, R. Ngono, R.D. Marini, P. Hubert, E. Ziemons, Comparing the qualitative performances of handheld NIR and Raman spectrophotometers for the detection of falsified pharmaceutical products, Talanta. 202 (2019) 469–478. https://doi.org/10.1016/j.talanta.2019.04.049.

[56]   K.X.E. Kay, A.H. Atabaki, W.B. Ng, Z. Li, G.P. Singh, S.W.L. Tan, R.J. Ram, Identification of illicit street drugs with swept-source Raman spectroscopy, Journal of Raman Spectroscopy. 53 (2022) 1321–1332. https://doi.org/10.1002/jrs.6357.

[57]   A. Guirguis, S. Girotto, B. Berti, J.L. Stair, Identification of new psychoactive substances (NPS) using handheld Raman spectroscopy employing both 785 and 1064 nm laser sources, Forensic Sci Int. 273 (2017) 113–123. https://doi.org/10.1016/j.forsciint.2017.01.027.

[58]   L.P. Santos, M.H.C. Nascimento, I.H.A.S. Barros, N.A. Santos, V. Lacerda, P.R. Filgueiras, W. Romão, Portable Raman spectroscopy applied to the study of drugs of abuse, J Forensic Sci. 67 (2022) 1399–1416. https://doi.org/10.1111/1556-4029.15011.

[59]   S. Assi, I. Abbas, K. Kielisczyzk, O. Wade, B. Arafat, Characterization of Street Drugs Using .., Spectroscopy. 38 (2023) 30–35.

[60]   J. Itkonen, L. Ghemtio, D. Pellegrino, P.J. Jokela, H. Xhaard, M.G. Casteleijn, Analysis of Biologics Molecular Descriptors towards Predictive Modelling for Protein Drug Development Using Time-Gated Raman Spectroscopy, Pharmaceutics. 14 (2022). https://doi.org/10.3390/pharmaceutics14081639.

[61] C. Domes, J. Popp, S. Hagel, M.W. Pletz, T. Frosch, Towards therapeutic drug monitoring of antibiotic levels - analyzing the pharmacokinetics of levofloxacin using DUV-resonance Raman spectroscopy, Analyst. (2023). https://doi.org/10.1039/d3an00402c.

[62] M. Mittal, S. Gupta, A.S. Rathore, Raman spectroscopy as process analytical technology tool for monitoring atomic layer deposition (ALD) of drug particles, Mater Chem Phys. 282 (2022). https://doi.org/10.1016/j.matchemphys.2022.125976.

[63] J. Ming, L. Chen, Y. Cao, C. Yu, B.S. Huang, K.L. Chen, Rapid identification of nine easily confused mineral traditional Chinese medicines using raman spectroscopy based on support vector machine, Journal of Spectroscopy. 2019 (2019). https://doi.org/10.1155/2019/6967984.

[64] C. Zhang, J.S. Springall, X. Wang, I. Barman, Rapid, quantitative determination of aggregation and particle formation for antibody drug conjugate therapeutics with label-free Raman spectroscopy, Anal Chim Acta. 1081 (2019) 138–145. https://doi.org/10.1016/j.aca.2019.07.007.

[65] G. Qun, L. Yan, C. Hui, C. Yifeng, L. Feng, Comparison of several chemometric methods of libraries and classifiers for the analysis of expired drugs based on Raman spectra, J Pharm Biomed Anal. 94 (2014) 58–64.

[66] J. Zhang, P.L. Xin, X.Y. Wang, H.Y. Chen, D.W. Li, Deep Learning-Based Spectral Extraction for Improving the Performance of Surface-Enhanced Raman Spectroscopy Analysis on Multiplexed Identification and Quantitation, Journal of Physical Chemistry A. 126 (2022) 2278–2285. https://doi.org/10.1021/acs.jpca.1c10681.

[67] Y. Park, U.J. Kim, S. Lee, H. Kim, J. Kim, H. Ma, H. Son, Y.Z. Yoon, J. soong Lee, M. Park, H. Choo, Q.H. Park, Y.G. Roh, On-chip Raman spectrometers using narrow band filter array combined with CMOS image sensors, Sens Actuators B Chem. 381 (2023). https://doi.org/10.1016/j.snb.2023.133442.

[68] C. Carey, T. Boucher, S. Mahadevan, P. Bartholomew, M.D. Dyar, Machine learning tools for mineral recognition and classification from Raman spectroscopy, Journal of Raman Spectroscopy. 46 (2015) 894–903. https://doi.org/10.1002/jrs.4757.

[69] Metrohm, Mira XTR DS, (2021).

[70] S. Krimm, C.Y. Liang, G.B.B.M. Sutherland, Infrared spectra of high polymers. II. Polyethylene, J Chem Phys. 25 (1956) 549–562. https://doi.org/10.1063/1.1742963.

[71]   K. Ben Mabrouk, T.H. Kauffmann, H. Aroui, M.D. Fontana, Raman study of cation effect on sulfate vibration modes in solid state and in aqueous solutions, Journal of Raman Spectroscopy. 44 (2013) 1603–1608. https://doi.org/10.1002/jrs.4374.

[72]   P. Larkin, IR and Raman Spectroscopy: Principles and spectral interpretation, 2011.

[73]   T. Shu, X. Yang, W. Li, X. Yao, Raman Spectroscopic Differences between Ephedrine and Pseudoephedrine, J Forensic Sci. 64 (2019) 1482–1485. https://doi.org/10.1111/1556-4029.14015.

[74]   R.W. Berg, T. Nrbygaard, P.C. White, S. Abdali, Ab initio calculations and raman and sers spectral analyses of amphetamine species, Appl Spectrosc Rev. 46 (2011) 107–131. https://doi.org/10.1080/05704928.2010.520180.

[75]   H.G.M. Edwards, T. Munshi, M. Anstis, Raman spectroscopic characterisations and analytical discrimination between caffeine and demethylated analogues of pharmaceutical relevance, Spectrochim Acta A Mol Biomol Spectrosc. 61 (2005) 1453–1459. https://doi.org/10.1016/j.saa.2004.10.022.

[76]   C.M. Liu, H.Y. He, L. Xu, Z.D. Hua, New qualitative analysis strategy for illicit drugs using Raman spectroscopy and characteristic peaks method, Drug Test  Anal. 13 (2021) 720–728. https://doi.org/10.1002/dta.2963.

[77]   D. Lv, Y. Cao, Z. Lou, S. Li, X. Chen, Y. Chai, F. Lu, Rapid on-site detection of ephedrine and its analogues used as adulterants in slimming dietary supplements by TLC-SERS, Anal Bioanal Chem. 407 (2015) 1313–1325. https://doi.org/10.1007/s00216-014-8380-9.

[78]   S. Thurrott, Here's Why Your Medication Contains Active and Inactive Ingredients, Banner Health. (2022). https://www.bannerhealth.com/healthcareblog/teach-me/why-your-medication-contains-active-and-inactive-ingredients.

[79]   R. Shaikh, D.P. O'Brien, D.M. Croker, G.M. Walker, Chapter 2 - The development of a pharmaceutical oral solid dosage forms, Computer Aided Chemical Engineering. 41 (2018) 27–65. https://doi.org/10.1016/B978-0-444-63963-9.00002-6.

[80]   Y.-L. Cheng, C.-Y. Lee, Y.-L. Huang, C.A. Buckner, R.M. Lafrenie, J.A. Dénommée, J.M. Caswell, D.A. Want, G.G. Gan, Y.C. Leong, P.C. Bee, E. Chin, A.K.H. Teh, S. Picco, L. Villegas, F. Tonelli, M. Merlo, J. Rigau, D. Diaz, M. Masuelli, S. Korrapati, P. Kurra, S. Puttugunta, S. Picco, L. Villegas, F. Tonelli, M. Merlo, J. Rigau, D. Diaz, M. Masuelli, M. Tascilar, F.A. de Jong, J. Verweij, R.H.J. Mathijssen, Cellulose and Its Derivatives Use in

the Pharmaceutical Compounding Practice Chap, in: Cellulose - Medical, Pharmaceutical and Electronic Applications, InTech, 2013: p. 145. https://doi.org/10.5772/56637.

[81]    T. Cooman, T. Trejos, A.H. Romero, L.E. Arroyo, Implementing machine learning for the identification and classification of compound and mixtures in portable Raman instruments, Chem Phys Lett. 787 (2022) 139283. https://doi.org/10.1016/j.cplett.2021.139283.

[82]    Z.-H. Zhou, Machine Learning, 1st ed., Springer Nature Singapore Pte Lt, Singapore, 2021.

[83]    I. Goodfellow, Y. Bengio, A. Courville, Deep Learning: Intro, MIT Press, 2016.

[84]    C. Janiesch, P. Zschech, K. Heinrich, Machine learning and deep learning, Electronic Markets. 31 (2021) 685–695. https://doi.org/10.1007/s12525-021-00475-2/Published.

[85]    I. Goodfellow, Y. Bengio, A. Courville, Deep Learning: CNN, MIT Press, 2016.

[86]    J. Sharma, Introduction to Supervised Deep Learning Algorithms!, Analytics Vidhya. (2021).

[87]    J. Brownlee, Supervised and Unsupervised Machine Learning Algorithms, Machine Learning Mastery. (2020).

[88]    J. Brownlee, A Gentle Introduction to the Rectified Linear Unit (ReLU), Machine Learning Mastery. (2020).

[89]    M. Riva, Batch Normalization in Convolutional Neural Networks, Baeldung.Com. (2023). https://www.baeldung.com/cs/batch-normalization-cnn#:~: (accessed May 22, 2023).

[90]    A. Biswal, Convolutional Neural Network Tutorial, Simplilearn.Com. (2023). https://www.simplilearn.com/tutorials/deep-learning-tutorial/convolutional-neural-network (accessed May 22, 2023).

[91]    A. Kuma, Difference: Binary, Multiclass & Multi-label Classification, Data Analytics. (2022). https://vitalflux.com/difference-binary-multi-class-multi-label-classification/1/9.

[92]    J. Brownlee, A Gentle Introduction to k-fold Cross-Validation, Machine Learning Mastery. (2020).

[93]    J. Brownlee, How to Calculate Precision, Recall, and F-Measure for Imbalanced Classification, Machine Learning Mastery. (2020). https://machinelearningmastery.com/precision-recall-and-f-measure-for-imbalanced-classification/#:~:text=Precision.

[94]   C.A.F. De Oliveira Penido, M.T.T. Pacheco, I.K. Lednev, L. Silveira, Raman spectroscopy in forensic analysis: Identification of cocaine and other illegal drugs of abuse, Journal of Raman Spectroscopy. 47 (2016) 28–38. https://doi.org/10.1002/jrs.4864.

[95]   P. Larkin, Infrared and Raman Spectroscopy: Principles and Spectral Interpretation, first, Elsevier, 2011.

[96]   R.B. Cody, J.A. , Laramée, D.H. Dupont, Versatile new ion source for the analysis of materials in open air under ambient conditions, Anal Chem. 77 (2005) 2297–2302. https://doi.org/10.1021/ac050162j.

[97]   R.R. Steiner, DART$^{TM}$ (Direct Analysis in Real Time) | Products | JEOL Ltd., JOEL. (n.d.). https://www.jeol.co.jp/en/products/detail/DART.html (accessed May 16, 2022).

[98]   J.H. Gross, Direct analysis in real time-a critical review on DART-MS, Anal Bioanal Chem. 406 (2014) 63–80. https://doi.org/10.1007/s00216-013-7316-0.

[99]   E. Sisco, T.P. Forbes, Forensic applications of DART-MS: A review of recent literature, Forensic Chemistry. 22 (2021). https://doi.org/10.1016/j.forc.2020.100294.

[100]  R.B. Cody, Dart Mass Spectrometry 2008 : 01 : Introduction, Technology Transition Workshop. (2008). https://www.youtube.com/watch?v=vWWvEDhCc-c (accessed May 18, 2022).

[101]  E. Sisco, T.P. Forbes, M.E. Staymates, G. Gillen, Rapid analysis of trace drugs and metabolites using a thermal desorption DART-MS configuration, Analytical Methods. 8 (2016) 6494–6499. https://doi.org/10.1039/c6ay01851c.

[102]  M.J. Pavlovich, B. Musselman, A.B. Hall, Direct analysis in real time—Mass spectrometry (DART-MS) in forensic and security applications, Mass Spectrom Rev. 37 (2018) 171–187. https://doi.org/10.1002/mas.21509.

[103]  H. Brown, B. Oktem, A. Windom, V. Doroshenko, K. Evans-Nguyen, Direct Analysis in Real Time (DART) and a portable mass spectrometer for rapid identification of common and designer drugs on-site, Forensic Chemistry. 1 (2016) 66–73. https://doi.org/10.1016/j.forc.2016.07.002.

[104]  A.D. Lesiak, R.B. Cody, A.J. Dane, R.A. Musah, Rapid detection by direct analysis in real time-mass spectrometry (DART-MS) of psychoactive plant drugs of abuse: The case of Mitragyna speciosa aka "Kratom," Forensic Sci Int. 242 (2014) 210–218. https://doi.org/10.1016/j.forsciint.2014.07.005.

[105] T.H. Chen, H.Y. Hsu, S.P. Wu, The detection of multiple illicit street drugs in liquid samples by direct analysis in real time (DART) coupled to Q-orbitrap tandem mass spectrometry, Forensic Sci Int. 267 (2016) 1–6. https://doi.org/10.1016/j.forsciint.2016.07.025.

[106] M.J. Bennett, R.R. Steiner, Detection of gamma-hydroxybutyric acid in various drink matrices via AccuTOF-DART, J Forensic Sci. 54 (2009) 370–375. https://doi.org/10.1111/j.1556-4029.2008.00955.x.

[107] R.R. Steiner, A Rapid Technique for the Confirmation of Iodine and Red Phosphorous using DART MS, Microgram Journal. 7 (2010) 3–6.

[108] S. Gwak, J.R. Almirall, Rapid screening of 35 new psychoactive substances by ion mobility spectrometry (IMS) and direct analysis in real time (DART) coupled to quadrupole time-of-flight mass spectrometry (QTOF-MS), Drug Test Anal. 7 (2015) 884–893. https://doi.org/10.1002/dta.1783.

[109] R. Lian, Z. Wu, X. Lv, Y. Rao, H. Li, J. Li, R. Wang, C. Ni, Y. Zhang, Rapid screening of abused drugs by direct analysis in real time (DART) coupled to time-of-flight mass spectrometry (TOF-MS) combined with ion mobility spectrometry (IMS), Forensic Sci Int. 279 (2017) 268–280. https://doi.org/10.1016/j.forsciint.2017.07.010.

[110] E. Sisco, J. Verkouteren, J. Staymates, J. Lawrence, Rapid detection of fentanyl, fentanyl analogues, and opioids for on-site or laboratory based drug seizure screening using thermal desorption DART-MS and ion mobility spectrometry, Forensic Chemistry. 4 (2017). https://doi.org/10.1016/j.forc.2017.04.001.

[111] E. Sisco, E.L. Robinson, A. Burns, R. Mead, What's in the bag? Analysis of exterior drug packaging by TD-DART-MS to predict the contents, Forensic Sci Int. 304 (2019) 109939. https://doi.org/10.1016/j.forsciint.2019.109939.

[112] A.S. Moorthy, E. Sisco, A New Library-Search Algorithm for Mixture Analysis Using DART-MS, J Am Soc Mass Spectrom. 32 (2021) 1725–1734. https://doi.org/10.1021/jasms.1c00097.

[113] A.S. Moorthy, S.S. Tennyson, E. Sisco, Updates to the Inverted Library Search Algorithm for Mixture Analysis, J Am Soc Mass Spectrom. 33 (2022) 1260–1266. https://doi.org/10.1021/jasms.2c00090.

[114] E. Sisco, M.G. Appley, S.S. Tennyson, A.S. Moorthy, Qualitative Analysis of Real Drug Evidence Using DART-MS and the Inverted Library Search Algorithm, J Am Soc Mass Spectrom. 33 (2022) 1784–1793. https://doi.org/10.1021/jasms.2c00166.

[115] M.G. Appley, E.L. Robinson, A. Thomson, E. Russell, E. Sisco, An Analytical Platform for Near Real-Time Drug Landscape Monitoring using Paraphernalia Residues, Forensic Chemistry. (2023) 100489. https://doi.org/10.1016/j.forc.2023.100489.

[116] A.N. Couch, J. Sharp, J.T. Davidson, Assessing the effectiveness of the NIST DART-MS Forensics Database and Data Interpretation Tool for designer drug screening with alternative instrumentation, Int J Mass Spectrom. 483 (2023). https://doi.org/10.1016/j.ijms.2022.116964.

[117] United Nations Office on Drugs and Crime (UNODC), Guidelines on Raman Handheld Field Identification Devices for Seized Material, (2017) 1–45.

[118] One Pill Can Kill, DEA. (n.d.). https://www.dea.gov/onepill (accessed January 29, 2023).

[119] Facts about Fentanyl, DEA. (n.d.). https://www.dea.gov/resources/facts-about-fentanyl (accessed January 29, 2023).

[120] Doj, Dea, DEA Joint Intelligence Report The Growing Threat of Xylazine and its Mixture with Illicit Drugs, 2022.

[121] FDA alerts health care professionals of risks to patients exposed to xylazine in illicit drugs _ FDA, FDA. (2022). https://www.fda.gov/drugs/drug-safety-and-availability/fda-alerts-health-care-professionals-risks-patients-exposed-xylazine-illicit-drugs (accessed May 30, 2023).

[122] C. Russell, J. Law, M. Bonn, J. Rehm, F. Ali, The increase in benzodiazepine-laced drugs and related risks in Canada: The urgent need for effective and sustainable solutions, International Journal of Drug Policy. 111 (2023). https://doi.org/10.1016/j.drugpo.2022.103933.

[123] UNODC, Main countries identified as departure or transit of methamphetamine shipments, UNODC. (n.d.).

[124] UNODC, Main countries identified as destination of methamphetamine shipments, UNODC. (n.d.).
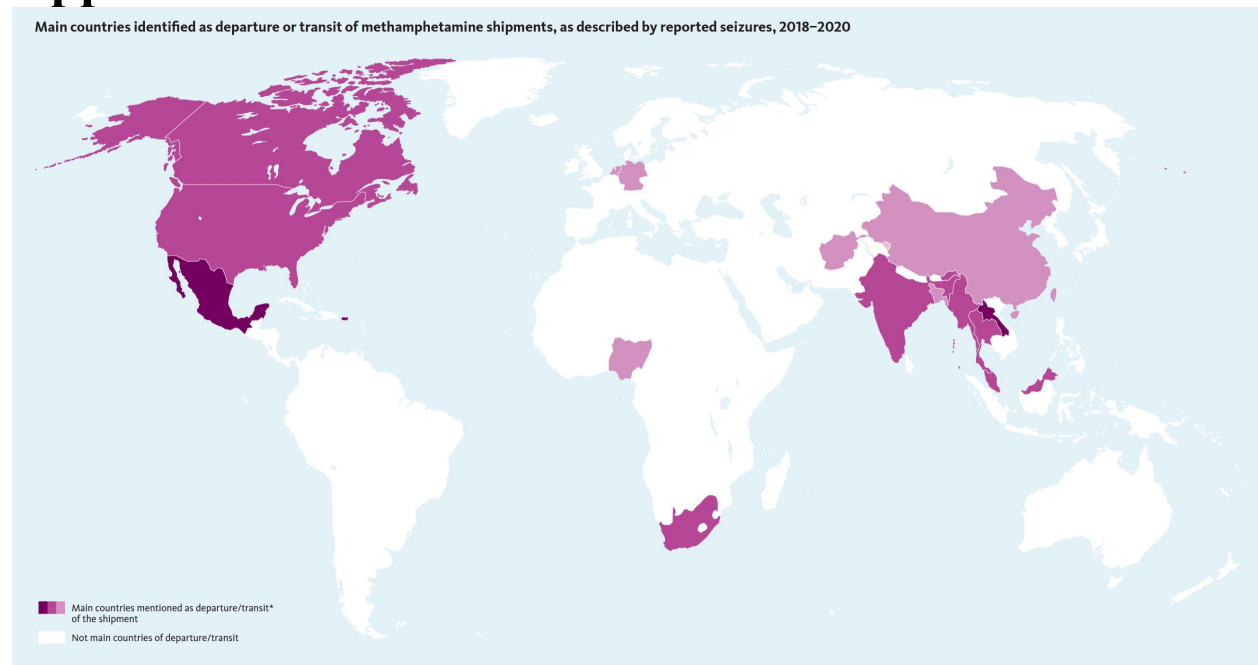
# Appendix



**Figure A - 1:** Graph from UNODC showing the major countries identified as departure or transit of methamphetamine shipments, as described by reported seizures, 2018 – 2020. [123]
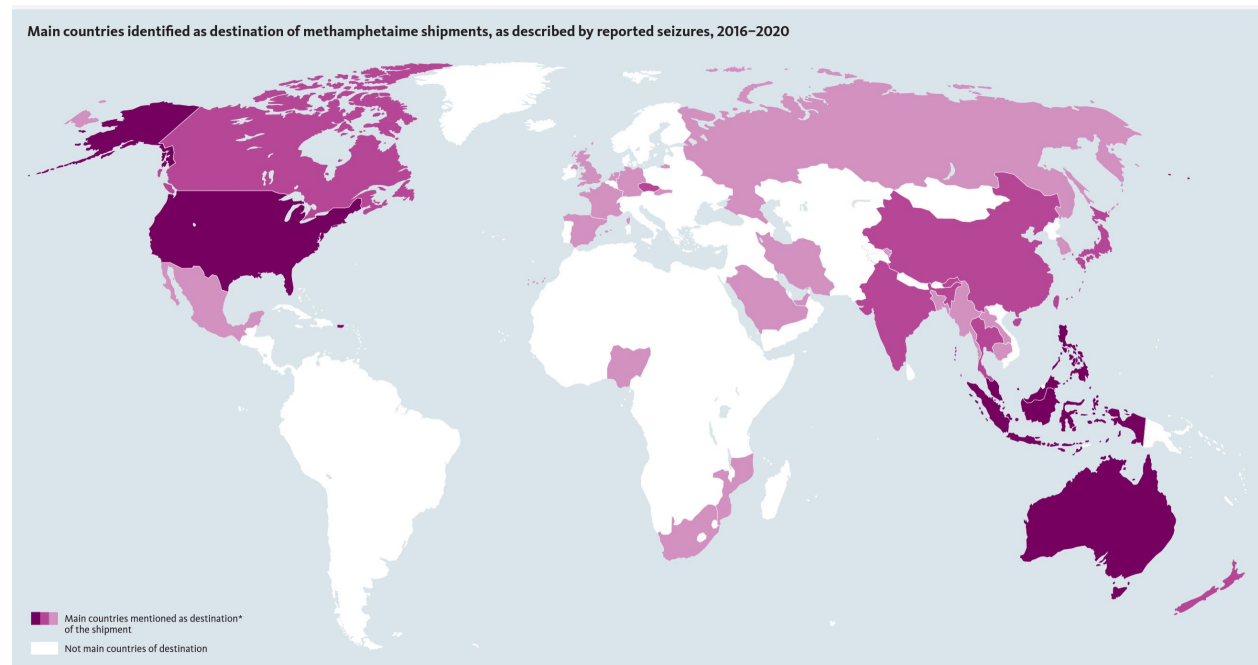


**Figure A - 2:** Graph from UNODC showing the major countries identified as destinations of methamphetamine shipments, as described by reported seizures, 2016 – 2020. [124]
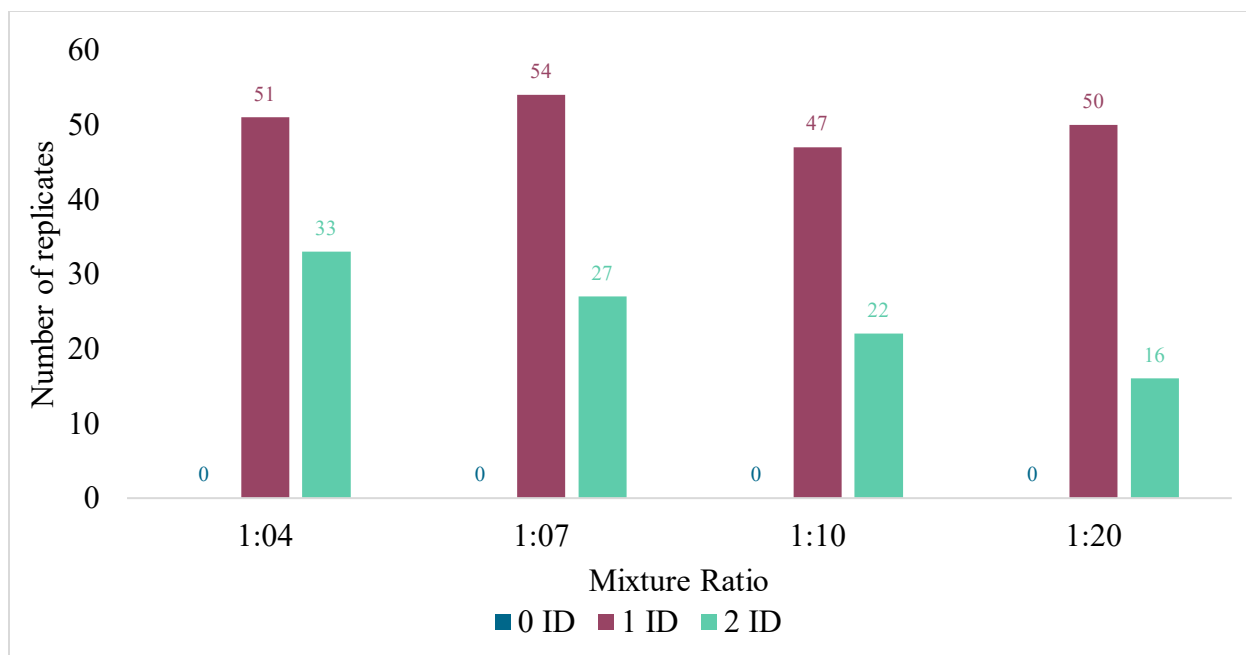
**Figure A - 3:** Percent identification for each ratio of the binary mixtures when using the individual results.

**Table A - 1:** The average precision, recall, and f1-score for each fold and the percent identification. The bolded numbers are the highest value for that metric/score. The "Individual ID %" is the percent identification when using the replicates as individual samples. The "Combined ID %" is the percent identification when combining the results into one overall result for each mixture.

| Fold | Precision | Recall | F1-score | Individual ID % | Combined ID % |
|---|---|---|---|---|---|
| 1 | 99.77 | 98.53 | 99.14 | 81.2 | 91.0 |
| 2 | 99.57 | 98.78 | 99.17 | 80.5 | 91.0 |
| 3 | 99.75 | 98.65 | 99.20 | 82.2 | 94.0 |
| 4 | 99.80 | 98.09 | 98.93 | 80.3 | 90.5 |
| 5 | 99.78 | 98.33 | 99.05 | 80.3 | 91.0 |
| 6 | 99.76 | 98.38 | 99.06 | 82.3 | 92.5 |
| 7 | 99.86 | 98.37 | 99.10 | 81.5 | 91.5 |
| 8 | 99.86 | 98.45 | 99.15 | 81.0 | 92.0 |
| 9 | 99.57 | 98.28 | 98.92 | 79.8 | 89.5 |
| 10 | 99.69 | 98.33 | 99.00 | 80.2 | 90.5 |

Potential matches:

Search: [                    ]

| | Compound | Δ m/z | FPIE | RevMF | IRD | Match Type |
|---|---|---|---|---|---|---|
| 1 | Codeine | -0.0010 | 0.324 | 0.447 | 0.000 | Protonated Molecule |
| 2 | Heterocodeine | -0.0010 | 0.250 | 0.239 | 0.000 | Protonated Molecule |
| 3 | Hydrocodone | -0.0010 | 0.837 | 0.861 | 0.000 | Protonated Molecule |
| 4 | Neopine | -0.0010 | 0.821 | 0.780 | 0.000 | Protonated Molecule |
| 5 | Pseudocodeine | -0.0010 | 0.885 | 0.845 | 0.000 | Protonated Molecule |

**Figure A - 4:** DIT results for codeine from the average mass spectra for codeine and acetaminophen at a 1:20 ratio. While codeine has low scores, other compounds similar to codeine like hydrocodone and pseudocodeine are above the threshold.

Potential matches:

| | Compound | Δ m/z | FPIE | RevMF | IRD | Match Type |
|---|---|---|---|---|---|---|
| 1 | 2,3-Dimethylmethcathinone | -0.0002 | 0.738 | 0.556 | 0.032 | Protonated Molecule |
| 2 | 2,4-Dimethylmethcathinone | -0.0002 | 0.542 | 0.402 | 0.032 | Protonated Molecule |
| 3 | 2-Ethylmethcathinone | -0.0002 | 0.706 | 0.648 | 0.032 | Protonated Molecule |
| 4 | 2-Methylethcathinone | -0.0002 | 0.747 | 0.595 | 0.032 | Protonated Molecule |
| 5 | 2-NMC | -0.0002 | 0.439 | 0.764 | 0.032 | Protonated Molecule |
| 6 | 3,4-Dimethylmethcathinone | -0.0002 | 0.591 | 0.431 | 0.032 | Protonated Molecule |
| 7 | 3-Ethylmethcathinone | -0.0002 | 0.919 | 0.602 | 0.032 | Protonated Molecule |
| 8 | 3-Methylbuphedrone | -0.0002 | 0.694 | 0.624 | 0.032 | Protonated Molecule |
| 9 | 3-Methylethcathinone | -0.0002 | 0.804 | 0.662 | 0.032 | Protonated Molecule |
| 10 | 4-Ethylmethcathinone | -0.0002 | 0.772 | 0.626 | 0.032 | Protonated Molecule |

**Figure A - 5:** DIT results from the average of 4-MEC and benzocaine at a 1:10 ratio. Ten different compounds are present for this target fragment, including the 4-MEC, highlighted in blue. However, they are all cathinones.

Measured *m/z*: 389.1654
Relative Intensity: 4.3 %

Potential matches:

Search: [ ]

| | Compound | Δ *m/z* | FPIE | RevMF | IRD | Match Type |
|---|---|---|---|---|---|---|
| 1 | Cetirizine | 0.0022 | 0.672 | 0.766 | -0.320 | Protonated Molecule |

**Figure A - 6:** False positive result from the cocaine and hydroxyzine at a 1:10 mixture. This false positive can be ruled out because the Δ*m/z* value is positive, whereas the values for the m/z range trended negatively.
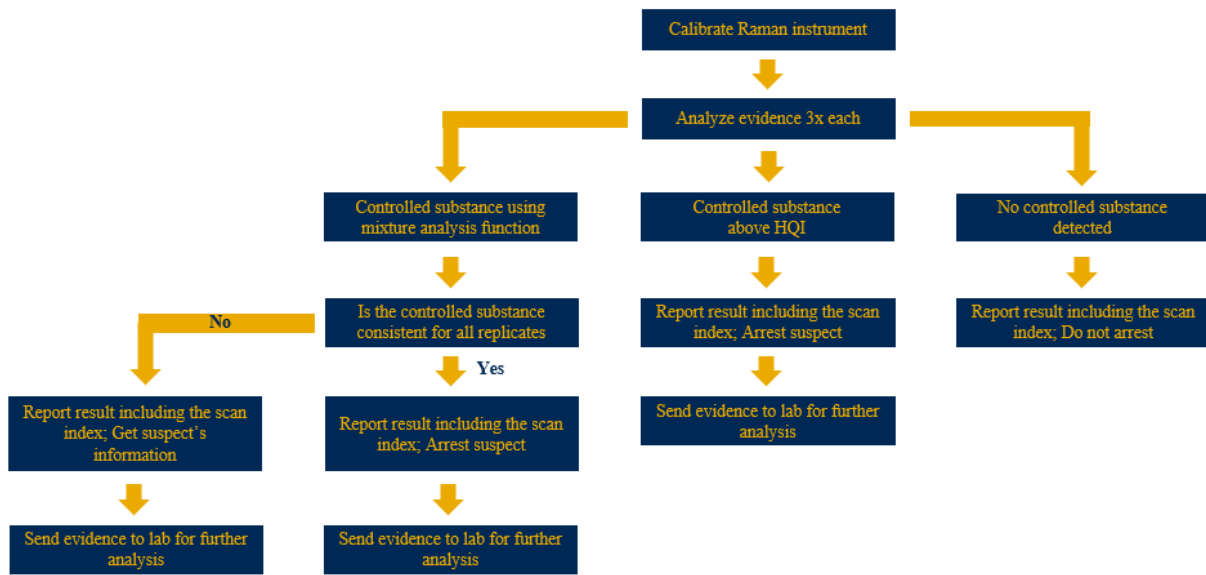


**Figure A - 7:** A decision tree for implementation of a portable Raman instrument for a controlled substance found at a crime scene.
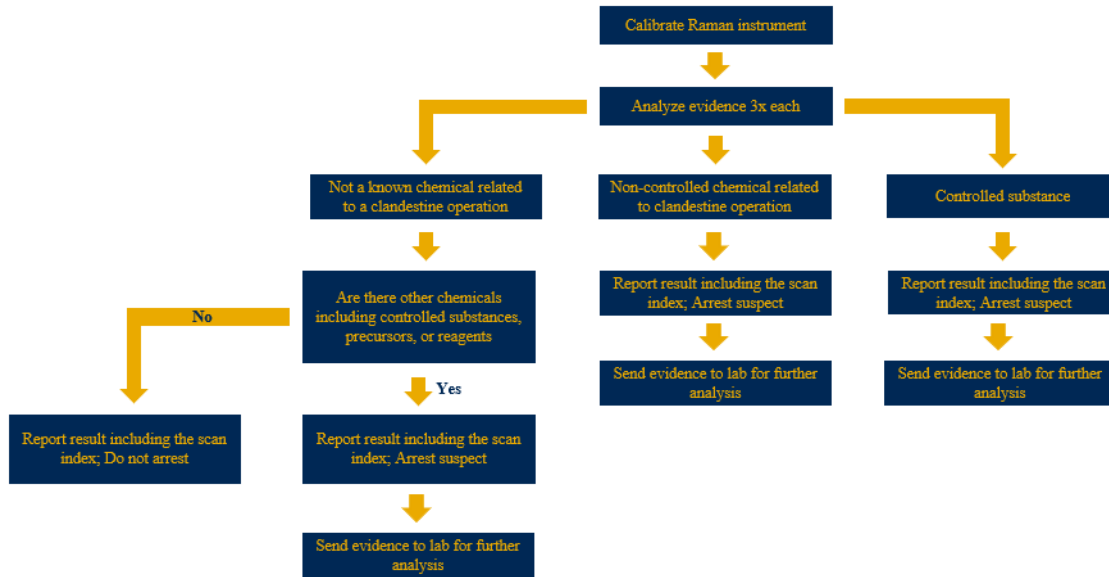
**Figure A - 8:** A decision tree for implementation of a portable Raman instrument for a potential clandestine laboratory.
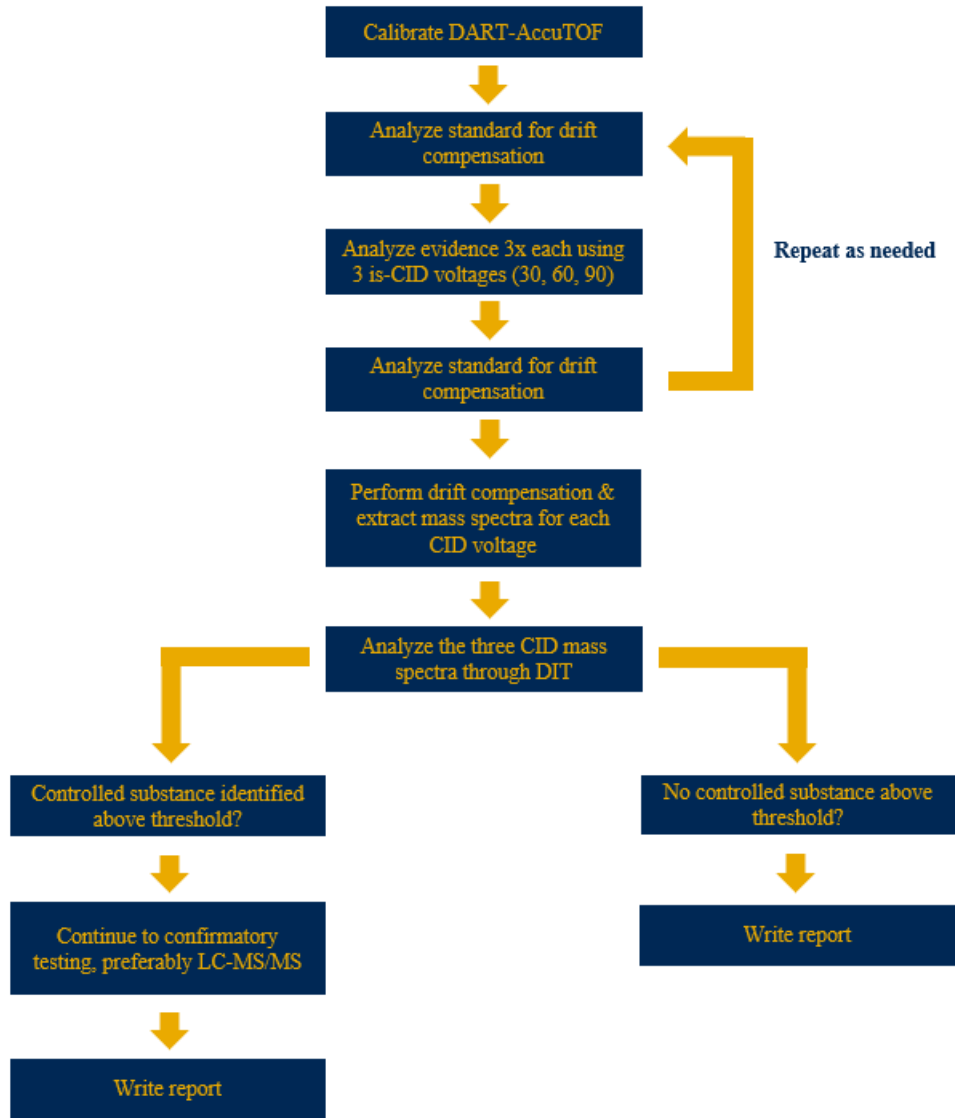
**Figure A - 9:** A decision tree for implementation of a DART-AccuTOF for a screening technique for a forensic laboratory.